# Parton Distribution Functions at the LHC

Robert Thorne

May 28th 2019

University College London

# Introduction to Parton Distribution Functions (PDFs)

Strong force makes it difficult to perform analytic calculations of scattering processes involving hadronic particles.

The weakening of $\alpha_S(\mu^2)$ at higher scales $\longrightarrow$ the **Factorization Theorem**.

Hadron scattering with an electron factorizes.

$Q^2$ – Scale of scattering

$x = \frac{Q^2}{2m\nu}$ – Momentum fraction of Parton ($\nu$=energy transfer)

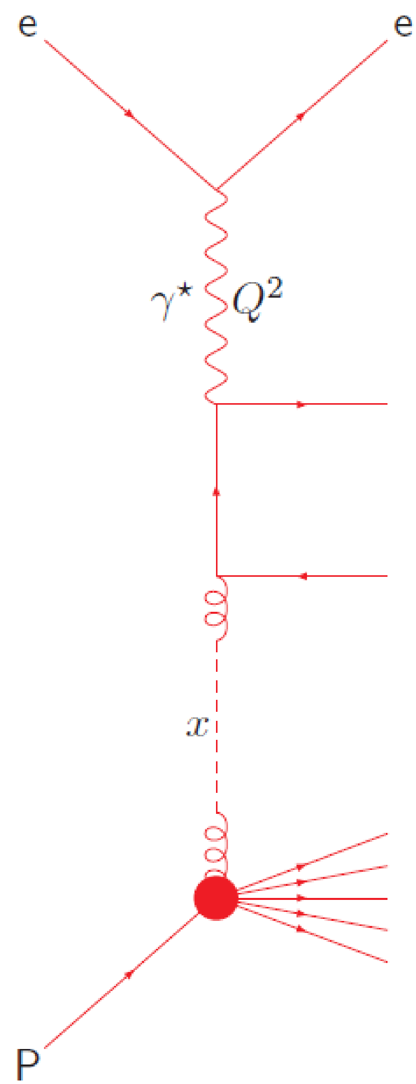


perturbative
calculable
coefficient function
$C_i^P(x, \alpha_s(Q^2))$

nonperturbative
incalculable
parton distribution
$f_i(x, Q^2, \alpha_s(Q^2))$

The coefficient functions $C_i^P(x, \alpha_s(Q^2))$ are process dependent (new physics) but are calculable as a power-series in $\alpha_s(Q^2)$.

$$C_i^P(x, \alpha_s(Q^2)) = \sum_k C_i^{P,k}(x)\alpha_s^k(Q^2).$$

Since the parton distributions $f_i(x, Q^2, \alpha_s(Q^2))$ are process-independent, i.e. **universal**, and evolution with scale is calculable, once they have been measured at one experiment, one can predict many other scattering processes.

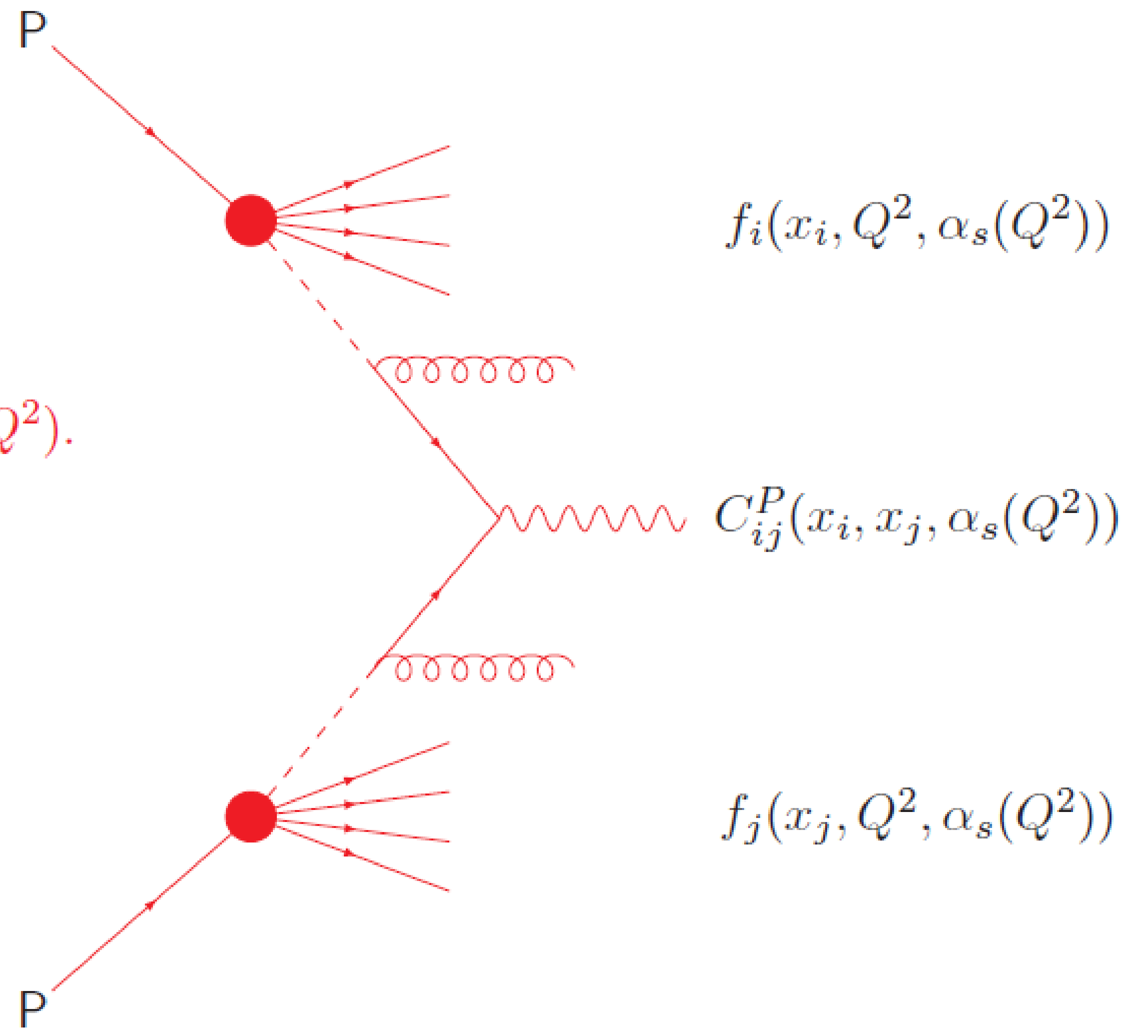

# LHC Physics

The kinematic range for particle production at the LHC is shown (W.J. Stirling).

$$x_{1,2} = x_0 \exp(\pm y), \quad x_0 = \frac{M}{\sqrt{s}}.$$

$x \sim 0.001 - 0.01$ parton distributions therefore vital for understanding standard production processes at the LHC.

However, even smaller (and higher) $x$ required when one moves away from zero rapidity, e.g. when calculating total cross-sections.

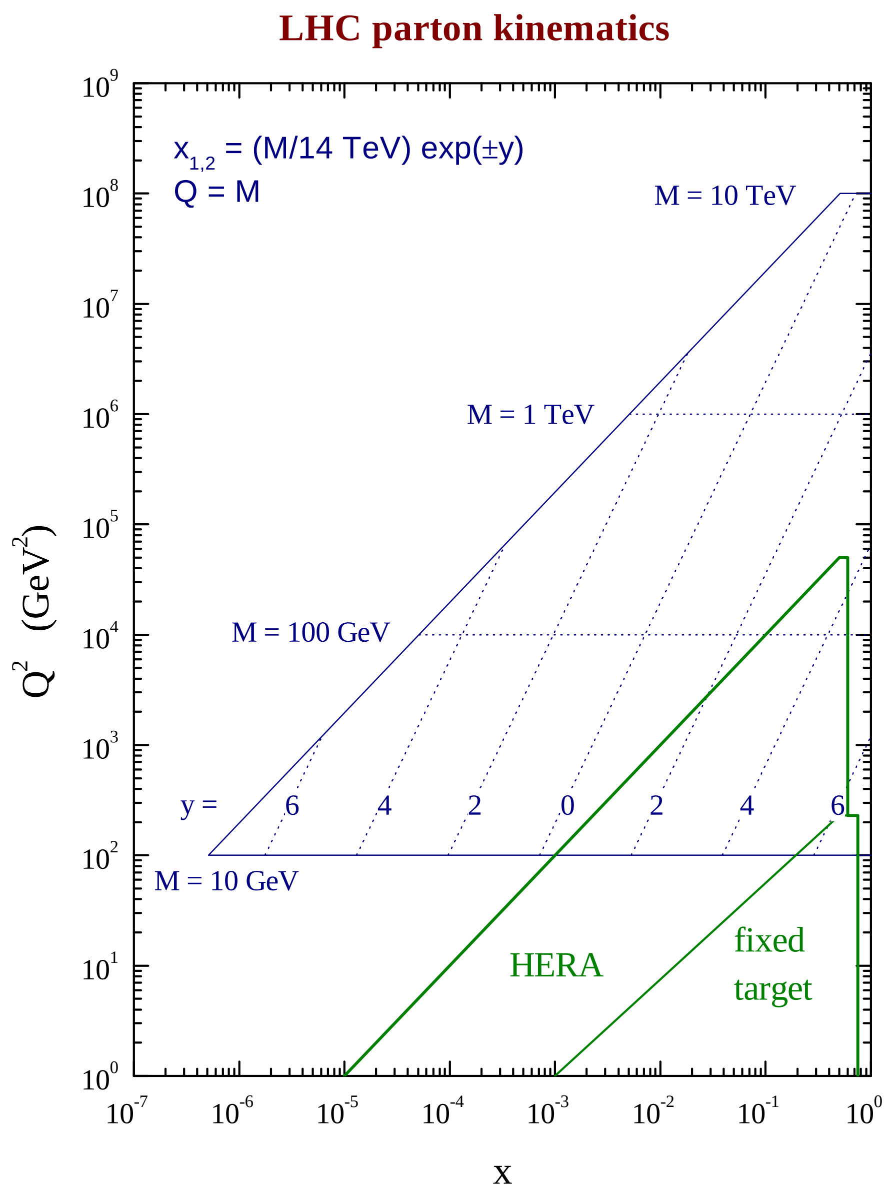

# Production Rates

Very quick estimates of benefits of increasing collider energy.

100 TeV dramatically increases the full cross-sections for most standard model processes, but even more enhancement as $M_X$ increases.

Precise PDFs needed for details.

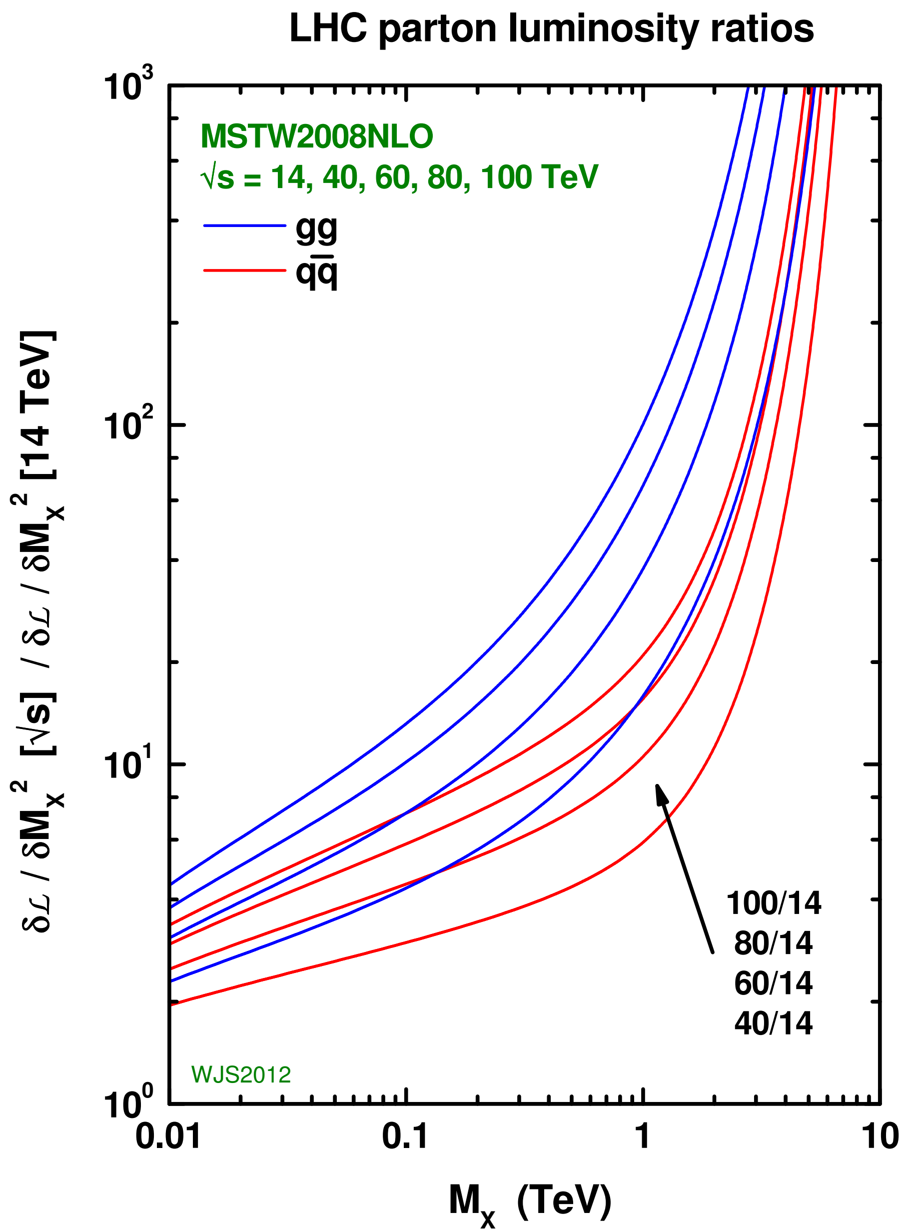

## Obtaining PDF sets – General procedure.

Start parton evolution at low scale $Q_0^2 \sim 1\mathrm{GeV}^2$. In principle 11 different partons to consider.

$$u, \bar{u}, \quad d, \bar{d}, \quad s, \bar{s}, \quad c, \bar{c}, \quad b, \bar{b}, \quad g$$

$m_c, m_b \gg \Lambda_{\mathrm{QCD}}$ so heavy parton distributions determined perturbatively. Leaves 7 independent combinations, or 6 if we assume $s = \bar{s}$.

$$u_V = u - \bar{u}, \quad d_V = d - \bar{d}, \quad \mathrm{sea} = 2 * (\bar{u} + \bar{d} + \bar{s}), \quad s + \bar{s}, \quad \bar{d} - \bar{u}, \quad g.$$

Input partons parameterised as, e.g. MMHT,

$$xf(x, Q_0^2) = A(1-x)^\eta x^\delta (1 + \textstyle\sum_n a_n T_n(y)).$$

Where $T_n$ are Chebyshev polynomials and $y = 1 - 2\sqrt{x}$.

Evolve partons upwards using LO, NLO or NNLO DGLAP equations.

$$\frac{df_i(x, Q^2, \alpha_s(Q^2))}{d \ln Q^2} = \textstyle\sum_j P_{ij}(x, \alpha_s(Q^2)) \otimes f_j(x, Q^2, \alpha_s(Q^2))$$

Fit data above $\sim 2\mathrm{GeV}^2$. Need many types for full determination.

- Lepton-proton collider HERA – (DIS) $\rightarrow$ small-$x$ quarks and gluons from evolution. Charged current data some limited info on flavour separation. Heavy flavour structure functions – gluon and charm, bottom distributions and masses.

- Fixed target DIS – higher $x$ – leptons (BCDMS, NMC, $\ldots$) $\rightarrow$ up quark (proton) or down quark (deuteron) and neutrinos (CHORUS, NuTeV, CCFR) $\rightarrow$ valence or singlet combinations.

- Di-muon production in neutrino DIS ($W+s \rightarrow c \rightarrow \mu$) – strange quarks.

- Drell-Yan production of dileptons – ($q\bar{q} \rightarrow \gamma^\star$) – high-$x$ sea quarks. Deuterium target – $\bar{u}/\bar{d}$ asymmetry.

- High-$p_T$ jets at colliders (Tevatron/LHC) – high-$x$ gluon distribution.

- $W$ and $Z$ production at colliders (Tevatron/LHC) – different quark contributions to DIS.

New types of data becoming available at LHC – later.

This procedure is generally successful and is part of a large-scale, ongoing project (MRST → MSTW → MMHT). Results in partons of the form shown.

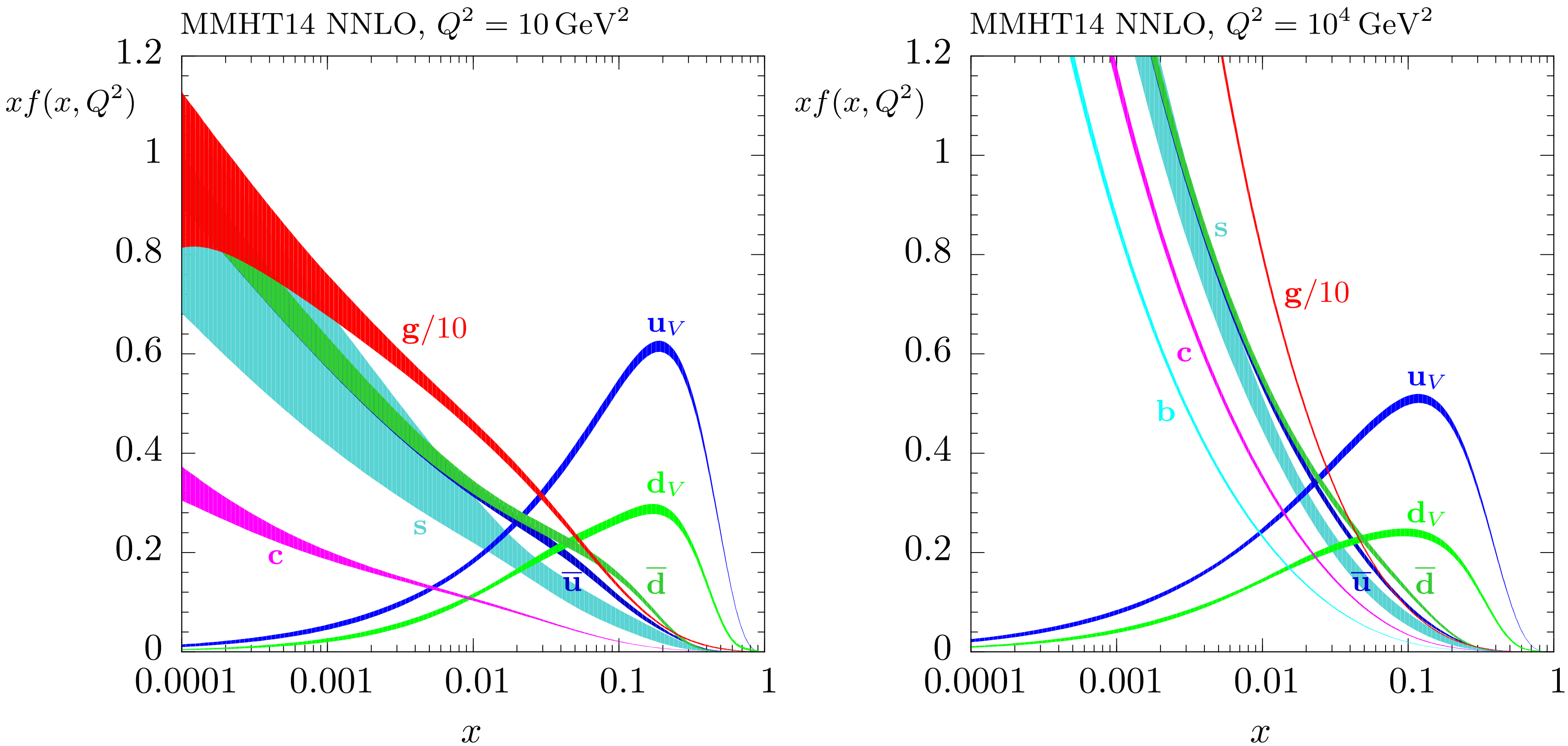


Various choices of PDF – MMMT, CTEQ, NNPDF, ABM(P), HERA, CJ *et al* *etc.*. All LHC cross-sections rely on our understanding of these partons.

**Parton Fits and Uncertainties.** Two main approaches.

Most groups use a parton parameterization and Hessian approach.

$$\chi^2 - \chi^2_{min} \equiv \Delta\chi^2 = \sum_{i,j} H_{ij}(a_i - a_i^{(0)})(a_j - a_j^{(0)})$$

Often $\Delta\chi^2 > 1$ to account for inconsistencies between data sets (or other sources), e.g *dynamical tolerance*.

Can find and rescale eigenvectors of $H$ leading to $\Delta\chi^2 = \sum_i z_i^2$

*2-dim (i,j) rendition of d-dim (~20) PDF parameter space*

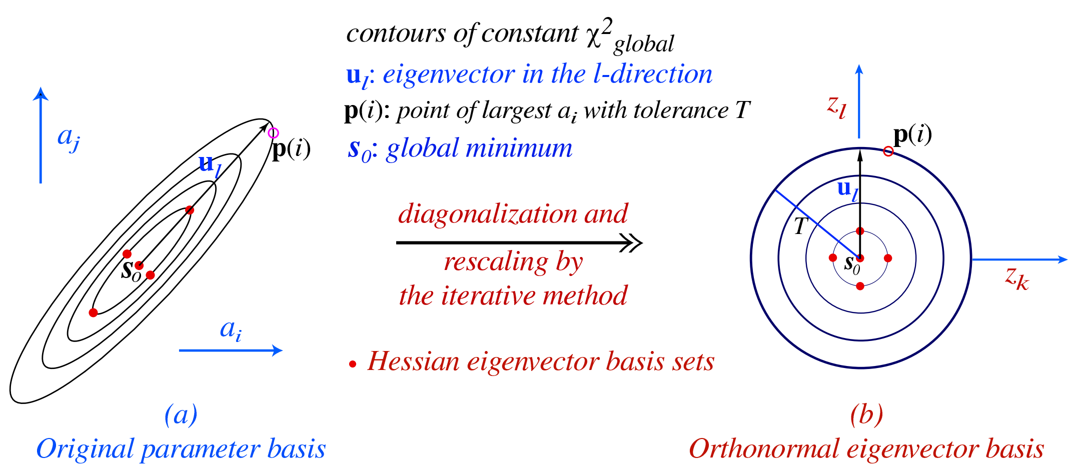


Uncertainty on physical quantity then given by

$$(\Delta F)^2 = \sum_i \left(F(S_i^{(+)}) - F(S_i^{(-)})/2\right)^2,$$

where $S_i^{(+)}$ and $S_i^{(-)}$ are PDF "error sets". (Can also allow for asymmetric uncertainties.)

**Neural Network** group (Ball *et al.*) limit parameterization dependence. Leads to alternative approach to “best fit” and uncertainties.

First part of approach, no longer perturb about best fit.

- Generate artificial data according to distribution

$$O_i^{(art)\,(k)} = (1 + r_N^{(k)}\,\sigma_N)\left[O_i^{(exp)} + \sum_{p=1}^{N_{sys}} r_p^{(k)}\,\sigma_{i,p} + r_{i,s}^{(k)}\,\sigma_s^i\right]$$

Where $r_p^{(k)}$ are Gaussian distributed random numbers. Hence, include information about measurements and errors in distribution of $O_{i,p}^{art,(k)}$.

Fit to the data replicas obtaining PDF replicas $q_i^{(net)(k)}$.

Mean $\mu_O$ and deviation $\sigma_O$ of observable $O$ then given by

$$\mu_O = \frac{1}{N_{rep}}\sum_1^{N_{rep}} O[q_i^{(net)(k)}], \quad \sigma_O^2 = \frac{1}{N_{rep}}\sum_1^{N_{rep}}(O[q_i^{(net)(k)}] - \mu_O)^2.$$

*Eliminates* parameterisation dependence by using a neural net which undergoes a series of (mutations via genetic algorithm) to find the best fit. In effect is a much larger sets of parameters – $\sim 37$ per distribution.

Can now transform between eigenvectors and replicas.

# Comparisons between different sets.

From a few years ago when LHC data started appearing. (Watt)

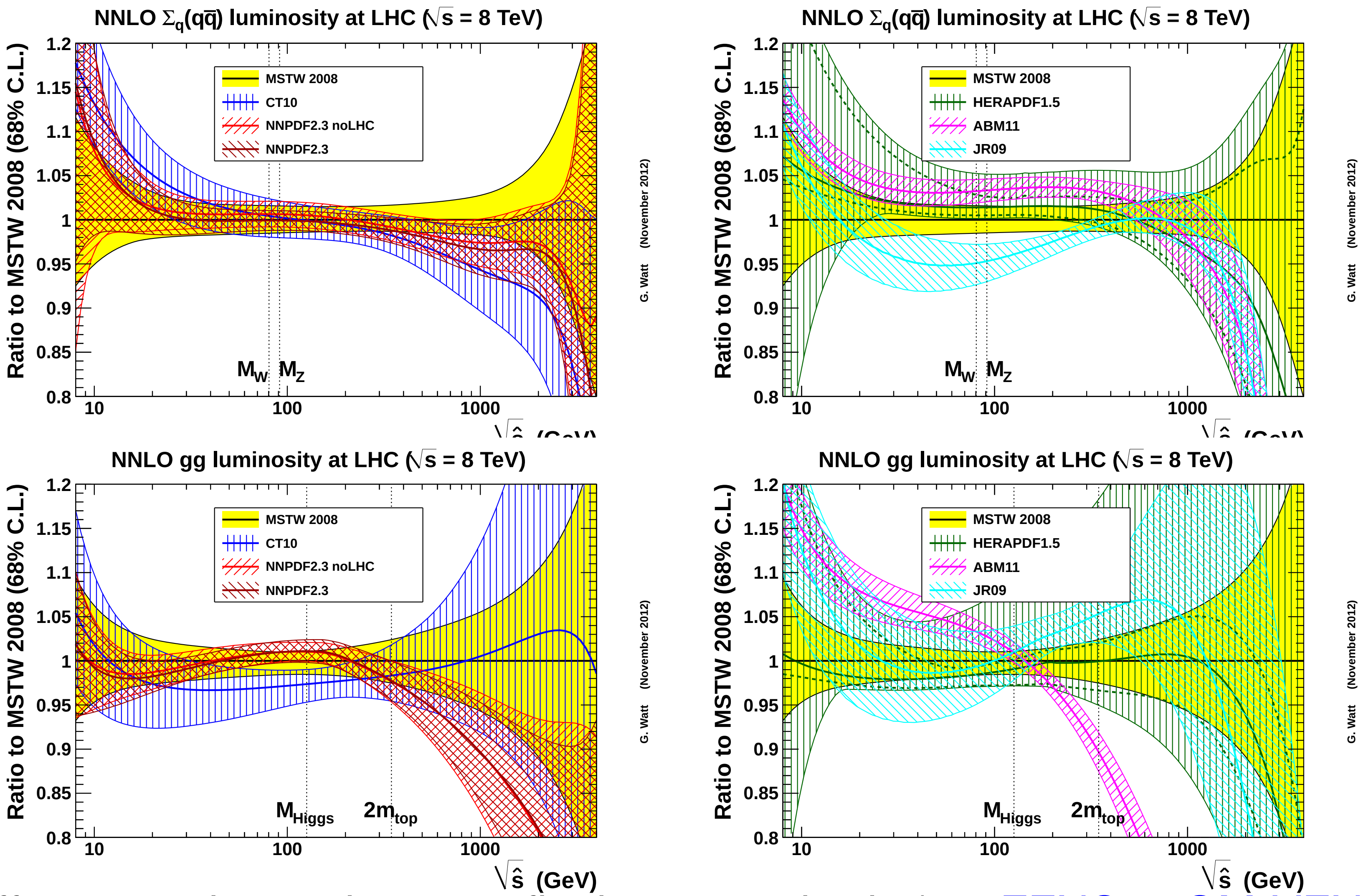


Differences due to data sets fit, theory methods (e.g FFNS or GM-VFNS for heavy flavour. Updates in the past few years have led to changes.

## PDF Updates

**ABM12 PDFs** – Include combined HERA charm DIS data, and ATLAS, CMS, LHCb Drell-Yan data. Also investigate top pair production data.

**CT14 PDF sets** - changes due to new data sets – ATLAS, CMS LHCb $W, Z$ data and ATLAS, CMS inclusive jet data.
Also **new parameterisation** – Bernstein polynomials.

**NNPDF3.0 PDFs** – newer HERA data, ATLAS, CMS inclusive jet data, ATLAS, CMS LHCb $W, Z, W+c, W p_T$ data and top pair production data.
**Improved methodology** - closure test improved procedures in finding best fit, i.e. inputs to algorithm, training length *etc.*

**MMHT2014 – Changes in theoretical procedures** – parameterisation with Chebyshev polynomials, freedom in deuteron corrections; improved $D$-meson branching ratio.
**Changes in data sets** - updates of HERA and Tevatron data; LHC data on $W, Z$ top pair production data. 25 eigenvector pairs (20 in MSTW).

## Developments soon after.

### HERAI+II combination data.

### Averaged cross sections: NC e⁻p

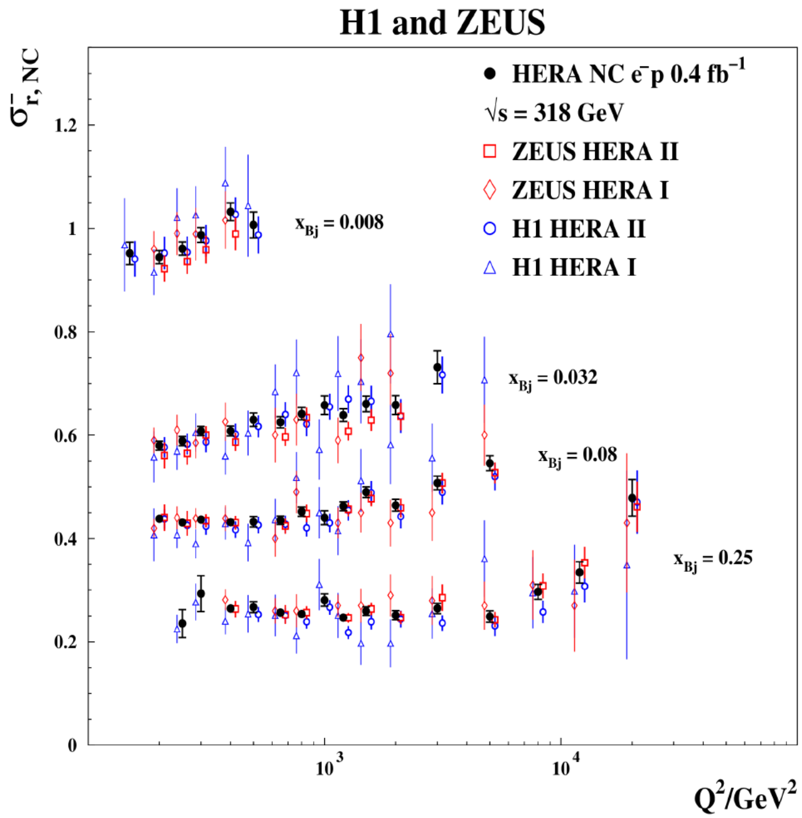


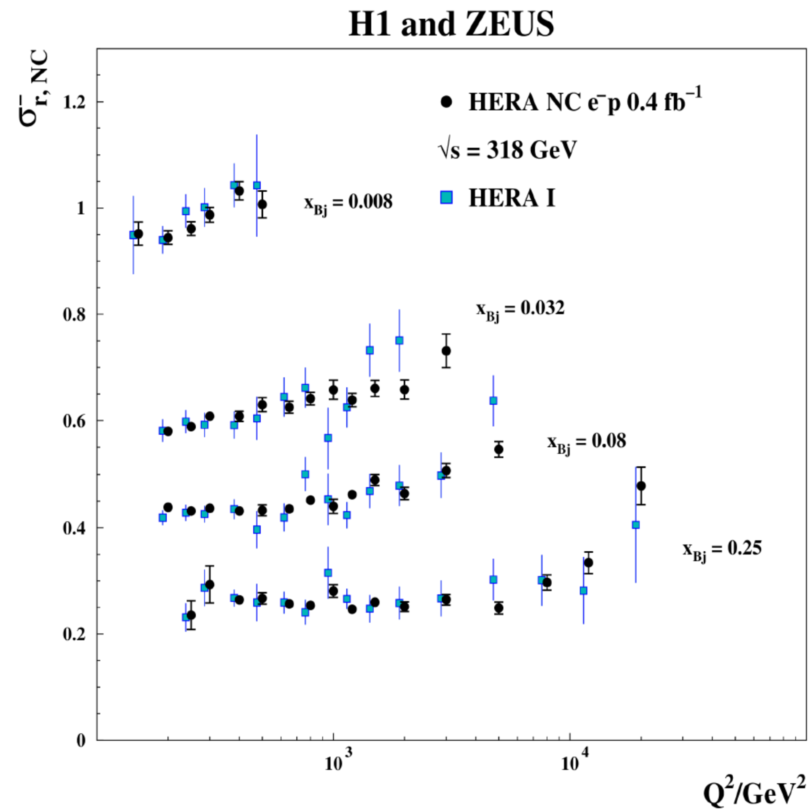


Makes HERAPDF PDFS more precise, but in general a bit further from other PDFs in some places, e.g high-$x$ up quark.

# HERA II Combined data in other PDFs

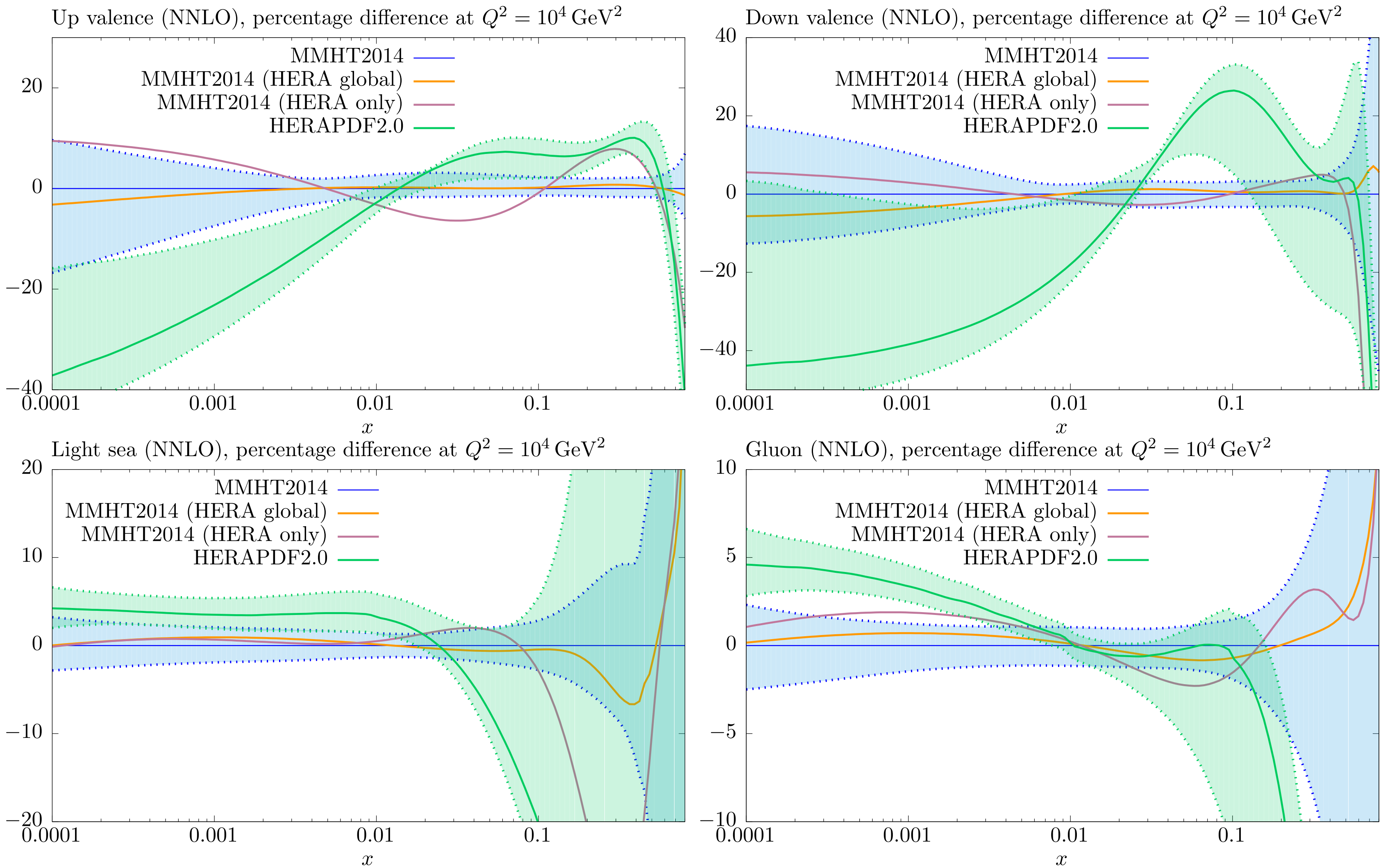


Updated PDFs very well within MMHT2014 uncertainties. PDFs from HERA II data only fit in some ways similar to HERAPDF2.0.

# Comparison PDFs in late 2015 - time of latest combination

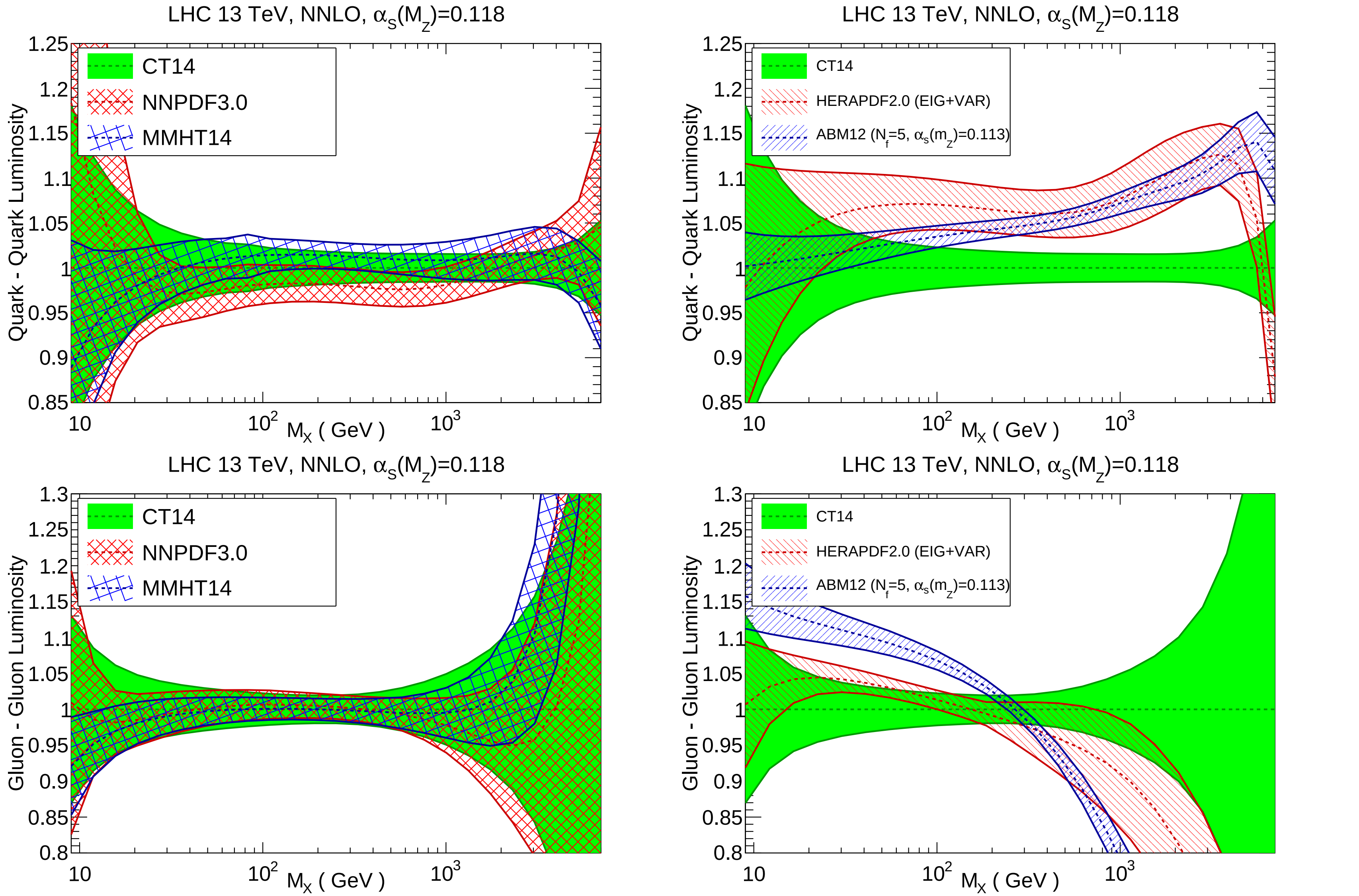


Some good agreement between CT14, MMHT2014 and NNPDF3.0.

Some differences in some PDF sets in central values and uncertainty.

# Comparison of Combination of CT, MMHT, NNPDF using "Monte Carlo" sets to the Individual PDFs

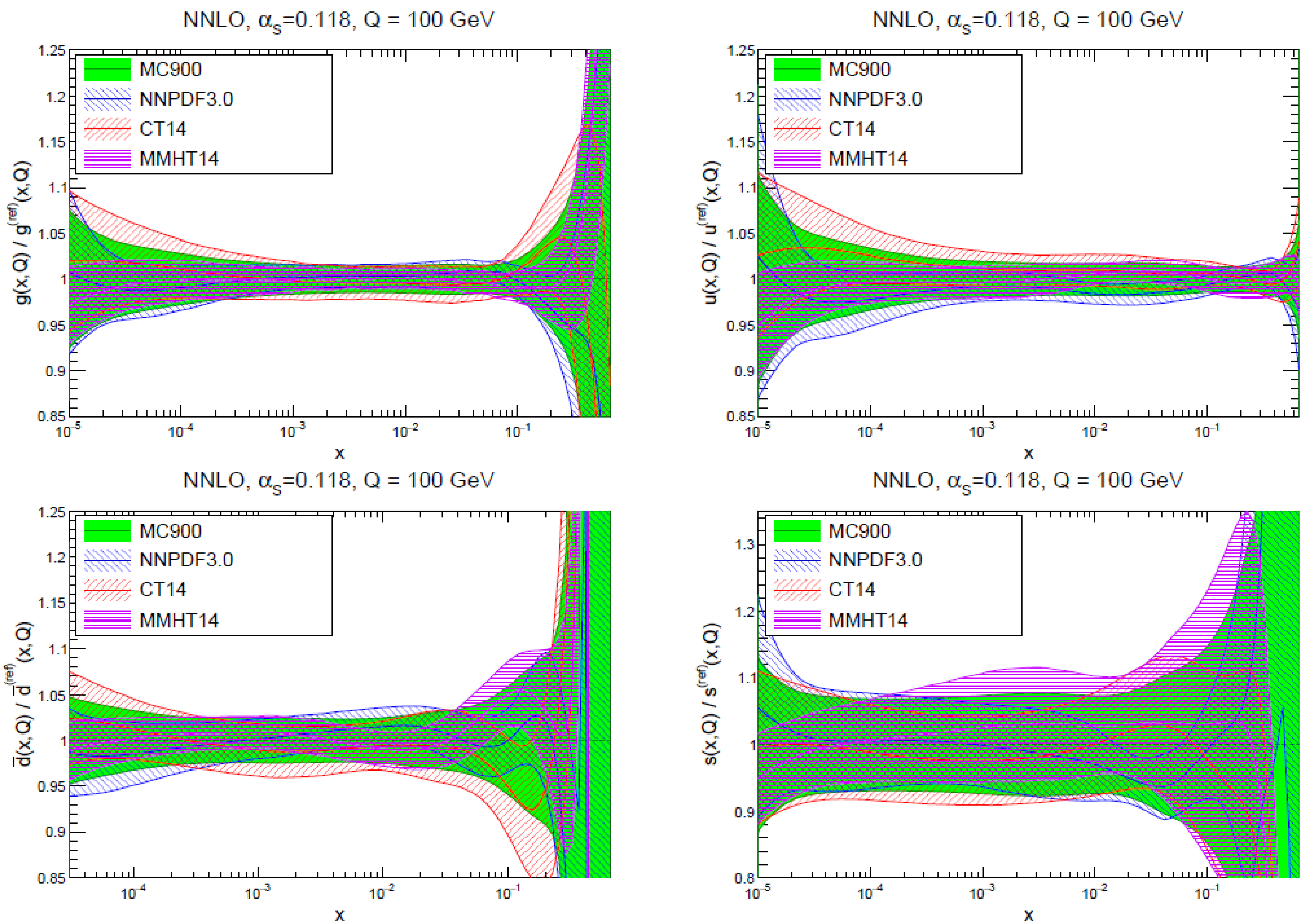


Works well if PDFs are fairly compatible.

# PDF fit framework

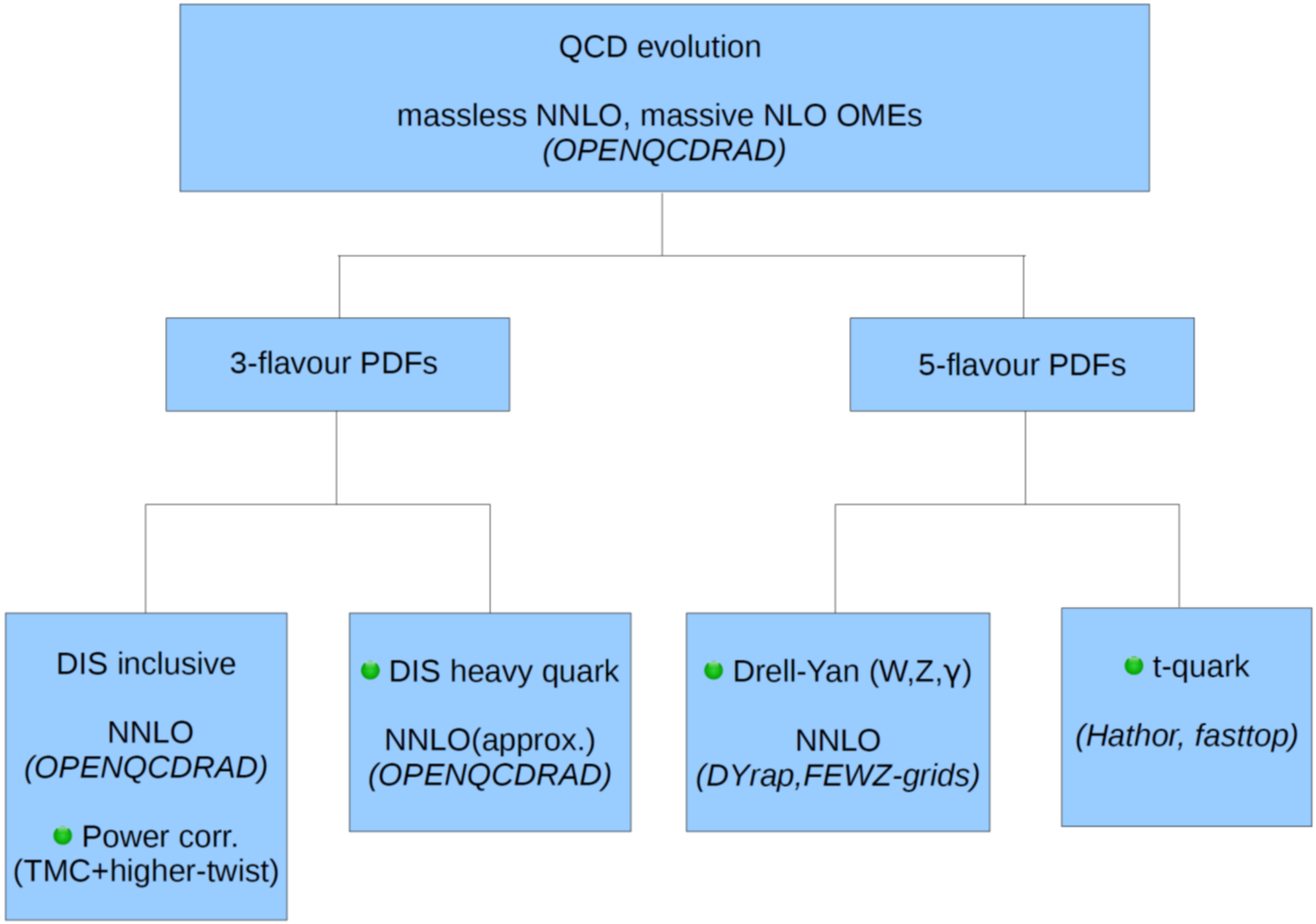


Alekhin DIS 2019

# ABMP16 PDFs – impact at high $x$ from LHC and Tevatron data.

## Impact of the forward Drell-Yan data

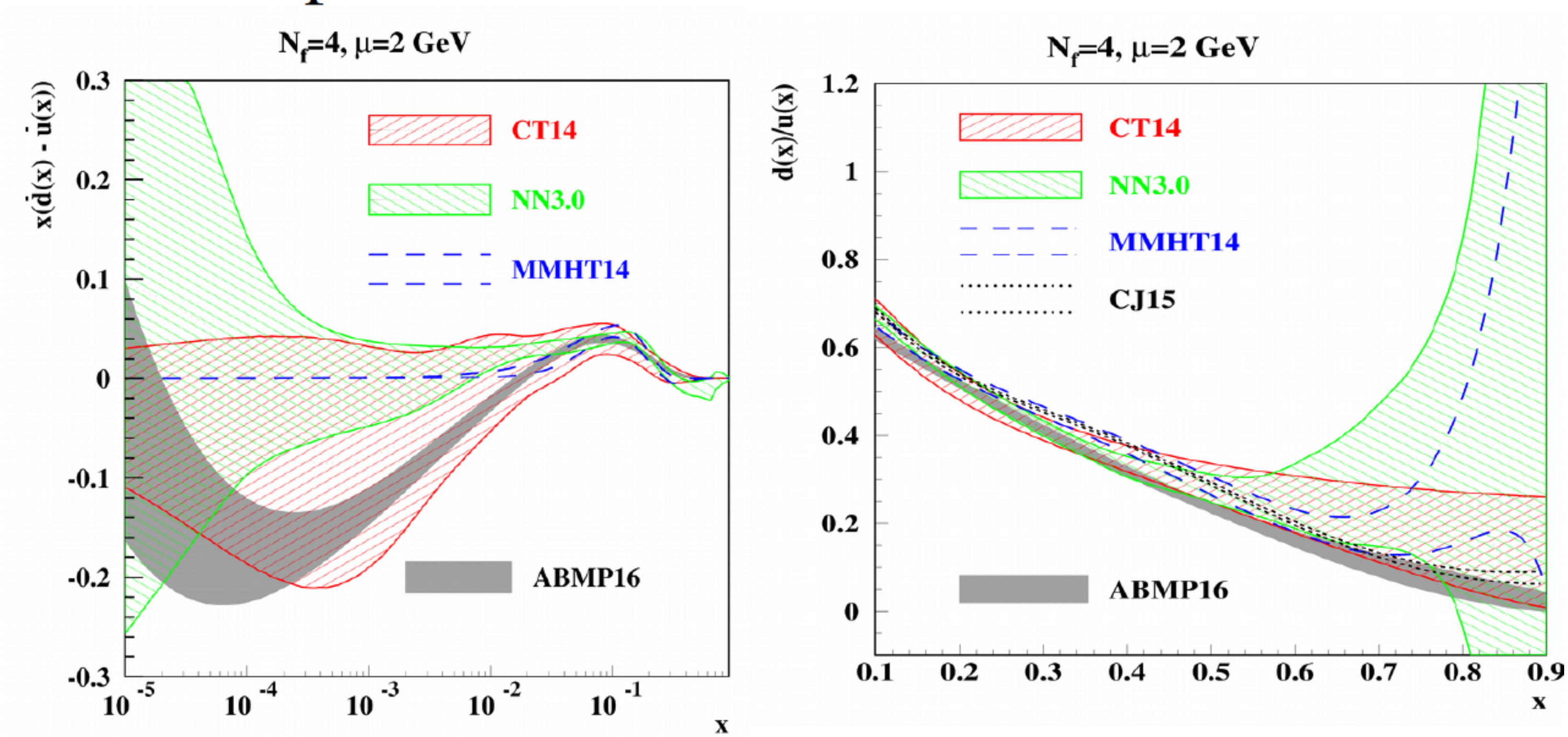


- Relaxed form of the sea iso-spin asymmetry I(x) at small x; Regge-like behaviour is recovered only at $x \sim 10^{-6}$; at large x it is still defined by the phase-space constraint
- Good constraint on the d/u ratio w/o deuteron data → independent extraction of the deuteron corrections **Accardi, Brady, Melnitchouk, Owens, Sato hep-ph/1602.03154;**
- Big spread between different PDF sets, up to factor of 30 at large x → poor control of the background to BSM effects without constraints from the DY data

# CJ15 PDFs – simultaneous study of precision proton and deuteron data fit/verify deuteron corrections.

## NUCL / HEP symbiosis

| Observable | Experiment | # points | $\chi^2$ LO | $\chi^2$ NLO | $\chi^2$ NLO (OCS) | $\chi^2$ NLO (no nucl) |
|---|---|---|---|---|---|---|
| DIS $F_2$ | BCDMS ($p$) [81] | 351 | 430 | **438** | 436 | 440 |
| | BCDMS ($d$) [81] | 254 | 297 | **292** | 289 | 301 |
| | SLAC ($p$) [82] | 564 | 488 | **434** | 435 | 441 |
| | SLAC ($d$) [82] | 582 | 396 | **376** | 380 | 507 |
| DIS $F_2$ tagged | Jefferson Lab ($n/d$) [21] | 191 | 218 | **214** | 213 | 219 |
| $W$/charge asymmetry | CDF ($e$) [88] | 11 | 11 | **12** | 12 | 13 |
| | DØ ($\mu$) [17] | 10 | 37 | **20** | 19 | 29 |
| | DØ ($e$) [18] | 13 | 20 | **29** | 29 | 14 |
| | CDF ($W$) [89] | 13 | 16 | **16** | 16 | 14 |
| | DØ ($W$) [19] | 14 | 39 | **14** | 15 | 82 |
| $Z$ rapidity | CDF ($Z$) [90] | 28 | 100 | **27** | 27 | 26 |

- Ignoring nuclear dynamics, SLAC(d) and D0(W) pull d quark in opposite directions
  - **D0 (W) data determine nuclear corrections !!**
  - other asymmetries inconclusive by themselves
  - **BONUS data validate DO(W) analysis**

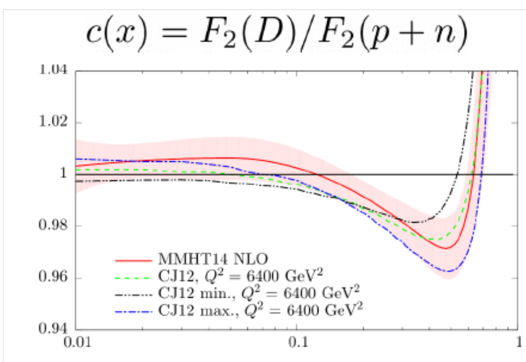


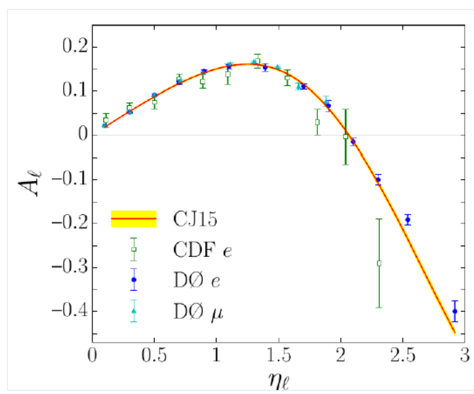


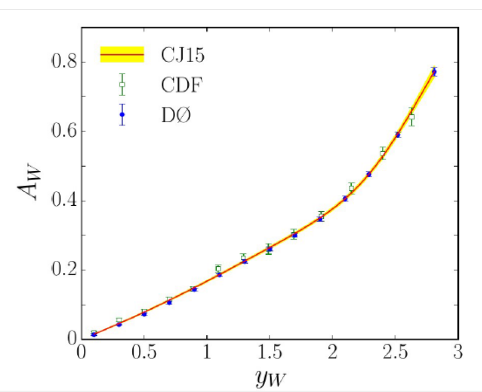

# NNPDF3.1 recently released.

## New datasets in NNPDF3.1

| Measurement | Data taking | Motivation |
|---|---|---|
| Combined HERA inclusive data | Run I+II | quark singlet and gluon |
| D0 legacy W asymmetries | Run II | quark flavor separation |
| ATLAS inclusive W, Z rap 7 TeV | 2011 | strangeness |
| ATLAS inclusive jets 7 TeV | 2011 | large-$x$ gluon |
| ATLAS low-mass Drell-Yan 7 TeV | 2010+2011 | small-$x$ quarks |
| ATLAS Z pT 7,8 TeV | 2011+2012 | medium-$x$ gluon and quarks |
| ATLAS and CMS tt differential 8 TeV | 2012 | large-$x$ gluon |
| CMS Z (pT,y) 2D xsecs 8 TeV | 2012 | medium-$x$ gluon and quarks |
| CMS Drell-Yan low+high mass 8 TeV | 2012 | small-$x$ and large-$x$ quarks |
| CMS W asymmetry 8 TeV | 2012 | quark flavor separation |
| CMS 2.76 TeV jets | 2012 | medium and large-$x$ gluon |
| LHCb W,Z rapidity dists 7 TeV | 2011 | large-$x$ quarks |
| LHCb W,Z rapidity dists 8 TeV | 2012 | large-$x$ quarks |

4 Juan Rojo DIS2017, Birmingham, 04/04/2017

Rojo DIS2017

# Theory developments

## Charm content of proton revisited

- The new LHC experiments provide additional constraints on **non-perturbative charm**
- Including the EMC charm data, we find **evidence for non-perturbative charm at the 1.5 sigma level.** Even without EMC data, **non-perturbative charm bounded < 1.0 % at the 90% CL**

$$[C(Q^2)] \equiv \int_0^1 dx\ \left(xc(x,Q^2) + x\bar{c}(x,Q^2)\right)$$

| PDF set | $C(Q = 1.65\ \mathrm{GeV})$ | $C(Q = 100\ \mathrm{GeV})$ |
|---|---|---|
| Perturbative charm | $(0.360 \pm 0.007)\%$ | $(3.77 \pm 0.02)\%$ |
| Fitted charm | $(0.45 \pm 0.40)\%$ | $(3.8 \pm 0.2)\%$ |
| Fitted charm with EMC data | $(0.52 \pm 0.14)\%$ | $(3.86 \pm 0.08)\%$ |

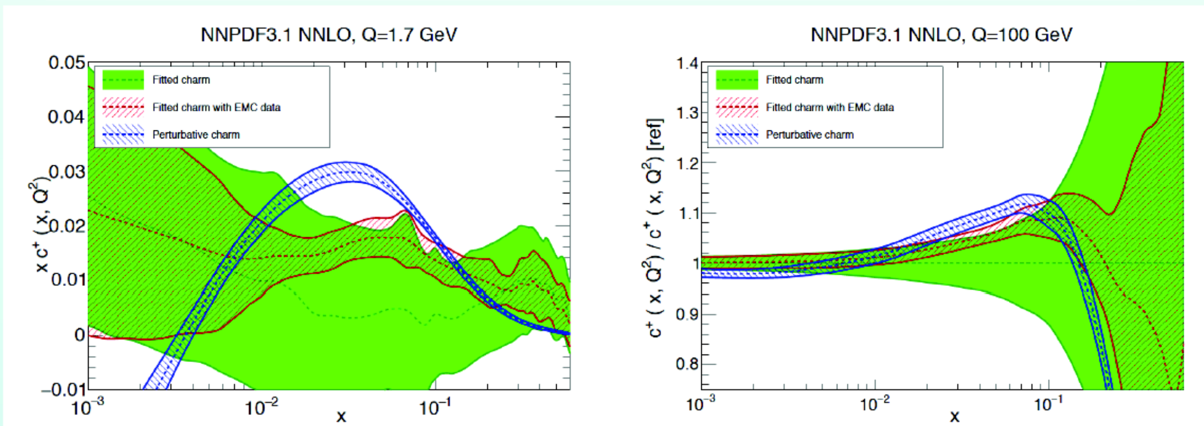


2

LHC $W, Z$ data prefer lower charm for $0.01 < x < 0.1$.

Rojo, DIS 2017

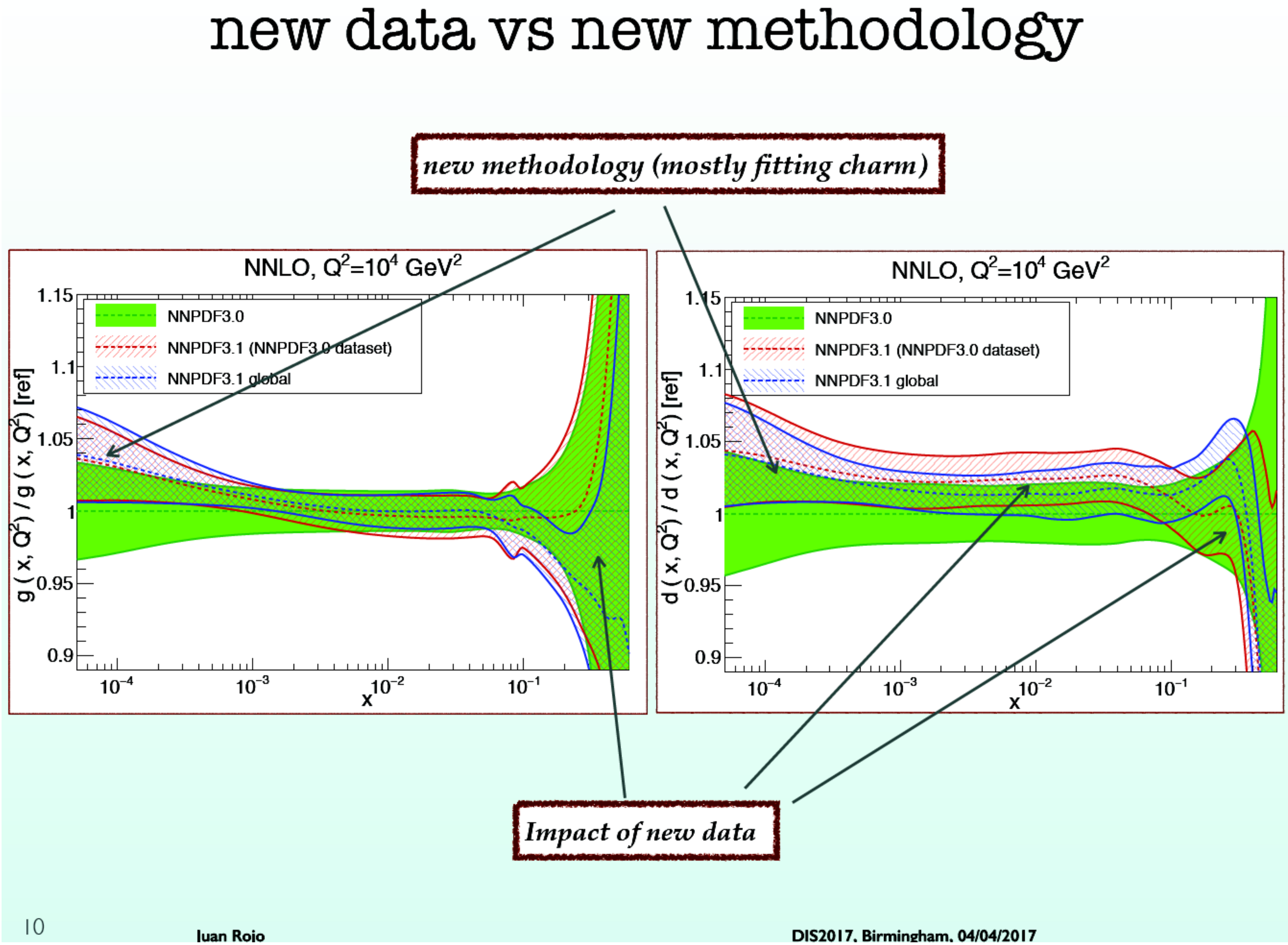


New methodology more significant.

# Higgs production cross-sections

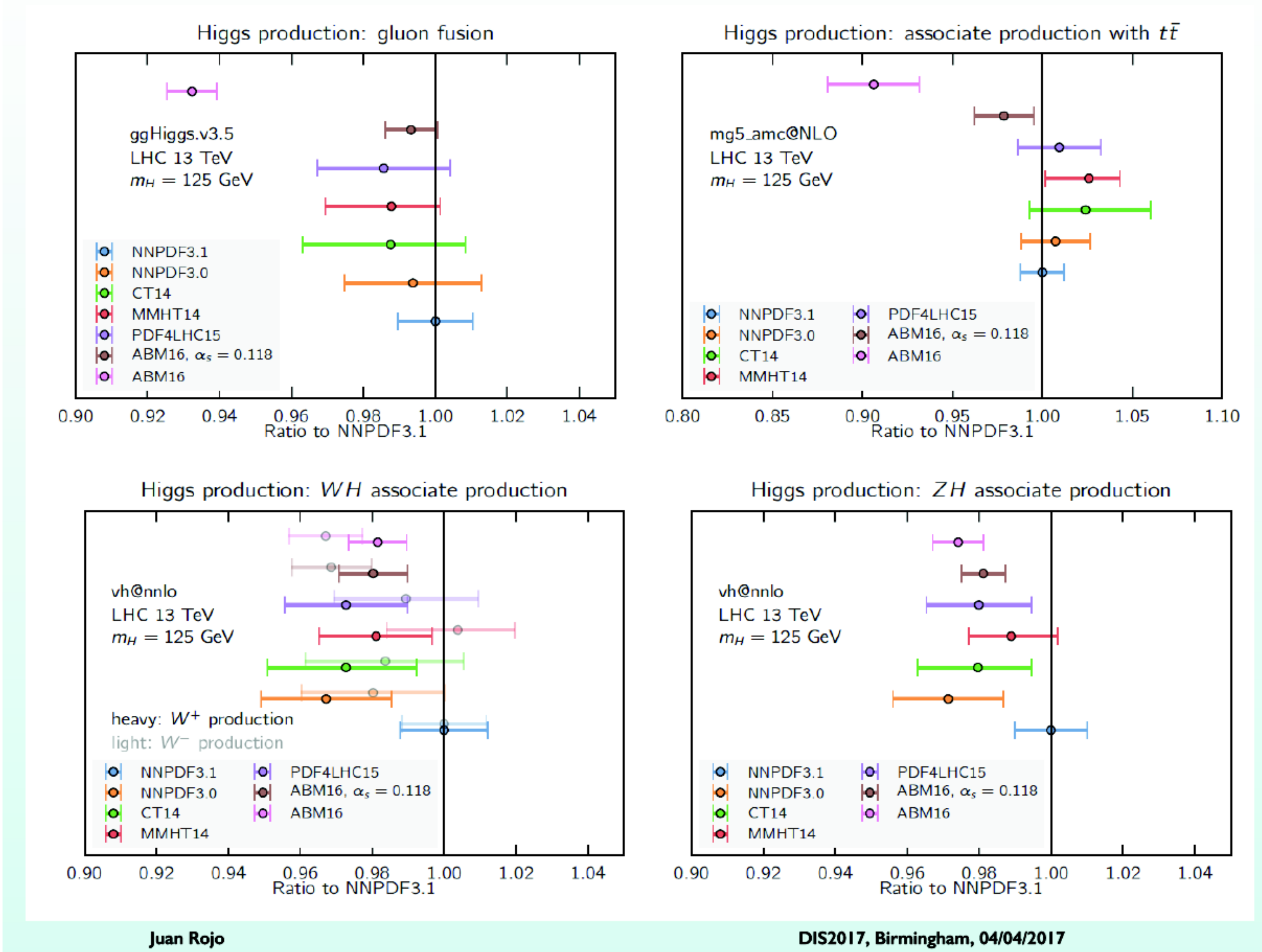


Some impact on cross sections.

# CT18 results

## 1. New LHC datasets for CT18

1. 245 1505.07024 LHCb Z (W) muon rapidity at 7 TeV(applgrid)
2. 246 1503.00963 LHCb 8 TeV Z rapidity (applgrid);
3. 249 1603.01803 CMS W lepton asymmetry at 8 TeV (applgrid)
4. 250 1511.08039 LHCb Z (W) muon rapidity at 8 TeV(applgrid)
5. 253 1512.02192 ATLAS 7 TeV Z pT (applgrid)
6. 542 1406.0324 CMS incl. jet at 7 TeV with R=0.7 (fastNLO)
7. 544 1410.8857 ATLAS incl. jet at 7 TeV with R=0.6 (applgrid)
8. 545 1609.05331 CMS incl. jet at 8 TeV with R=0.7 (fastNLO)
9. 580 1511.04716 ATLAS 8 TeV tT pT and mtT diff. distributions (fastNNLO)
10. 573 1703.01630 CMS 8 TeV tT (pT , yt ) double diff. distributions (fastNNLO)

11. 248 1612.03016 ATLAS 7 TeV Z and W rapidity (applgrid)->CT18Z
- also uses a special small-x factorization scale, charm mass $m_c$=1.4 GeV
- serious changes in PDFs, so warrants a separate PDF

2018-04-09 P. Nadolsky, DIS'2019 workshop, Torino 4

Two different sets proposed – one with precision ATLAS $W, Z$ data.

# Data has now filled in a lot of the $x - Q^2$ plane.

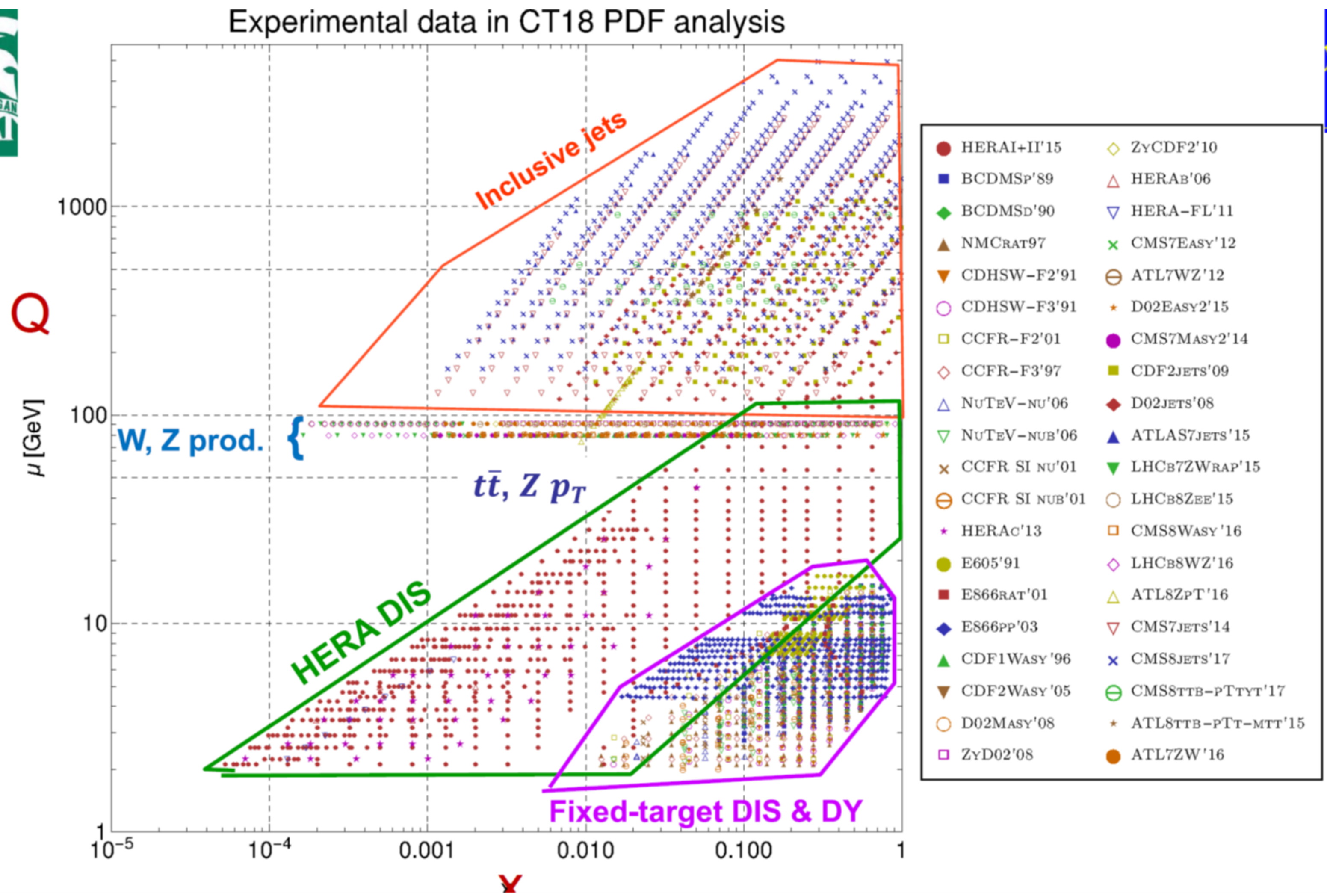


Yuan DIS 2019

# Sensitivity of hadronic experiments to PDFs

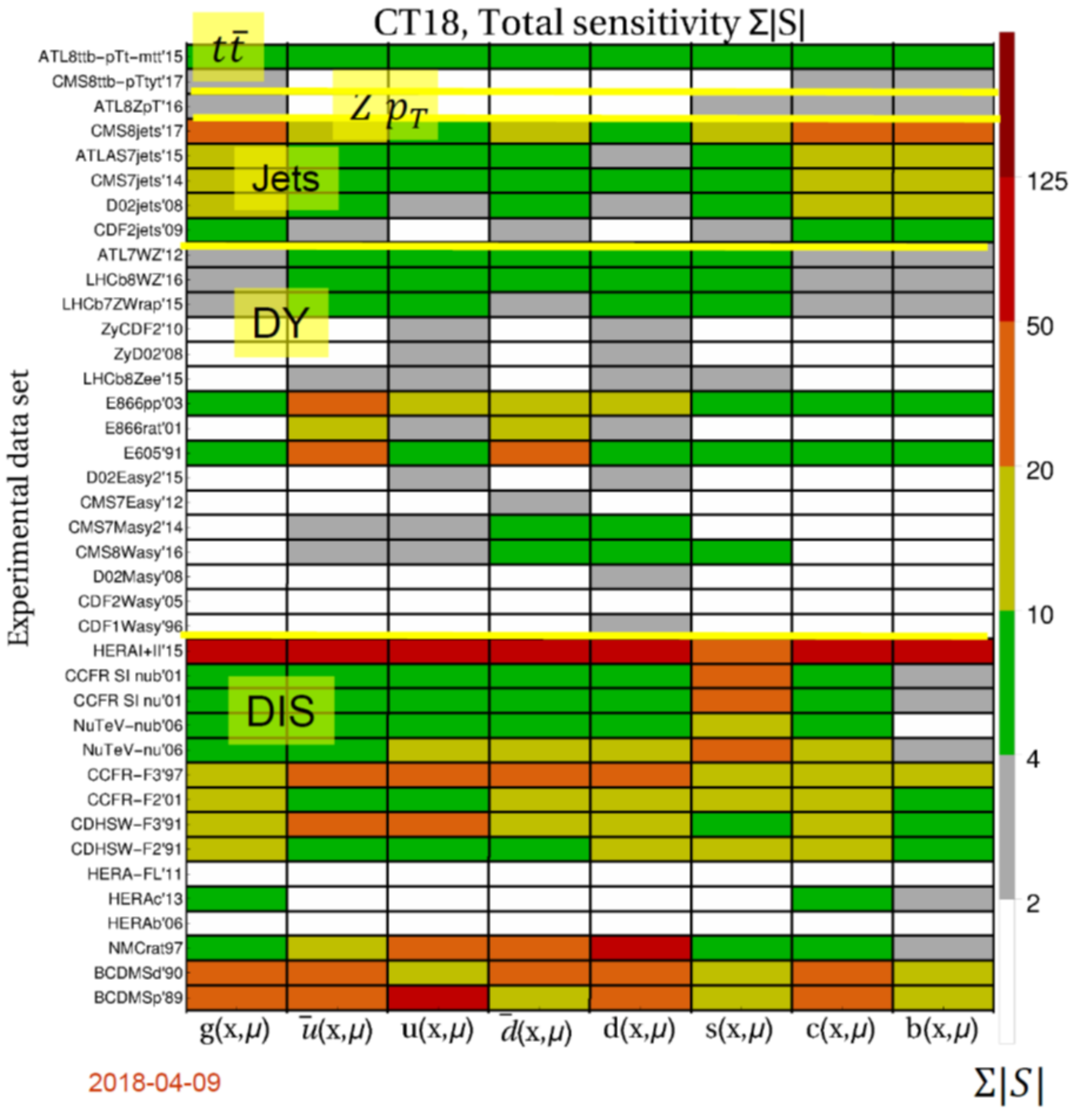


Total sensitivity to $f_a(x_i, \mu_i)$ , **summed over data points**

$$\sum_{points} |S_{f,i}|$$

Computed using the **PDFSense** code **[arXiv:0803.02777]**

2018-04-09 10

# PDF Luminosities at 13 TeV LHC
# CT18, MMHT14 and NNPDF3.1



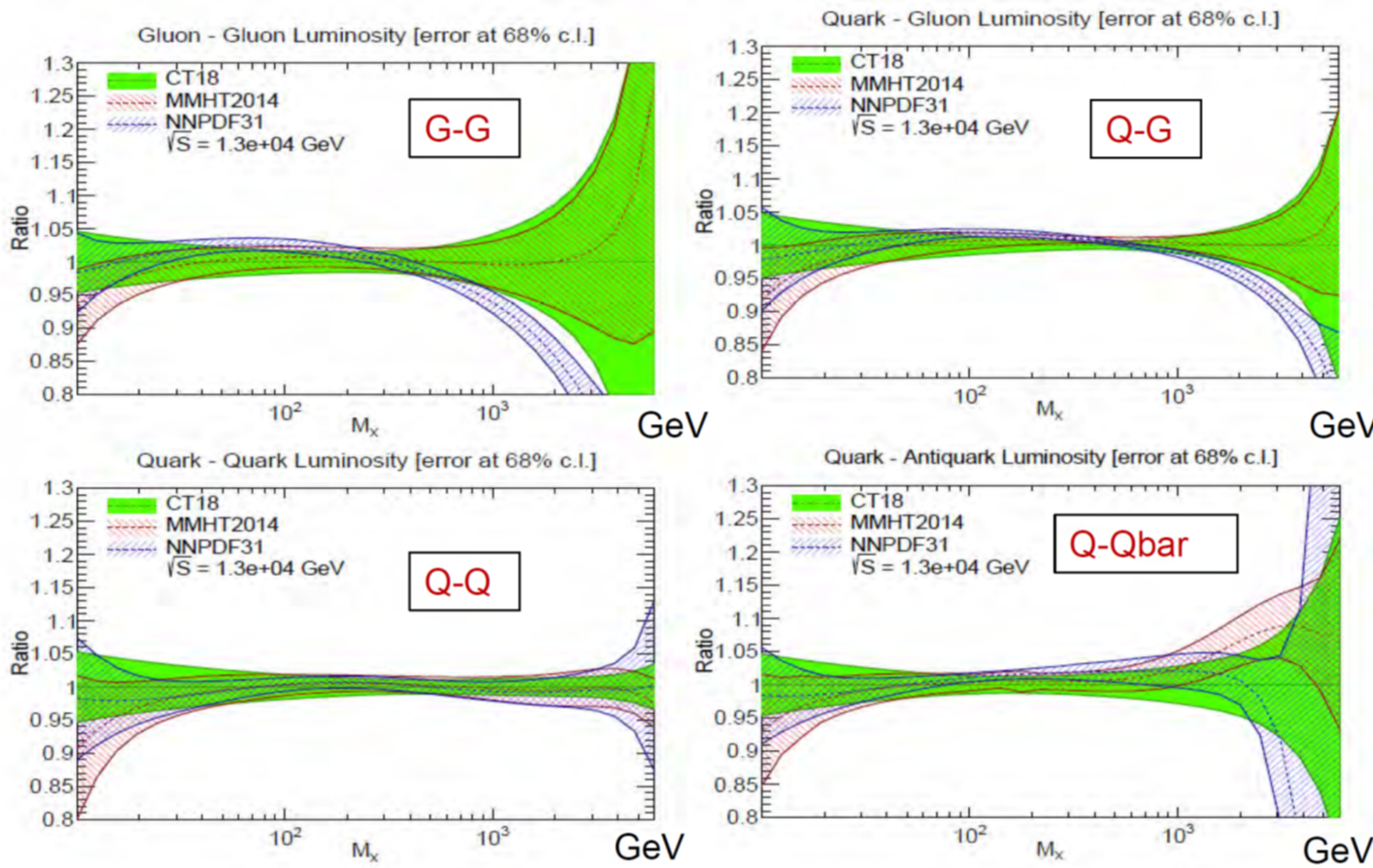


PDF errors at 68% CL

Quarks now in better agreement, but gluons worse.

Yuan DIS 2019

# CT18 (CT18Z) NNLO

13 (14) new LHC experiments with 665 (711) data points

- New LHC experiments tend to have larger $S_n$
- ATLAS 7 TeV $Z, W$ production has $S_n \approx 5.2$, included in CT18Z fit only

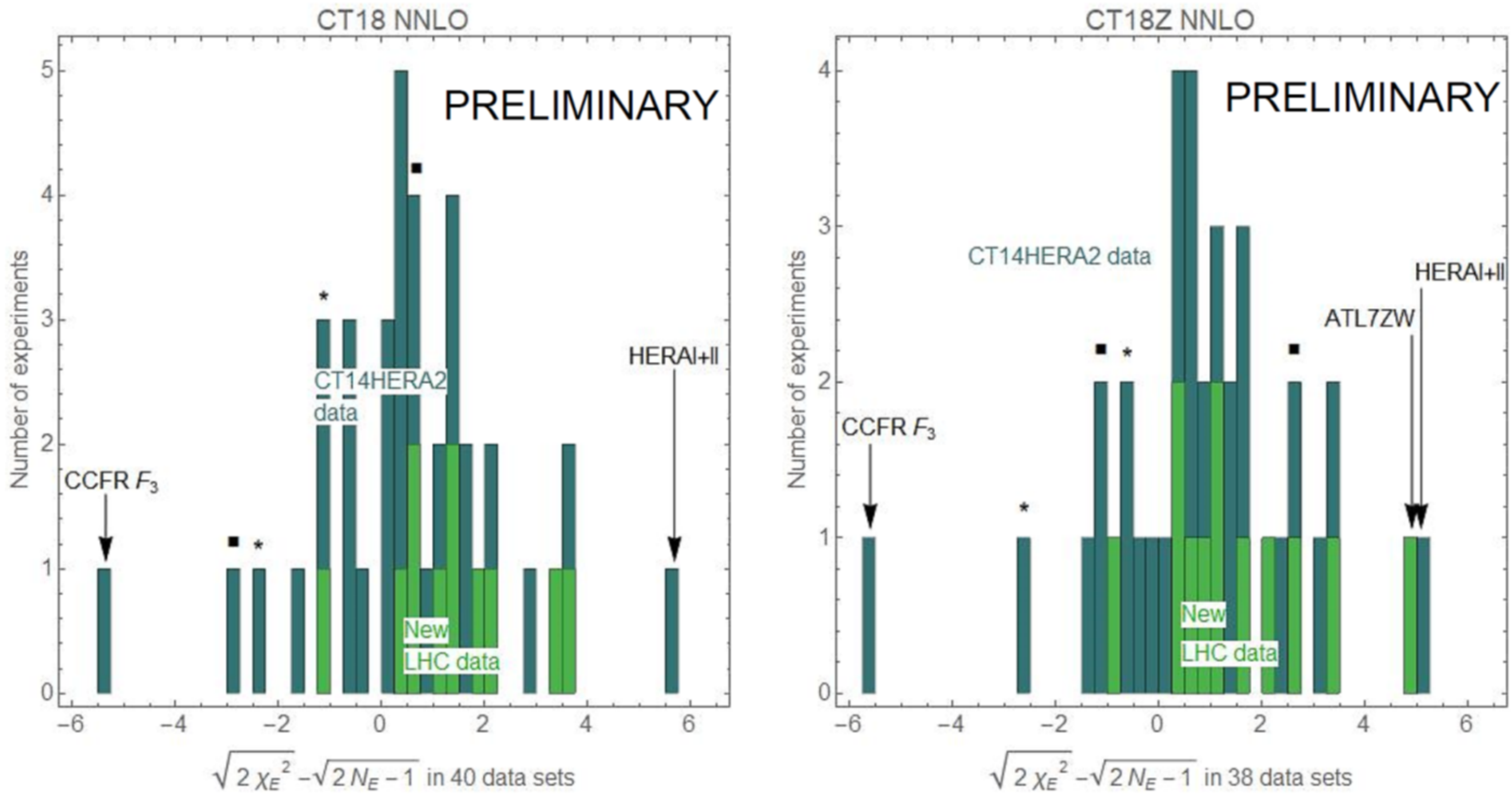


2018-04-09 P. Nadolsky, DIS'2019 workshop, Torino 19

Degree of inconsistency between data sets $\rightarrow$ tolerance in $\Delta\chi^2$.

Some differences between alternative sets.

# CT18Z vs.CT18 PDFs

u and d increase at small-x

s increases at small-x

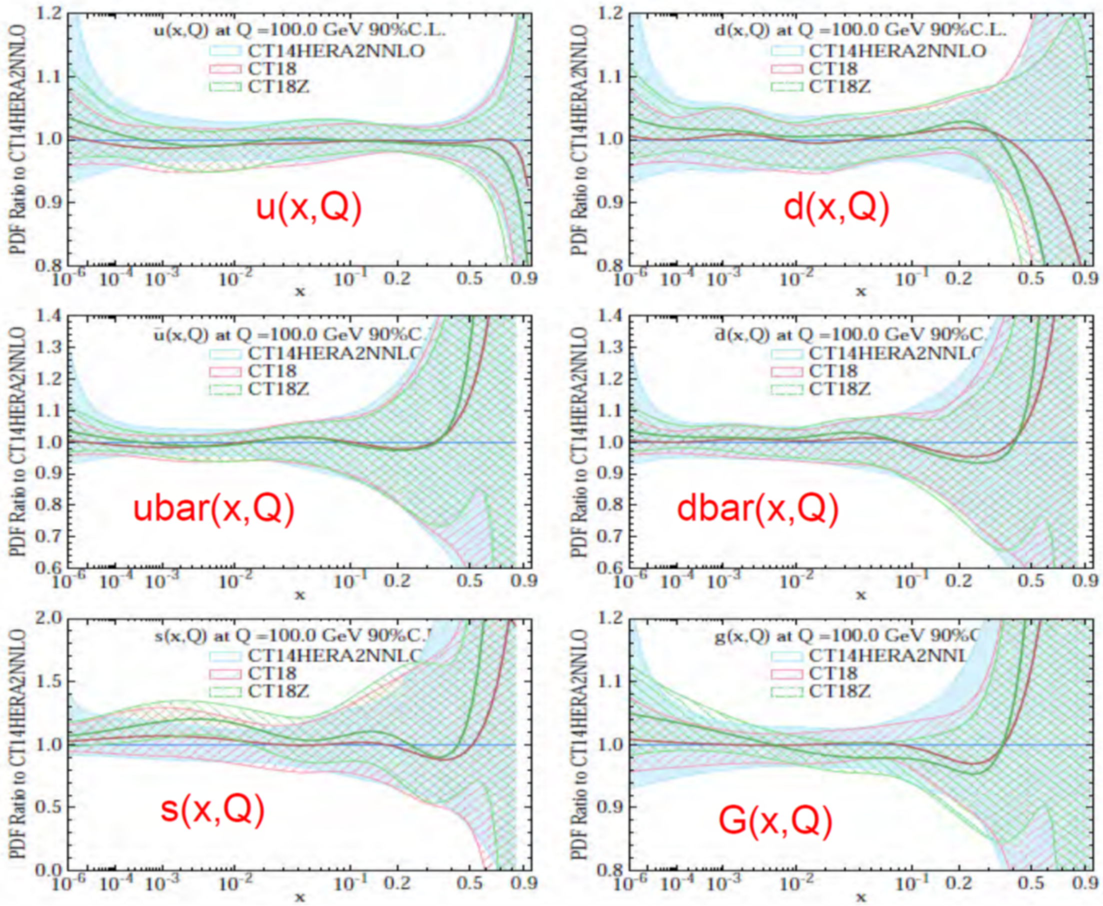


d increases at $x \sim 0.2 - 0.3$

Q=100 GeV; at 90%CL

G increases at small-x, and decreases at $x \sim 0.01 - 0.3$

Yuan DIS 2019

## MMHT preliminary set (2016) - fit to new hadron collider data

Fit new LHCb data at $7$ and $8\ \mathrm{TeV}$, $W + c$ jets from CMS, CMS $W^{+,-}$ data, and also the final $e$ asymmetry data from D0.

| | no. points | NLO $\chi^2_{pred}$ | NLO $\chi^2_{new}$ | NNLO $\chi^2_{pred}$ | NNLO $\chi^2_{new}$ |
|---|---|---|---|---|---|
| $\sigma_{t\bar{t}}$ Tevatron +CMS+ATLAS | 18 | 19.6 | 20.5 | 14.7 | 15.5 |
| LHCb 7 TeV $W+Z$ | 33 | 50.1 | 45.4 | 46.5 | 42.9 |
| LHCb 8 TeV $W+Z$ | 34 | 77.0 | 58.9 | 62.6 | 59.0 |
| LHCb 8TeV $e$ | 17 | 37.4 | 33.4 | 30.3 | 28.9 |
| CMS 8 TeV $W$ | 22 | 32.6 | 18.6 | 34.9 | 20.5 |
| CMS 7 TeV $W+c$ | 10 | 8.5 | 10.0 | 8.7 | 8.0 |
| D0 $e$ asymmetry | 13 | 22.2 | 21.5 | 27.3 | 25.8 |
| total | 3738/3405 | 4375.9 | 4336.1 | 3741.5 | 3723.7 |

Predictions good, and no real tension with other data when refitting, i.e. changes in PDFs relatively small, mainly in $d_V(x,Q^2)$.

$\Delta\chi^2 < 10$ for the remainder of the data at NLO and NNLO.

Some reduction in details of flavour decomposition uncertainties, e.g. low-$x$ valence quarks.

# Recent extremely high precision data on $W, Z$ from ATLAS

## Differential $W \to \ell\nu$ Measurements

- shape of differential $W$ cross sections generally well described
- particularly good description of the differential lepton charge asymmetry $A_\ell$
- differences in PDF sets seen in the overall normalisation
- a precise measurement of the absolute cross section provides valuable information despite larger uncertainties

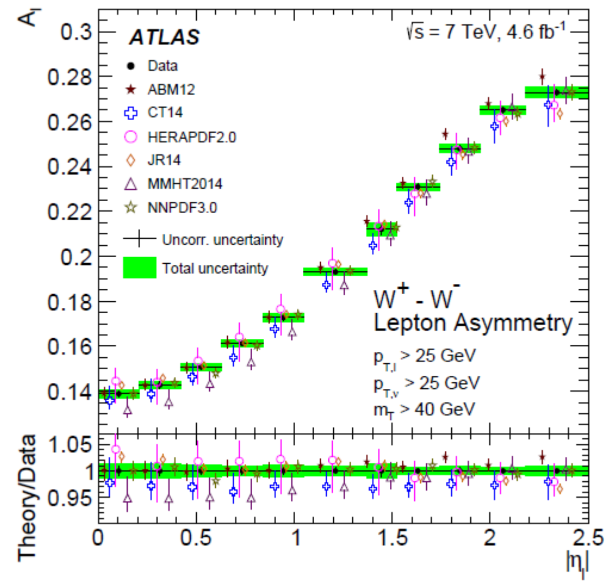


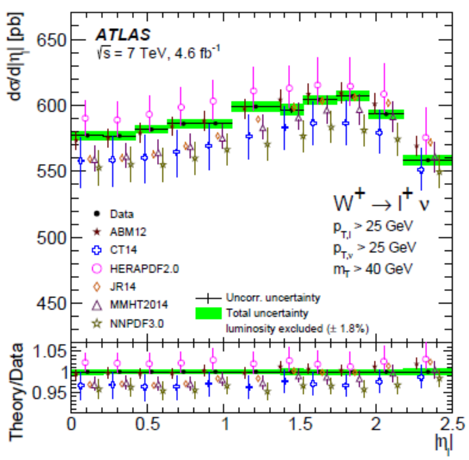


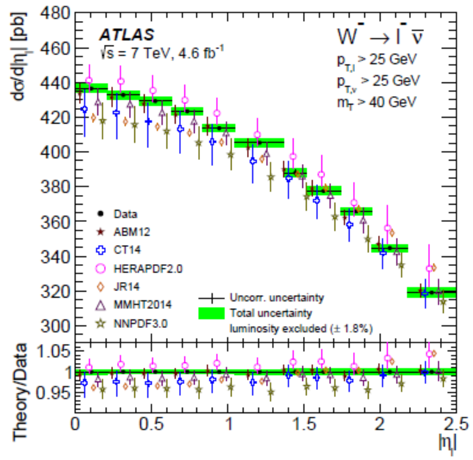


Sommer DIS2017

# Differential $Z \to \ell\ell$ Measurements

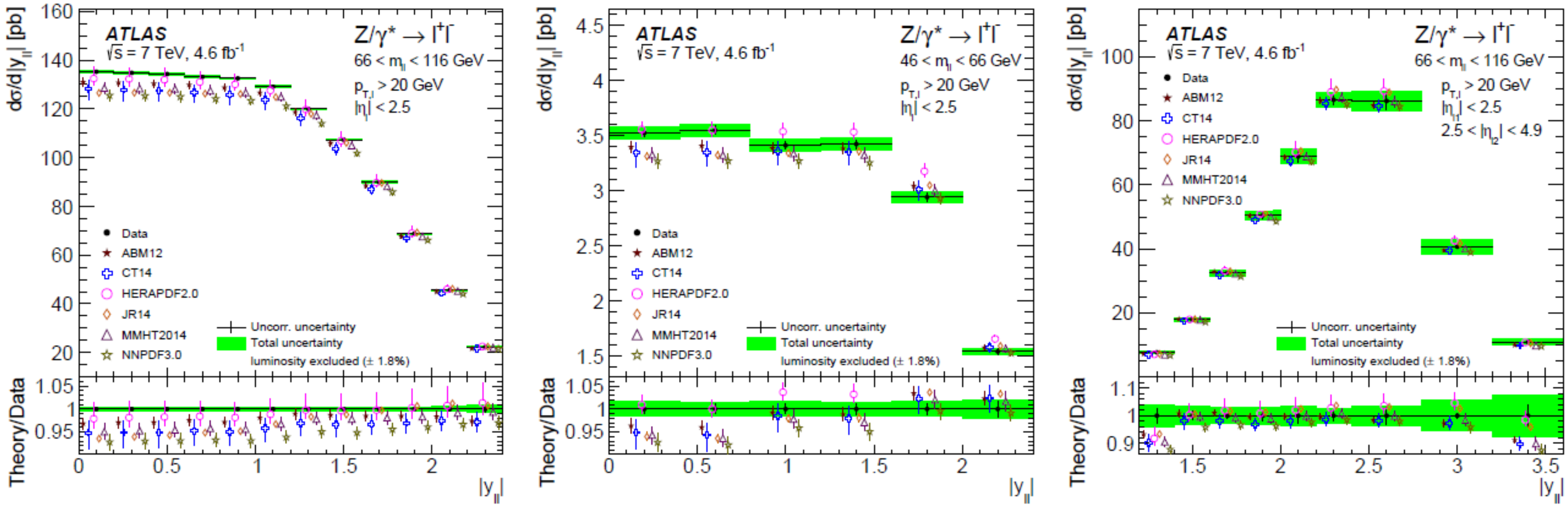


- differences in the rapidity dependence between data and theoretical predictions

Fixed by increase in strange quark fraction in ATLAS study.

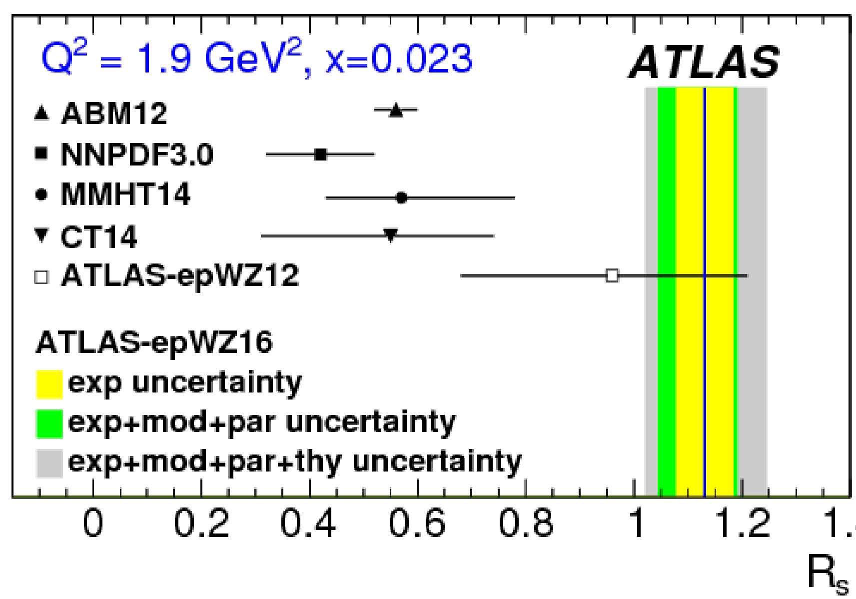

## Studied by NNPDF - smaller strange enhancement.

| PDF set | $R_s(x = 0.023, Q = 1.65$ GeV$)$ | $R_s(x = 0.013, Q = M_Z)$ |
|---|---|---|
| NNPDF3.0 | 0.47±0.09 | 0.79±0.04 |
| NNPDF3.1 | 0.62±0.12 | 0.83±0.05 |
| NNPDF3.1 collider-only | 0.86±0.17 | 0.94±0.07 |
| NNPDF3.1 HERA + ATLAS $W, Z$ | 0.96±0.20 | 0.98±0.09 |
| ATLAS $W, Z$ 2011 `xFitter` (Ref. [93]) | $1.13^{+0.11}_{-0.11}$ | - |
| ATLAS $W, Z$ 2010 `HERAfitter` (Ref. [120]) | $1.00^{+0.25}_{-0.28}$ (*) | $1.00^{+0.09}_{-0.10}$ (*) |

- **Confirmed the strange symmetric fit** preferred by the ATLAS W,Z 2011 measurements, though we find PDF uncertainties larger by a factor 2

- The **global fit** accommodates both the neutrino data and the ATLAS W,Z 2011 ( $\chi^2_{nutev}$**=1.1,** $\chi^2_{AWZ11}$**=2.1** ) finding a compromise value for **R$_S$=0.62+-0.12**

- **Mild tension** in the global fit (1.5-sigma level at most) when simultaneously included neutrino data, CMS W+charm and ATLAS W,Z 2010+2011

$\sigma_W \propto c\bar{s}$, $\sigma_Z \propto g_s * s\bar{s} + g_c * c\bar{c}$, where $g_s > g_c$.

Smaller strange correlated with smaller charm, i.e. $\sigma_Z/\sigma_W$ rises with smaller charm.

Improved fit to older ATLAS $W, Z$ data with larger $m_c$ evident in MMHT2014. Usually interplay with fitting HERA data.

# Updates in ATLAS Analysis – $W+$ jet.

## Including new data in a new fit …

- So far ATLAS has produced several fits using inclusive W and Z data†
  - ATLAS epWZ 12 (2010 data, 7 TeV 35 pb$^{-1}$)
  - ATLAS epWZ 16 (2010 data, 7 TeV 4.6 fb$^{-1}$)
  - ATLAS epWZ top 18 - with fully differential top data data to stabilise the gluon - **see Francesco's presentation tomorrow**

- Starting point for the new fit is the inclusive W, ATLAS data used in the the ATLAS epWZ16 fit plus the new W + jets data at 8 TeV from [JHEP 05 (2018) 077]

## W+jet production at 8 TeV data

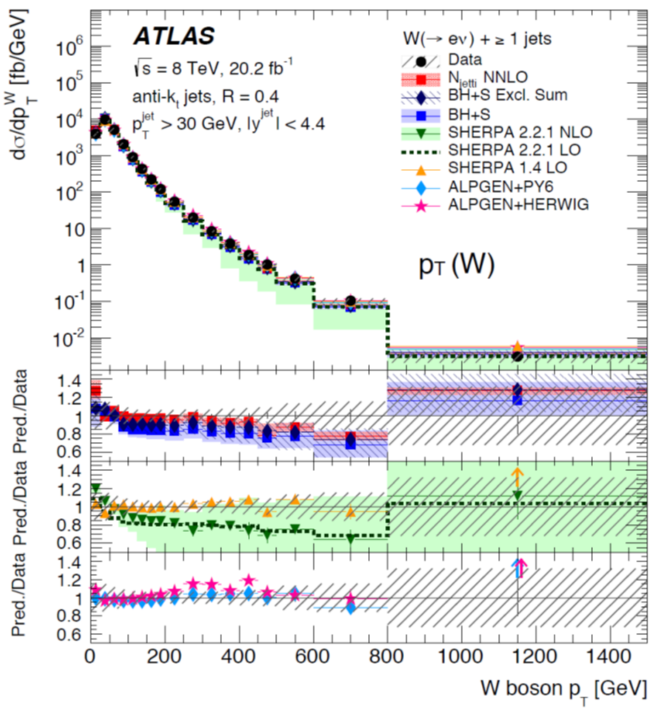


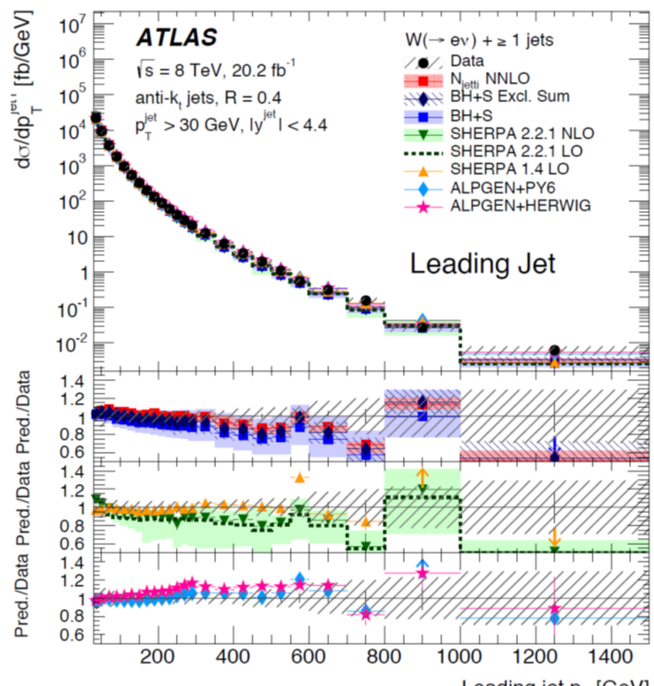


- [JHEP 05 (2018) 077]

- Multiple distributions
  - $P_T(W)$, $P_T$(leading jet)
  - Unfortunately, correlations between different spectra not available, so unable to fit distributions simultaneously

M Sutton - The proton PDF including W+jet data at ATLAS

8

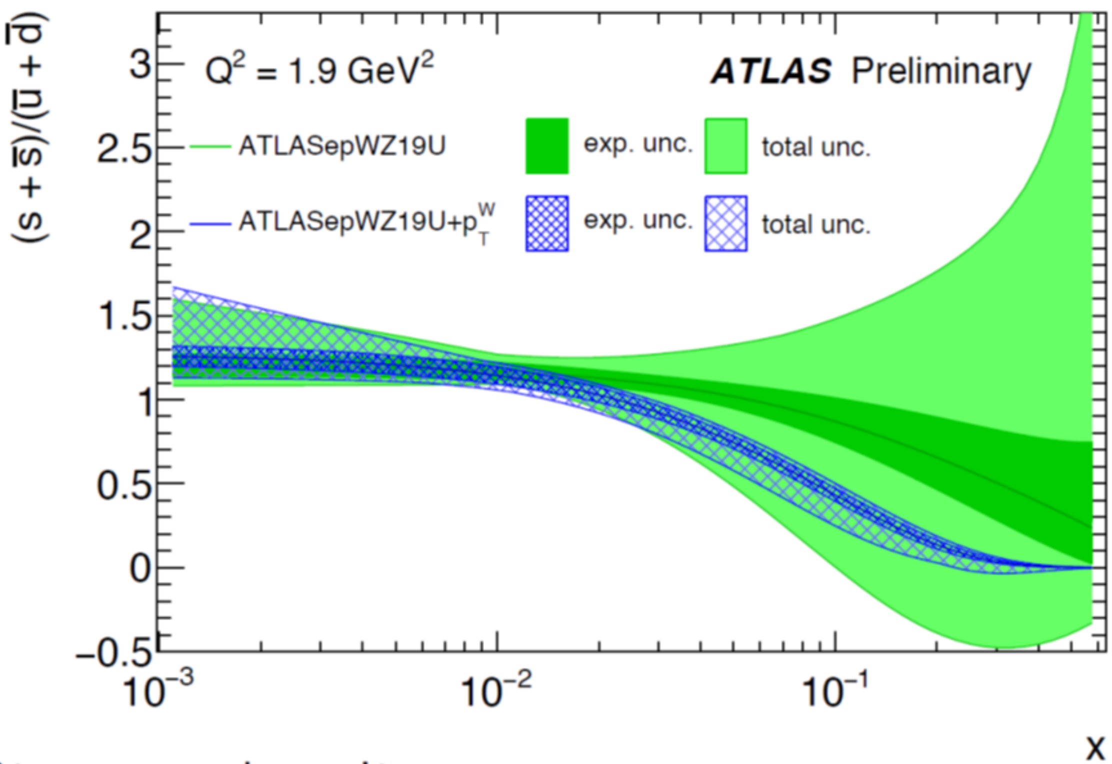


# Strange density

- Fit to epWZ uncombined data with larger error consistent with new epWZ fit with W $P_T$
- W+ jets fits with PT(W) and PT(leading jet) are themselves consistent
- Including the W + jet data reduces the strange density at higher-x

- Still consistent with enhanced strange at low-x

M Sutton - The proton PDF including W+jet data at ATLAS studies.

## **MMHT – updated fits also with high precision ATLAS W, Z data.**

Including ATLAS W, Z data in fit goes from $\chi^2/N_{pts} \sim 387/61 \to \chi^2/N_{pts} \sim 108/61$.

Deterioration in fit to other data $\Delta\chi^2 \sim 54$. CMS double differential $Z/\gamma$, CCFR/NuTeV dimuon data, Drell-Yan asymmetry.

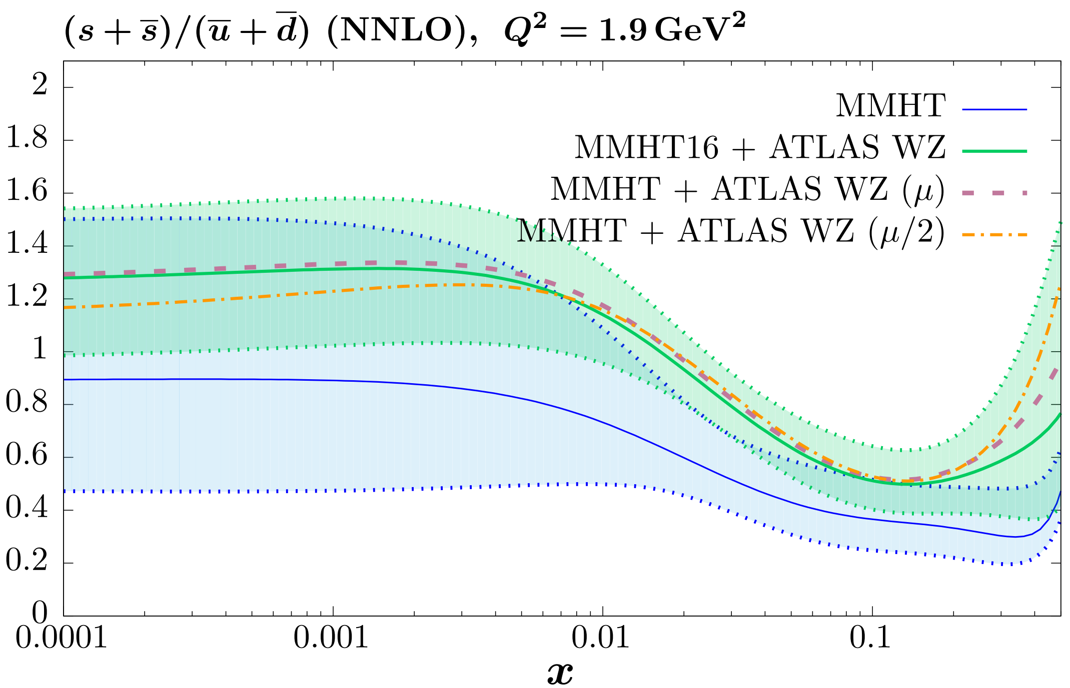


$(s+\bar{s})/(\bar{u}+\bar{d})$, i.e. $R_s$ at $Q^2 = 1.9\ \mathrm{GeV}^2$.

At $x = 0.023$ $R_s \sim 0.83 \pm 0.15$. Compare to ATLAS with $R_s = 1.13^{+0.08}_{-0.13}$

Details of tension of $W, Z$ data may be mitigated by NNLO corrections to dimuon production (Phys. Rev. Lett. 116 (2016), Berger *et al.*, J. Gao, `arXiv:1710.04258`).

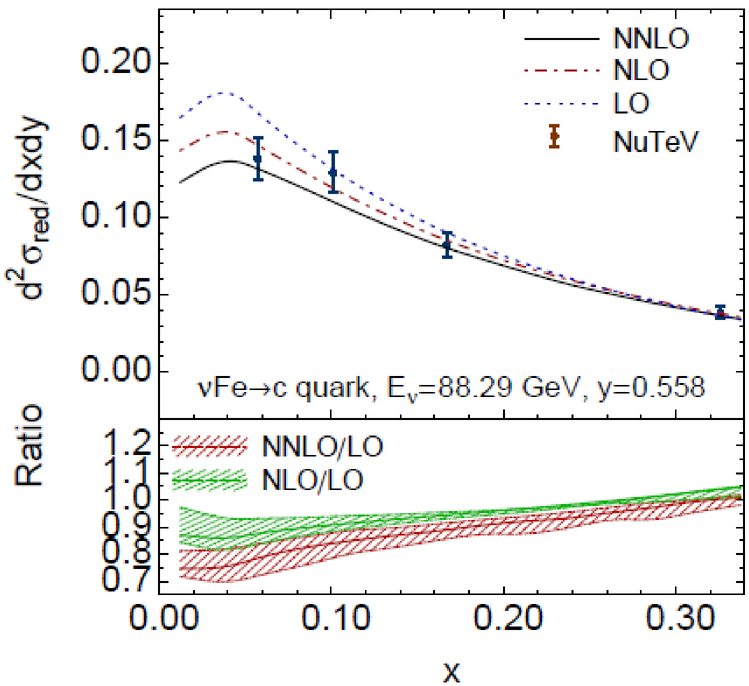


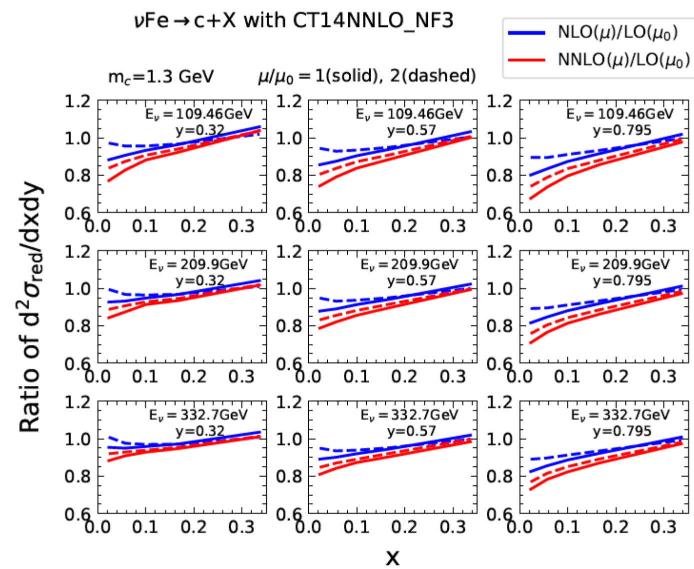


NNLO correction negative, but larger in size at lower $x$

Now include these in fit (Bailey) (required some improvement in threshold treatment for charged-current VFNS scheme).

| | BR$(c \to \mu)$ | CCFR/NuTeV $\chi^2$ | ATLAS $W, Z \chi^2$ | Total $\chi^2$ |
|---|---|---|---|---|
| MMHT+HERAII | 0.090 | 120.5 | | 3526.3 |
| MMHT+HERAII (NNLO dimuon ) | 0.102 | 122.7 | | 3527.3 |
| MMHT+HERAII (NNLO VFNS dimuon) | 0.101 | 123.9 | | 3531.3 |
| MMHT+HERAII+ATLAS$(W, Z)$ | 0.073 | 127.3 | 108.6 | 3684.7 |
| MMHT+HERAII+ATLAS$(W, Z)$ (NNLO dimuon ) | 0.084 | 137.8 | 106.8 | 3688.4 |
| MMHT+HERAII+ATLAS$(W, Z)$ (NNLO VFNS dimuon) | 0.086 | 137.0 | 106.8 | 3688.5 |
| $N_{pts}$ | | 126.25 | 61 | 3337 |

The default value of BR$(c \to \mu) = 0.092 \pm 10\%$.

## $s + \bar{s}$ illustration without full NNLO, i.e. as in MMHT2014.

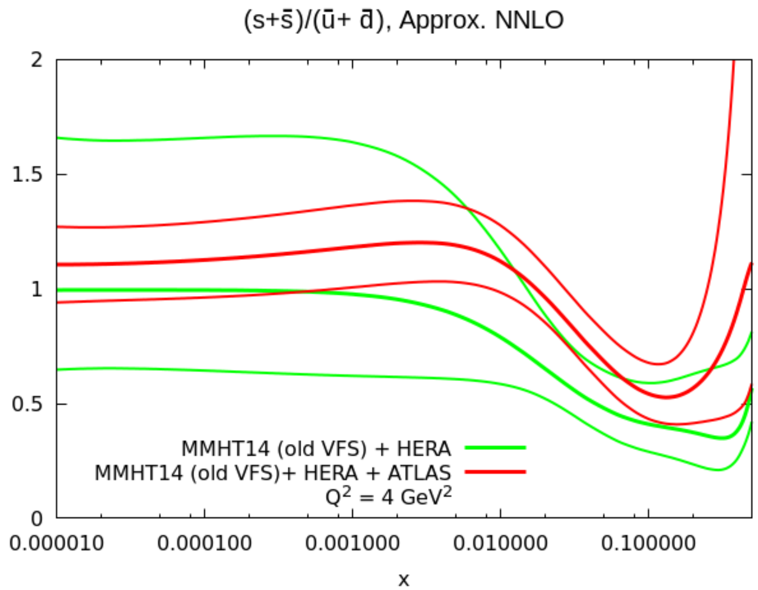


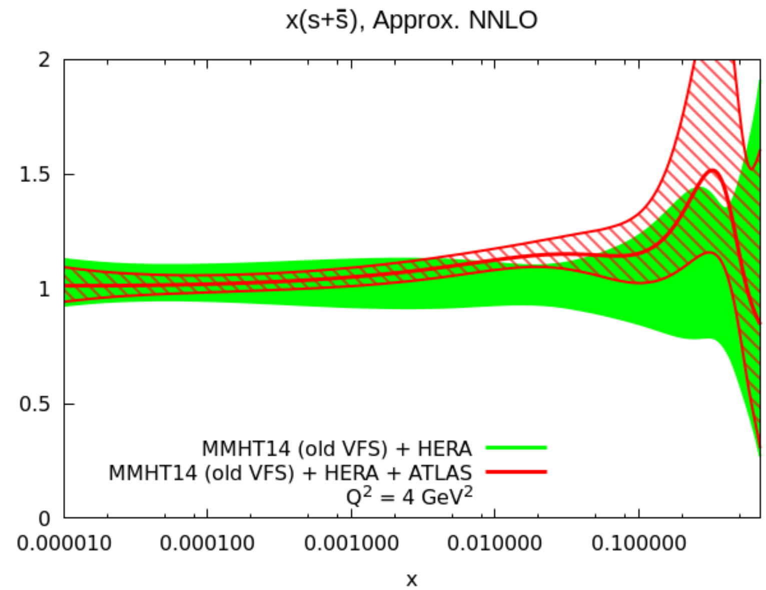


## $s + \bar{s}$ illustration with full NNLO and updated VFNS.

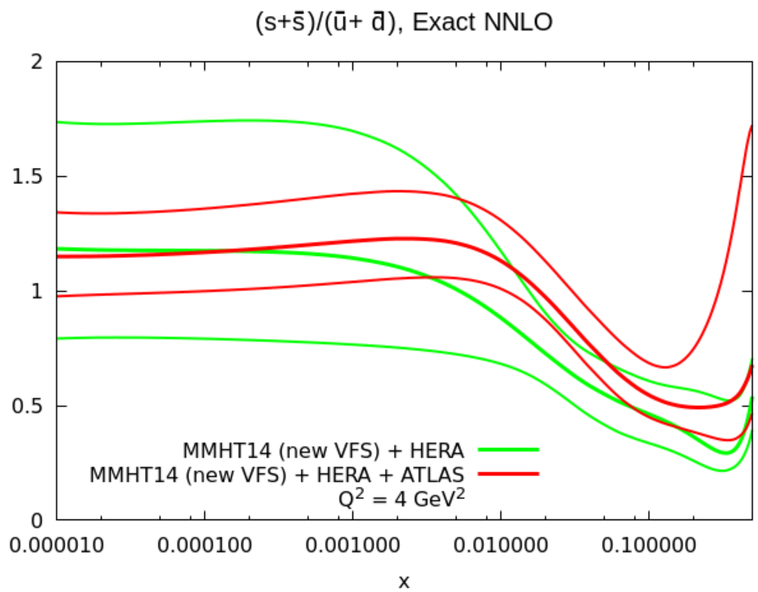


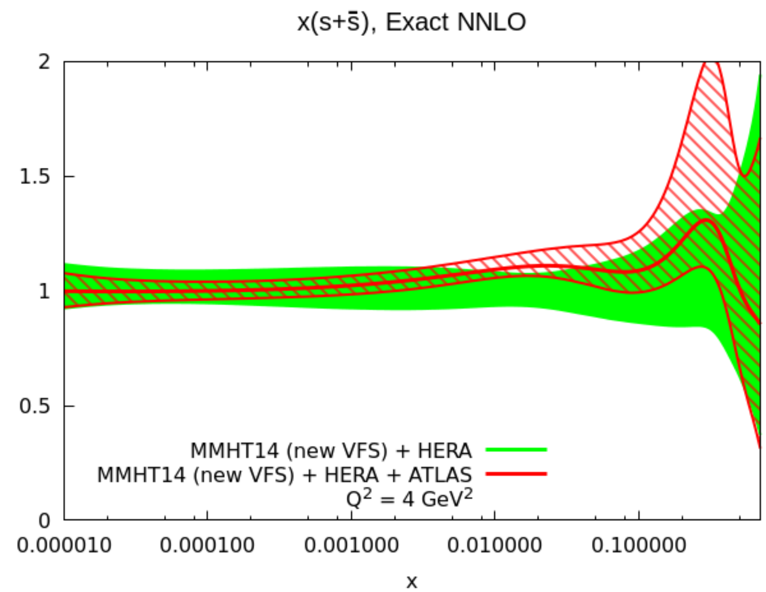

## Newer CMS data at 13 TeV – doesn't favour very large $s + \bar{s}$.

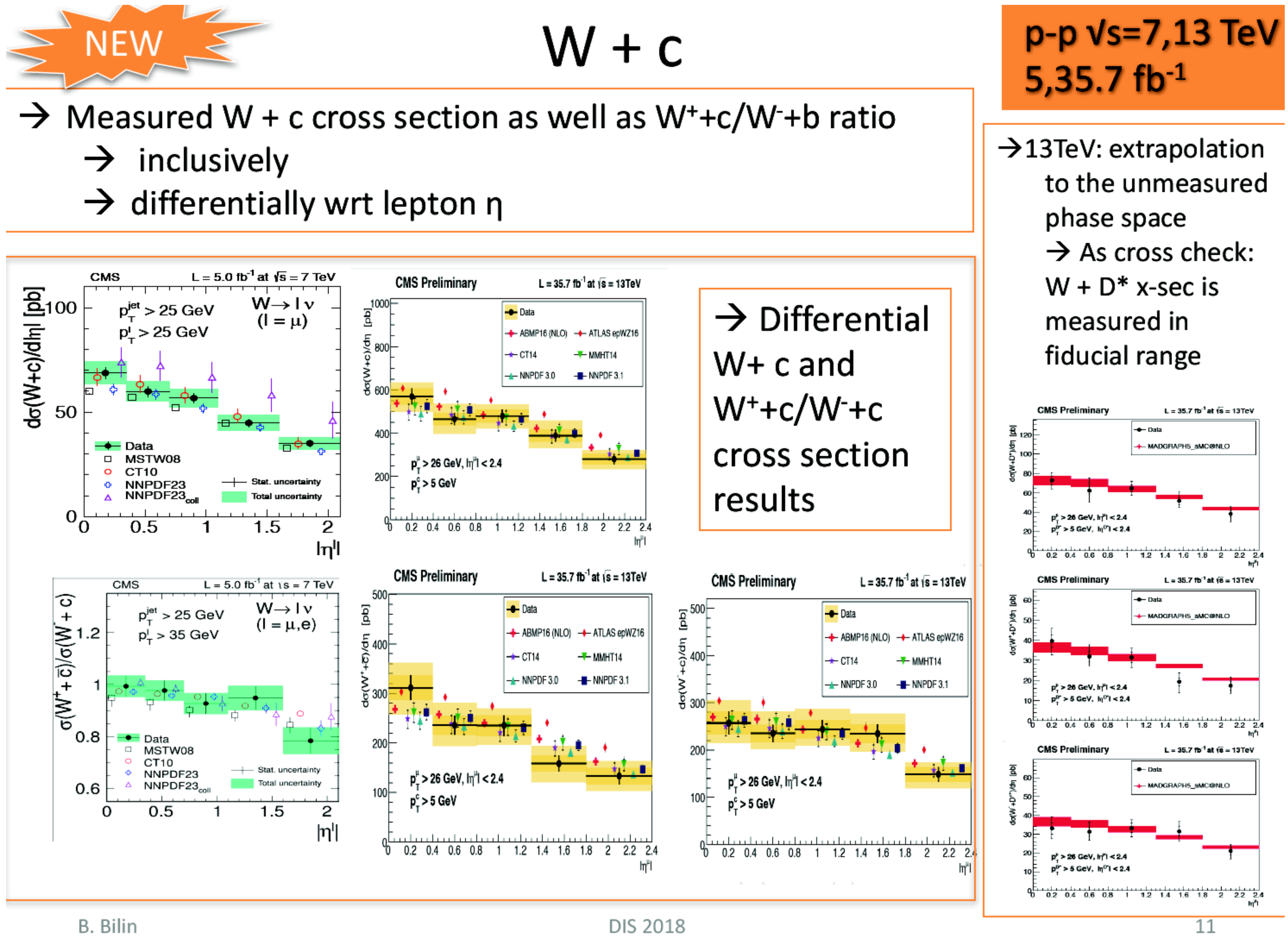

## Fit to high luminosity ATLAS 7 TeV inclusive jet data – MMHT (JHEP 02 (2015) 153)

Difficulty simultaneously fitting all rapidity bins. Mismatch in one bin different in form to neighbouring bin constraining PDFs of similar $x, Q^2$.

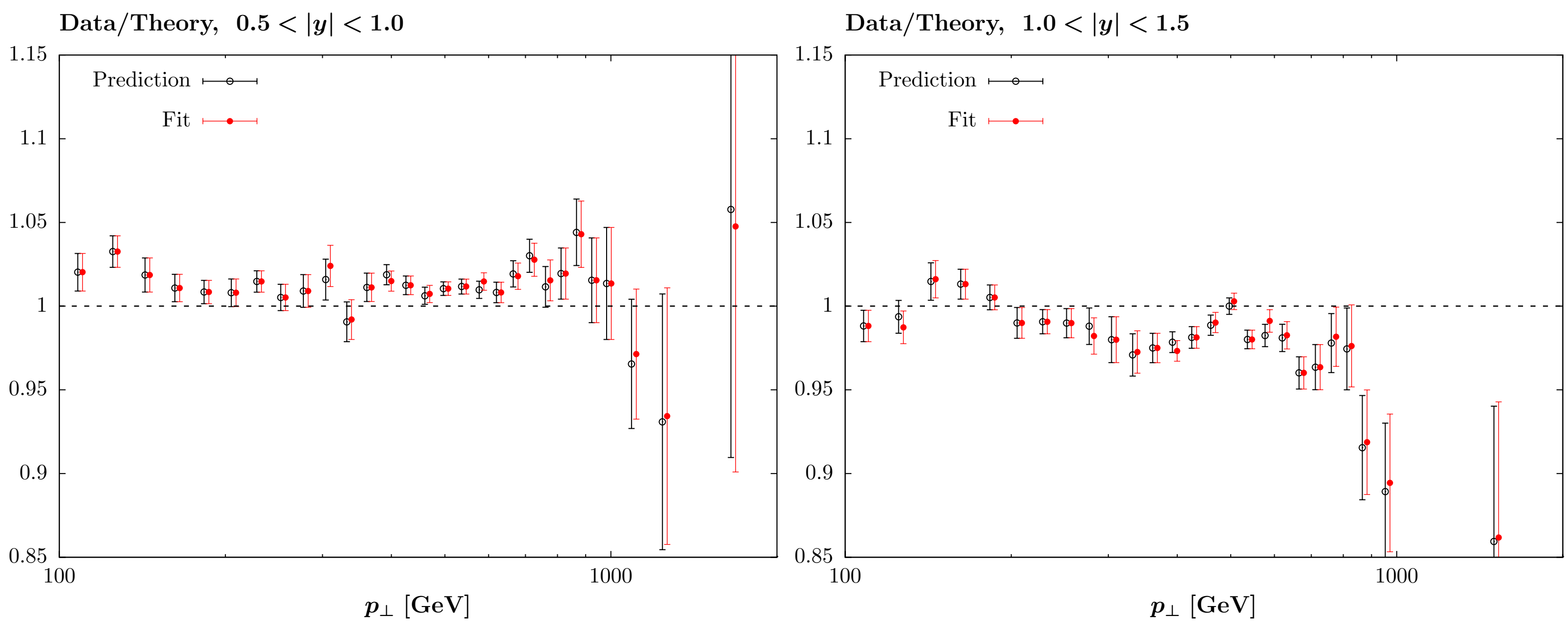


Similar results also seen by other groups.

Qualitative conclusion shown to be independent of jet radius $R$, choice of scale or inclusion of NNLO corrections.

## Exercise on decorrelating uncertainties

We consider the effect of decorrelating two uncertainty sources, i.e. making them independent between the 6 rapidity bins. More extensive decorrelation study in ATLAS – JHEP 09 020 (2017).

| | Full | 21 | 62 | 21,62 |
|---|---|---|---|---|
| $\chi^2/N_{\rm pts.}$ | 2.85 | 1.56 | 2.36 | 1.27 |

Similar results using new NNLO results.

| | $R_{\rm low},\, p_\perp^{\rm jet}$ | $R_{\rm low},\, p_\perp^{\rm max}$ | $R_{\rm high},\, p_\perp^{\rm jet}$ | $R_{\rm high},\, p_\perp^{\rm max}$ |
|---|---|---|---|---|
| NLO | 210.0 (187.1) | 189.1 (181.7) | 175.1 (193.5) | 164.9 (191.2) |
| NNLO | 172.3 (177.8) | 199.3 (187.0) | 149.8 (182.3) | 152.5 (185.4) |

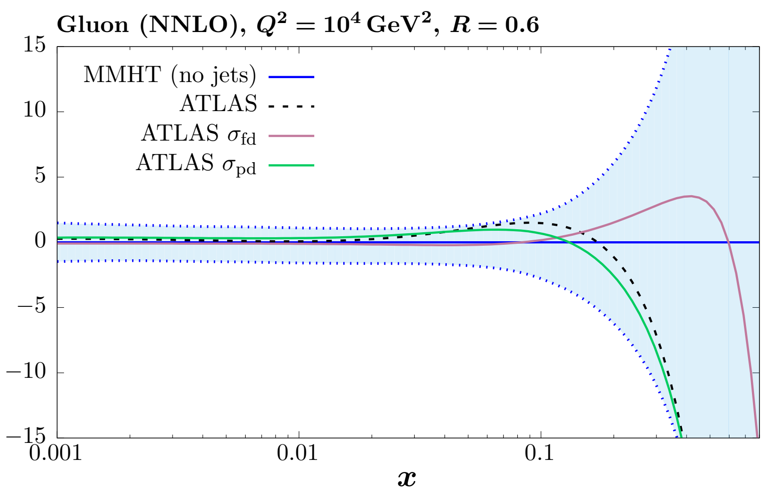


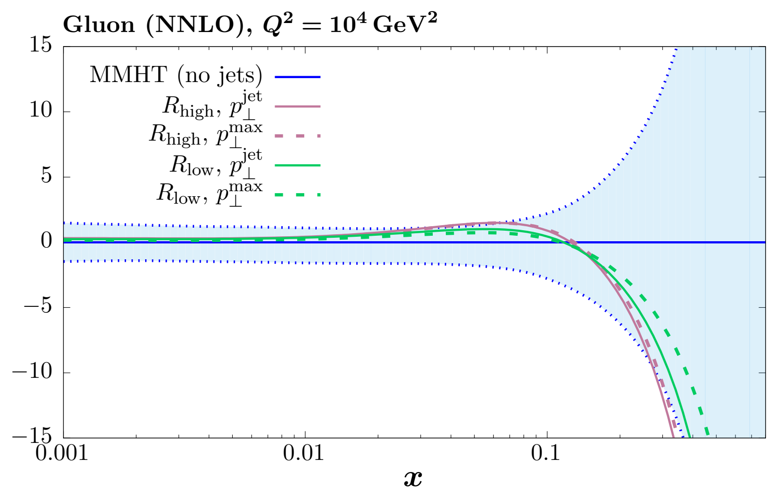


Results insensitive to decorrelation. Find softer gluon, reduced uncertainty. Also relatively little sensitivity to scales and jet radius.

## **Differential $t\bar{t}$ data.** Bailey

A similar issue noticed in differential top-antitop production –(NNLO Differential top-antitop production now available Czakon *et al*).

Distributions differential in $y_t, y_{\bar{t}t}, p_T^t, M_{\bar{t}t}$, and statistical correlations available (not fully implemented yet).

Find similar issues with correlated uncertainties when fitting all together, and fitting $y_t, y_{\bar{t}t}$ individually (seen by MMHT, CT, ATLAS not NNPDF.)

| | | Fitted data set(s) | | | | |
|---|---|---|---|---|---|---|
| | | $p_T$ | $y_t$ | $y_{t\bar{t}}$ | $M_{t\bar{t}}$ | All |
| Contribution | $p_T$ | 0.08 | | | | 2.38 |
| | $y_t$ | | 1.23 | | | 1.84 |
| | $y_{t\bar{t}}$ | | | 1.09 | | 2.22 |
| | $M_{t\bar{t}}$ | | | | 0.29 | 1.81 |
| | Penalty | 0.24 | 1.83 | 2.35 | 0.17 | 0.88 |
| | Total | 0.32 | 3.06 | 3.44 | 0.47 | 2.96 |

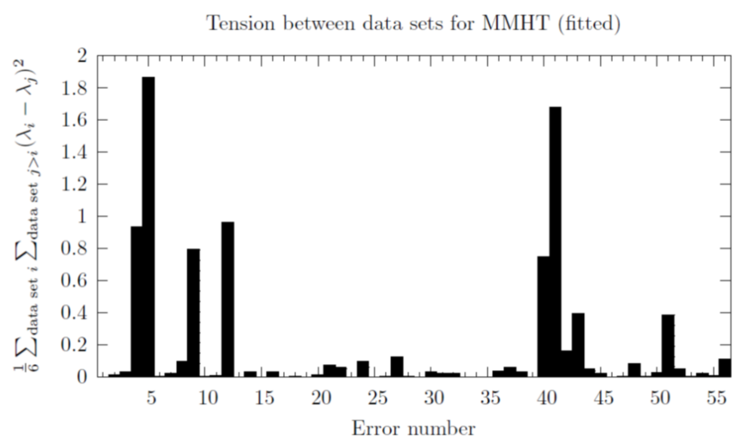


$\chi^2/N$ high in simultaneous fit and for rapidity distributions.

Highly sensitive to correlations in 3 large systematics – hard-scattering model, ISR/FSR and parton Shower. All Monte Carlo related.

$y_{\bar{t}t}, y_t$ fits still poor when decorrelating between types of distribution only.

For $y_{\bar{t}t}$ desired shift varies considerably between points.

Try decorrelating for individual distribution and between sets. (Between data sets only actually best $\chi^2$.)

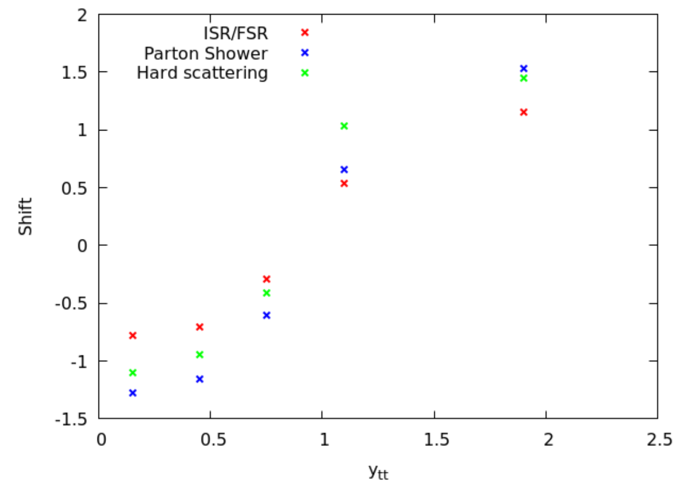


Two types of decorrelation for parton shower.

$$\beta_i^1 = \left(\frac{y_{tt,i} - y_{tt,min}}{y_{tt,max} - y_{tt,min}}\right)\beta_i^{tot}, \qquad \beta_i^2 = \left[1 - \left(\frac{y_{tt,i} - y_{tt,min}}{y_{tt,max} - y_{tt,min}}\right)\right]^{\frac{1}{2}}\beta_i^{tot}$$

$$\beta_i^1 = \cos\left[\pi\left(\frac{y_{tt,i} - y_{tt,min}}{y_{tt,max} - y_{tt,min}}\right)\right]\beta_i^{tot}, \qquad \beta_i^2 = \sin\left[\pi\left(\frac{y_{tt,i} - y_{tt,min}}{y_{tt,max} - y_{tt,min}}\right)\right]\beta_i^{tot}$$

| | Before decorrelating | After decorrelating |
|---|---|---|
| pT | 2.38 | 0.57 |
| yt | 1.84 | 1.86 |
| ytt | 2.21 | 1.59 |
| mtt | 1.81 | 0.39 |
| pen | 0.88 | 0.83 |
| tot | 2.96 | 1.81 |

| | Before decorrelating | After decorrelating |
|---|---|---|
| pT | 2.38 | 0.52 |
| yt | 1.84 | 2.11 |
| ytt | 2.21 | 0.79 |
| mtt | 1.81 | 0.72 |
| pen | 0.88 | 0.72 |
| tot | 2.96 | 1.67 |

Sine-cosine decorrelation works better.

Results on the gluon moderately independent of decorrelation and method.

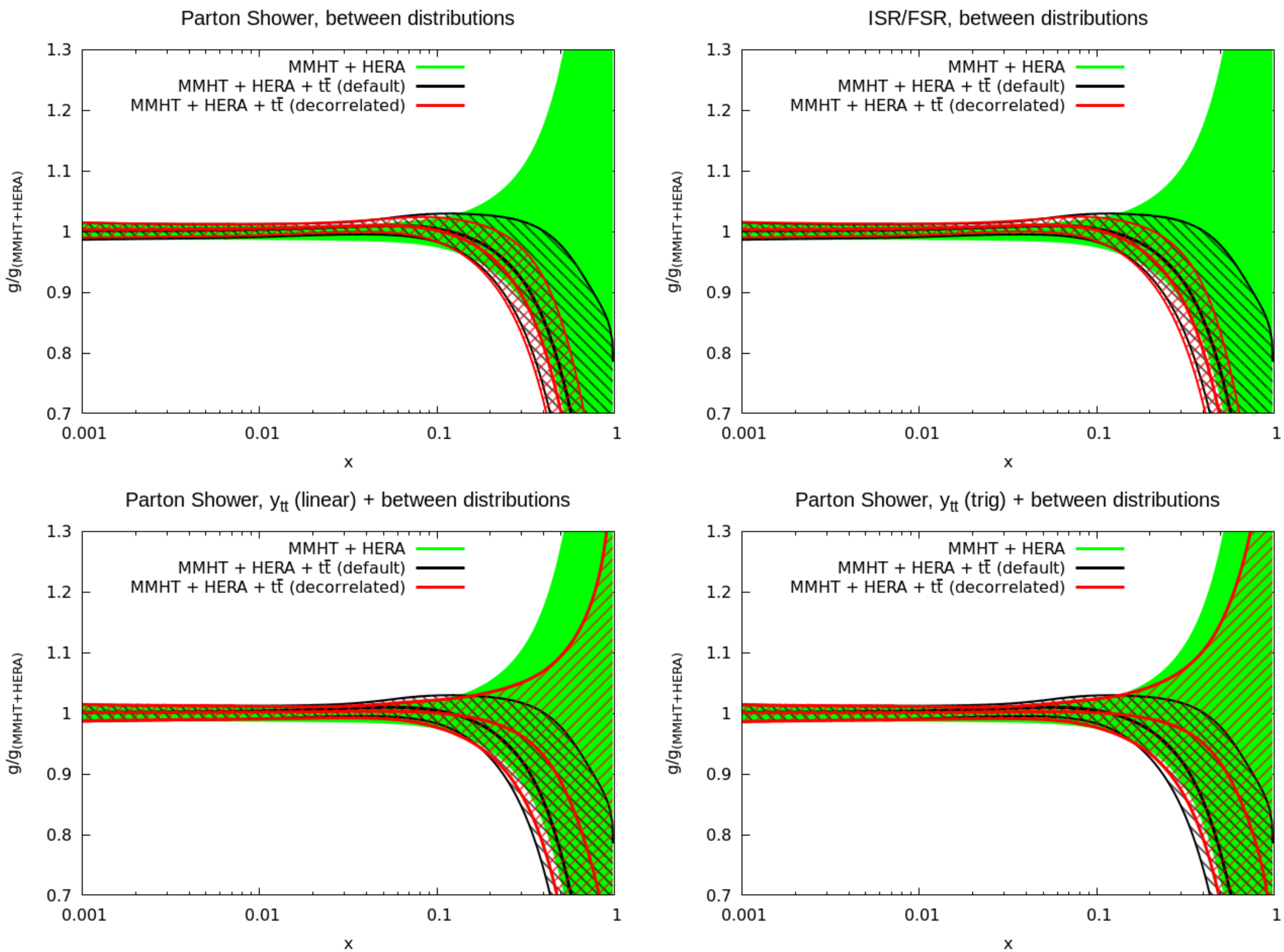


Perhaps better justification than jets.

Also noticed in ATL-PHYS-PUB-2018-017 .

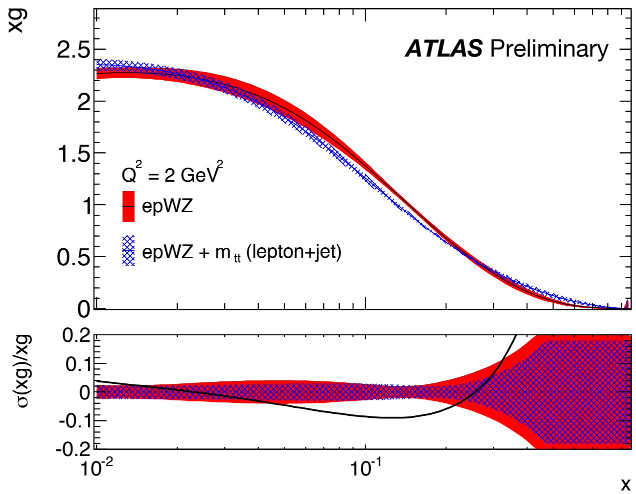


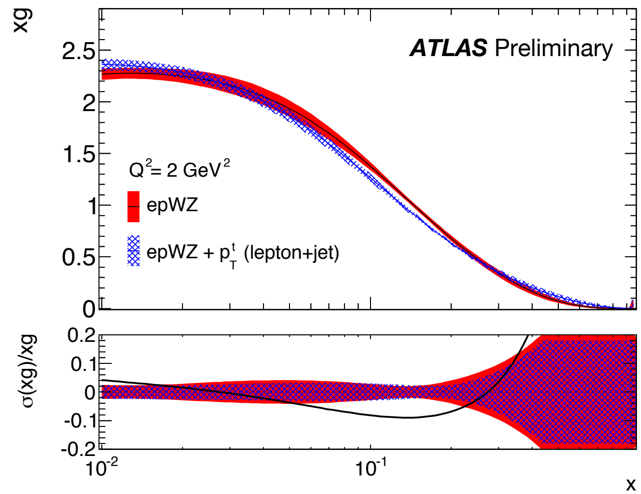


Distributions in $m_{t\bar{t}}$ and $p_T^t$ both fit well with similar pulls on gluon. However, $\chi^2$ in joint fit very poor.

| | | lepton+jets spectra | | | |
|---|---|---|---|---|---|
| | | $p_T^t$ and $y_t$ with statistical correlations | $p_T^t$ and $y_t$ without statistical correlations | $p_T^t$ and $m_{tt}$ with statistical correlations | $p_T^t$ and $m_{tt}$ without statistical correlations |
| Total $\chi^2$/NDF | | 1264 / 1068 | 1260 / 1068 | 1290 / 1070 | 1287 / 1070 |
| Partial $\chi^2$/NDP | HERA | 1148 / 1016 | 1147 / 1016 | 1162 / 1016 | 1162 / 1016 |
| Partial $\chi^2$/NDP | ATLAS $W, Z/\gamma^*$ | 82.7 / 55 | 83.5 / 55 | 83.2 / 55 | 83.1 / 55 |
| Partial $\chi^2$/NDP | ATLAS $t\bar{t}$ | 33 / 13 | 30 / 13 | 45 / 15 | 42 / 15 |

Again because some correlated systematic uncertainties require very different pulls. All related to 2-point model uncertainties.

| Systematic uncertainty source | lepton+jets spectrum | | | |
|---|---|---|---|---|
| | $p_T^t$ | $y_t$ | $y_{tt}$ | $m_{tt}$ |
| Hard scattering model | +0.74± 0.31 | +0.48± 0.22 | +0.92± 0.37 | -0.43± 0.20 |
| Parton shower model | -1.32± 0.43 | -0.79± 0.26 | -0.51± 0.17 | +0.39±0.13 |
| ISR/FSR model | -0.47± 0.18 | -0.87±0.30 | -1.27± 0.38 | +0.33± 0.10 |

## Extension of parameterisation. (Cridge)

General parameterisation used $A(1-x)^{\eta}x^{\delta}(1+\sum_{i=1}^{n} a_i T_i(1-2x^{\frac{1}{2}}))$,, where $T_i(1-2x^{\frac{1}{2}}))$ are Chebyshev polynomials.

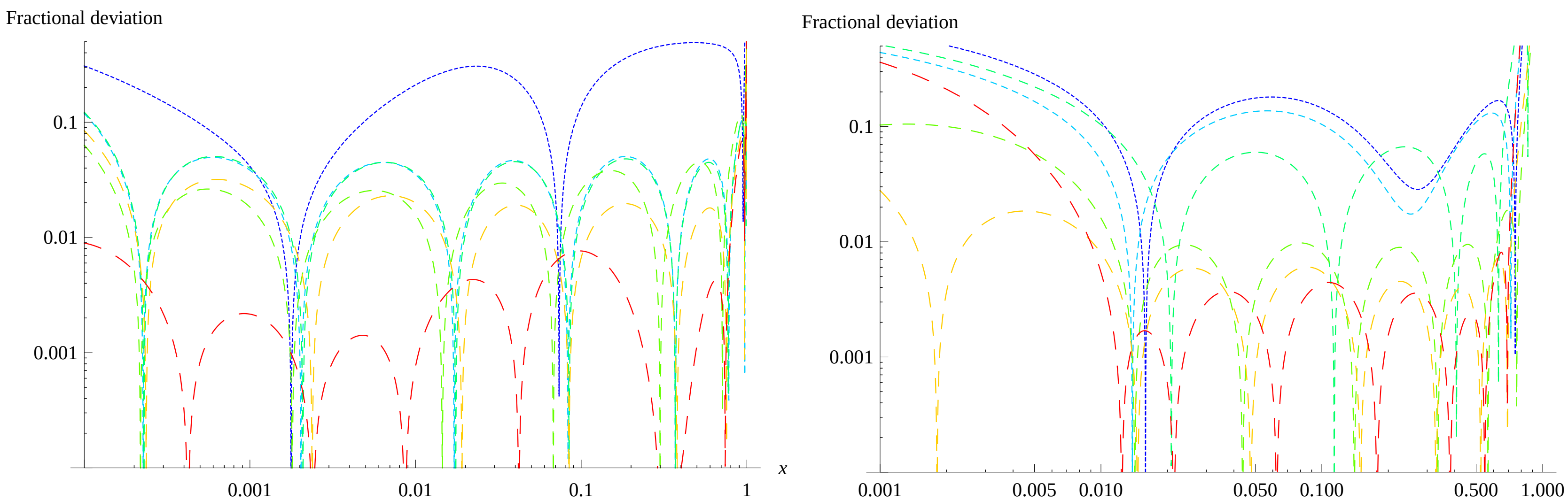


Illustration of precision possible with increasing $n$, sea-like (left) and valence-like (right) (where pseudo-data for $x > 0.01$).

For many inputs parameterisation using $n = 4$ is default for MMHT2014 - $g(x, Q_0^2)$ has a negative term, $s^+(x, Q_0^2)$ has two parameters tied to the sea and $(\bar{d} - \bar{u})(x, Q_0^2)$ and $s^-(x, Q_0^2)$ have fewer parameters.

Using $n = 6$ would lead to much better than $1\%$ precision.

For $(\bar{d}-\bar{u})(x,Q_0^2)$ by default use 4 parameters,

$$(\bar{d}-\bar{u})(x,Q_0^2) = A(1-x)^{\eta_{sea}+2}x^{\delta}(1+\gamma x+\Delta x^2),$$

Extend to $(\bar{d}-\bar{u})(x,Q_0^2) = A(1-x)^{\eta_{sea}+2}x^{\delta}(1+\sum_{i=1}^{4} a_i T_i(1-2x^{\frac{1}{2}})),$

Allows multiple turning points. Improves fit by $> 10$ points - eases ATLAS $W, Z$ and DY ratio tension.

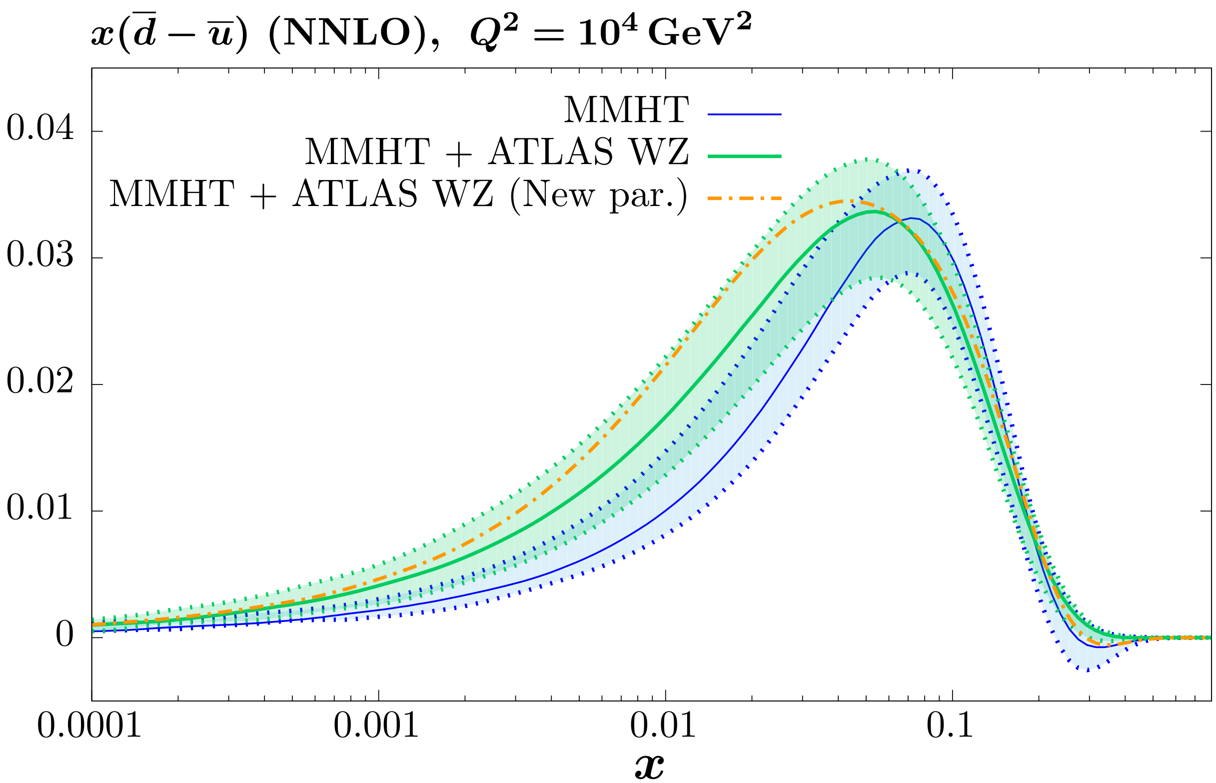

Extend the parameters of other PDFs sequentially, using $n = 6$ in Chebyshev polynomial for $u_v(x,Q_0^2), d_v(x,Q_0^2),\ sea(x,Q_0^2),\ s^+(x,Q_0^2)$ (two common parameters), and gluon

$$g(x,Q_0^2) = A(1-x)^{\eta}x^{\delta}(1+\sum_{i=1}^{4} a_i T_i(1-2x^{\frac{1}{2}})) - A_-(1-x)^{\eta_-}x^{\delta_-}.$$

Change of 36 to a maximum of 48 parton parameters.

Main improvements after extension of $(\bar{d}-\bar{u})(x,Q_0^2)$ from additionally introducing $d_V(x,Q_0^2)$ and $g(x,Q_0^2)$.

Go from 25 eigenvector pairs to 30 – one extra parameter for each PDF other than the light sea (and $s^-(x,Q_0^2)$).

Extra possible eigenvectors highly non-quadratic $\rightarrow$ little extra uncertainty.

# Improvements in Global Fit.

| Data set | $-\Delta\chi^2 \quad (\bar{d}-\bar{u})$ | $-\Delta\chi^2 \quad (\bar{d}-\bar{u}), d_V$ | $-\Delta\chi^2$ All |
|---|---|---|---|
| Total | 17.6 | 34.0 | 48.9 |
| BCDMS $F_2^p$ | -4.6 | -3.3 | -2.7 |
| BCDMS $F_2^d$ | -2.7 | 4.9 | 8.5 |
| NMC $F_2^n/F_2^p$ | 6.5 | 6.1 | 6.0 |
| NuTeV $F_3^N$ | -0.3 | 1.7 | 3.2 |
| E866 $\sigma(pd)/\sigma(pp)$ | 8.2 | 10.1 | 11.0 |
| NuTeV dimuon | 0.7 | 1.0 | 3.0 |
| HERA I+II $\sigma(e^+p)$ 920 GeV | 1.1 | 1.7 | 4.6 |
| CMS $pp \to l^+l^-$ | 0.7 | 1.8 | 3.1 |
| D0 $\sigma(e^+) - \sigma(e^-)$ | -1.2 | -3.4 | -1.4 |
| CMS $8\ \mathrm{TeV}\sigma(l^+) - \sigma(l^-)$ | 4.4 | 5.0 | 4.6 |
| ATLAS $7\ \mathrm{TeV}\ \ W, Z$ | -0.5 | 2.2 | 4.3 |
| CMS $7\ \mathrm{TeV}$ jets | -0.5 | 0.2 | 3.2 |

Improvement reduces tension between DY ratio and LHC data, not improves intrinsic fit quality to DY ratio (MMHT fit nearly optimal).

LHC lepton asymmetry improved, but D0 worse.

Gluon improvement only partially from HERA data.

Mean tolerance $T = 3.31$

27 eigenvector directions constrained primarily by LHC data sets – largely $7\,\mathrm{TeV}$ ATLAS $W, Z$ data and CMS $W$ (and $W + c$) data but some others including LHCb top and jets.

E866 Drell Yan asymmetry absolutely vital for constraining $\bar{d} - \bar{u}$.

Tevatron data of various types primary constraint for 8 eigenvectors.

Fixed target DIS data (BCDMS, NMC, NuTeV, CCFR) still constrains 12 eigenvectors (mainly high-$x$).

Fully global fit necessary for full constraint with (almost) no assumptions/models.

The biggest change is in $d_V(x,Q^2)$ - largely due to $7\ \mathrm{TeV}$ ATLAS $W, Z$ data, and extra parameterisation has a significant effect.

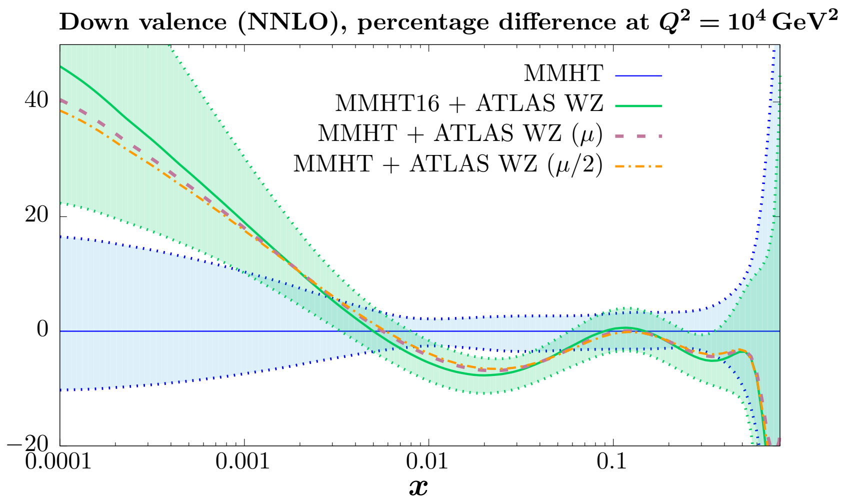


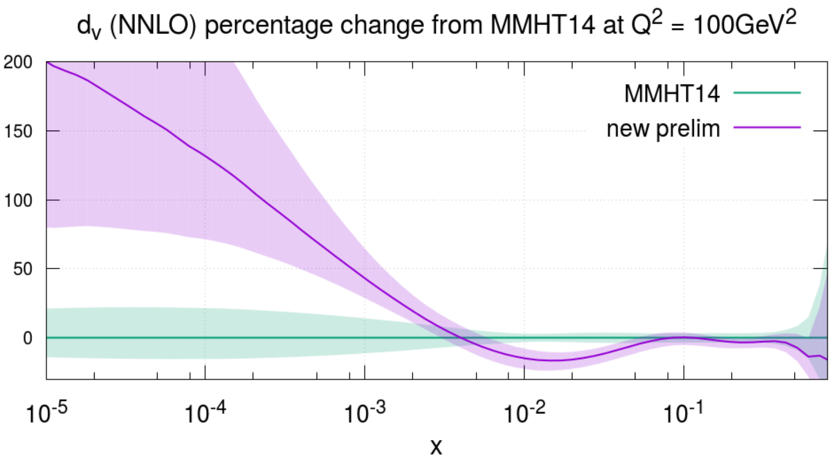


Left – new data. Right – newdata and extended parameterisation.

Note increased uncertainty at very large and small $x$ due to extended parameterisation. Former a feature of many PDFs.

## Plots of $(\bar{d}-\bar{u})(x,Q^2)$ and $(s-\bar{s})(x,Q^2)$

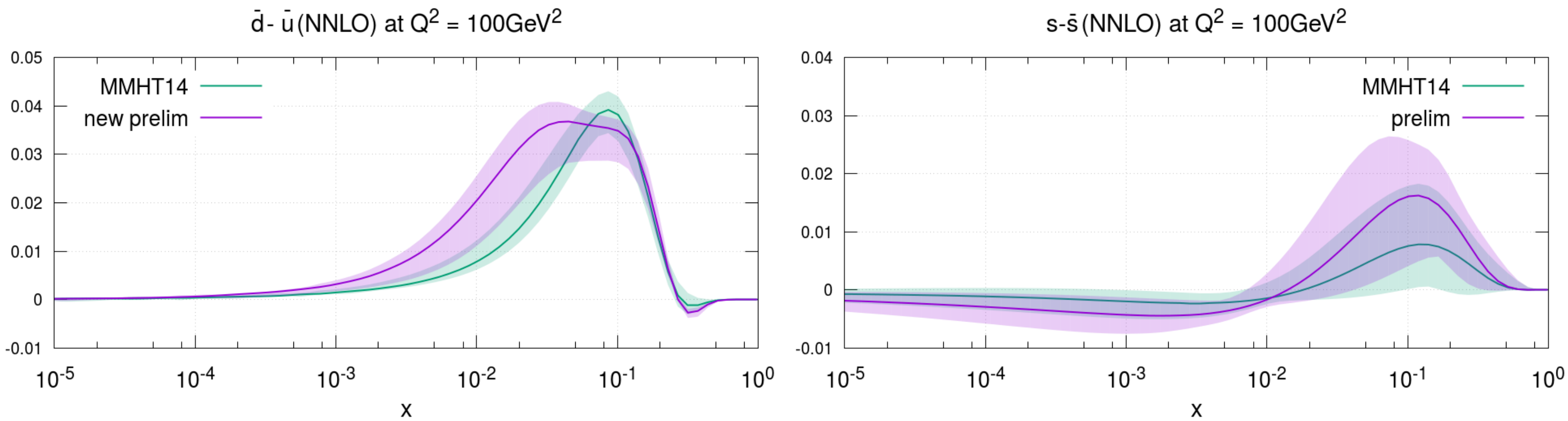


Data prefer a distinctly different shape in $(\bar{d}-\bar{u})(x,Q^2)$ and extra parameter gives extra uncertainty.

Increase in size of $(s-\bar{s})(x,Q^2)$ driven by data – overwhelmingly $7\ \mathrm{TeV}$ ATLAS $W,Z$ data. No change in parameterisation.

Plots of $g(x, Q^2)$ at high and lower $Q^2$.

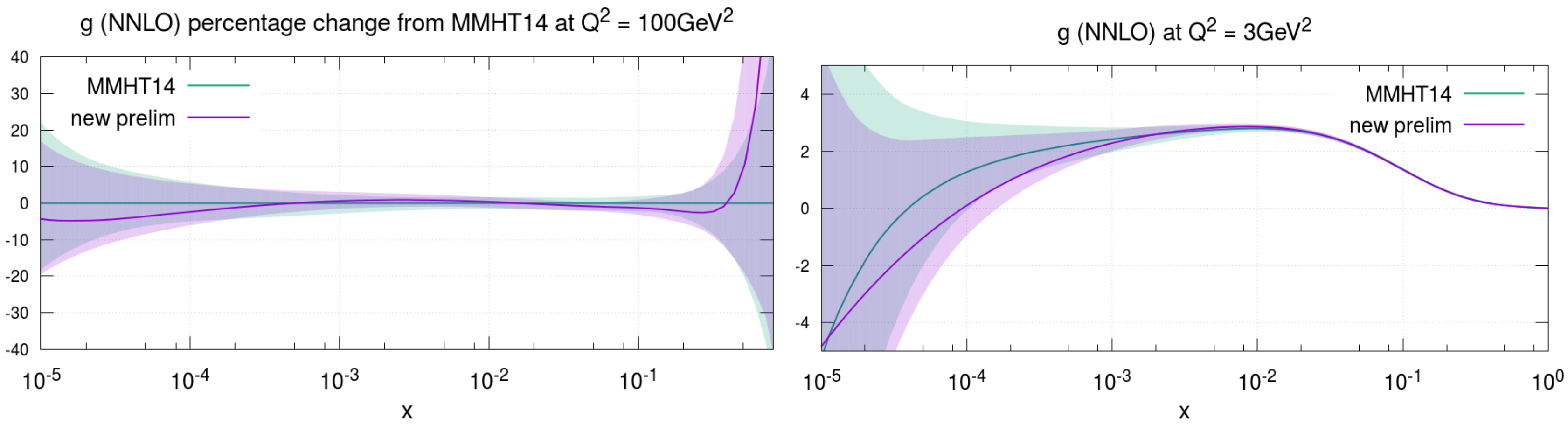


Some features in common with change in `arXiv:1902.11125`, but initial parameterisation much more free here.

Plots of $s^+(x,Q^2)$ and $\bar{u}(x,Q^2)$

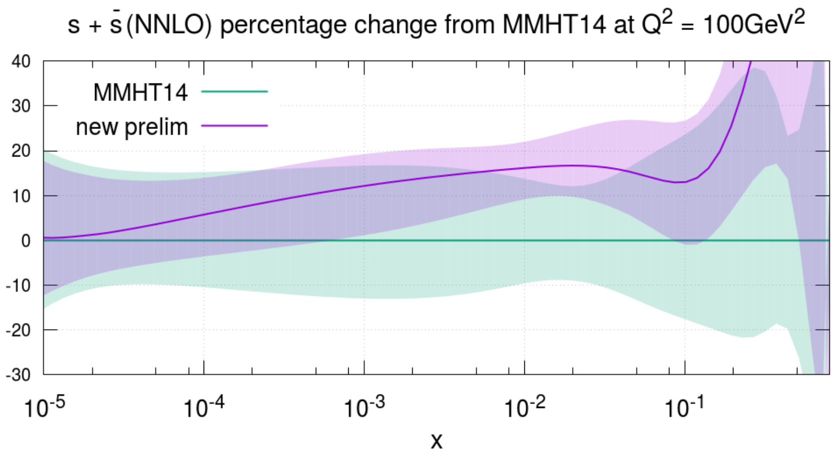


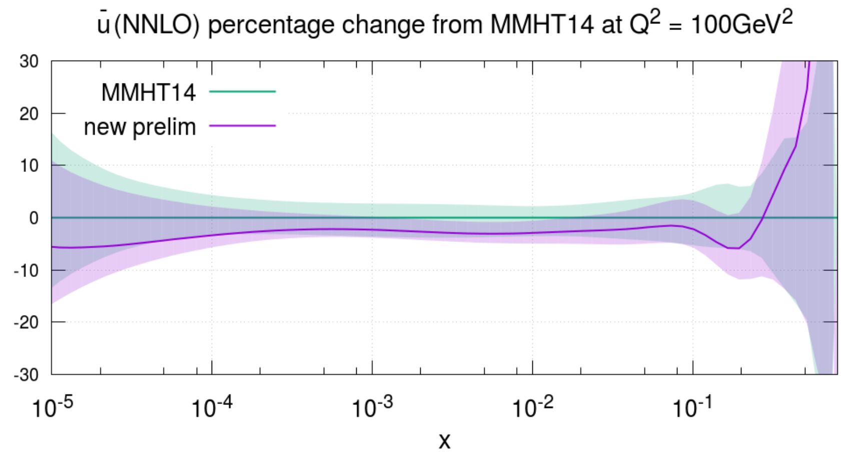


Significant change in shape of $s^+(x,Q^2)$ (note NNLO dimuon correction not included here).

Little change in $\bar{u}(x,Q^2)$. Slightly lower due to generally increased $s^+(x,Q^2)$.

Note – increased uncertainty for $x > 0.6$.

# **Photon** PDF in proton

LUXqed photon PDF (A. Manohar et al., PRL 117, 242002 (2016), JHEP 1712, 046 (2017)) relates photon to structure functions.

## LUXqed

- Recent study of arXiv:1607.04266:

CERN-TH/2016-155

How bright is the proton?
A precise determination of the photon PDF

Aneesh Manohar,[1,2] Paolo Nason,[3] Gavin P. Salam,[2,*] and Giulia Zanderighi[2,4]
[1]Department of Physics, University of California at San Diego, La Jolla, CA 92093, USA
[2]CERN, Theoretical Physics Department, CH-1211 Geneva 23, Switzerland
[3]INFN, Sezione di Milano Bicocca, 20126 Milan, Italy
[4]Rudolf Peierls Centre for Theoretical Physics, 1 Keble Road, University of Oxford, UK

- Show how photon PDF can be expressed in terms of $F_2$ and $F_L$. Use measurements of these to provide well constrained LUXqed photon PDF.

$$x f_{\gamma/p}(x,\mu^2) = \frac{1}{2\pi\alpha(\mu^2)} \int_x^1 \frac{dz}{z} \left\{ \int_{\frac{x^2 m_p^2}{1-z}}^{\frac{\mu^2}{1-z}} \frac{dQ^2}{Q^2} \alpha^2(Q^2) \left[ \left( z p_{\gamma q}(z) + \frac{2x^2 m_p^2}{Q^2} \right) F_2(x/z, Q^2) - z^2 F_L\left(\frac{x}{z}, Q^2\right) \right] - \alpha^2(\mu^2) z^2 F_2\left(\frac{x}{z}, \mu^2\right) \right\}, \quad (6)$$

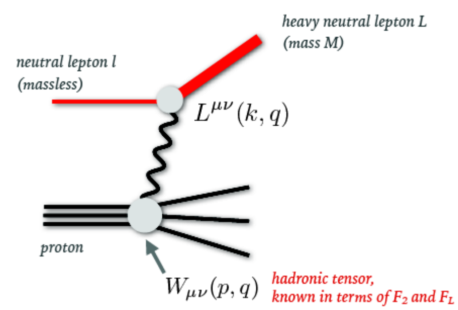


22

Breakdown into well-known elastic (coherent) contribution and moderately model dependent inelastic part Harland-Lang *et al.* PRD94 (2016) 074008. Much better constraint on input.

## NNPDFLux PDFs with QED corrections

Iterative procedure starting with LUX type photon.

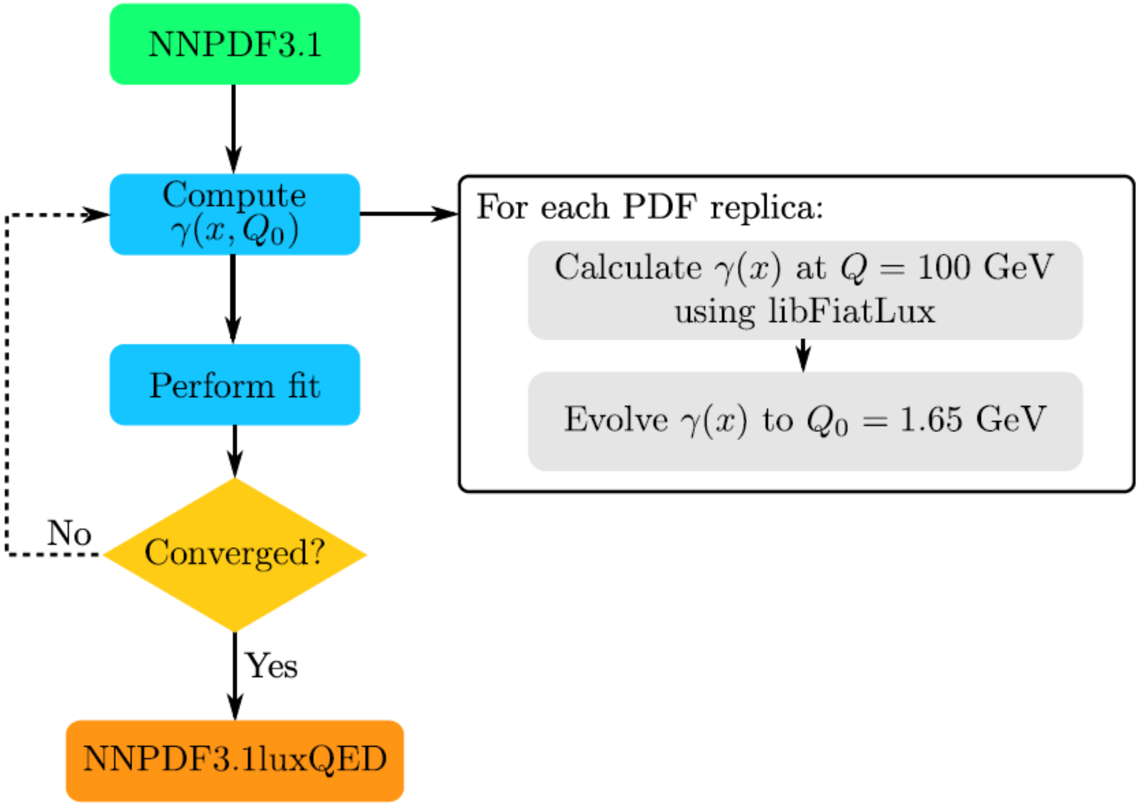


Calculate $\gamma(x, Q^2)$ at $Q^2 = 100\mathrm{GeV}^2$ using LUX procedure, but NNPDF PDFs.

Evolve down perturbatively to $Q_0^2 = (1.65)^2\mathrm{GeV}^2$ and use as input for new fit – iterate.

## MMHT PDFs with QED corrections – Nathvani

We now base photon input for PDFs at low $Q^2$ on LUX – much better constraint.

Effect of photon evolution fully incorporated to couple with that of quarks and gluon for both proton and neutron.

The photon input is defined at $Q_0^2 = 1\mathrm{GeV}^2$, the same as our other PDFs. Input momentum $0.00195$.

Input defined by integrating LUX expression up to scale $\mu^2 = Q_0^2$.

PDFs evolve up using DGLAP splitting functions to given order in $\alpha_s$ with $\alpha, \alpha\alpha_S$ and $\alpha^2$ corrections (De Florian *et al*) included.

In addition the photon receives contributions/corrections from "higher twist" sources above $Q_0^2 = 1\mathrm{GeV}^2$ – elastic, target mass, kinematic cuts, higher twist (renormalon) corrections to $F_2(x, Q^2)$.

## Change in PDFs due to refit

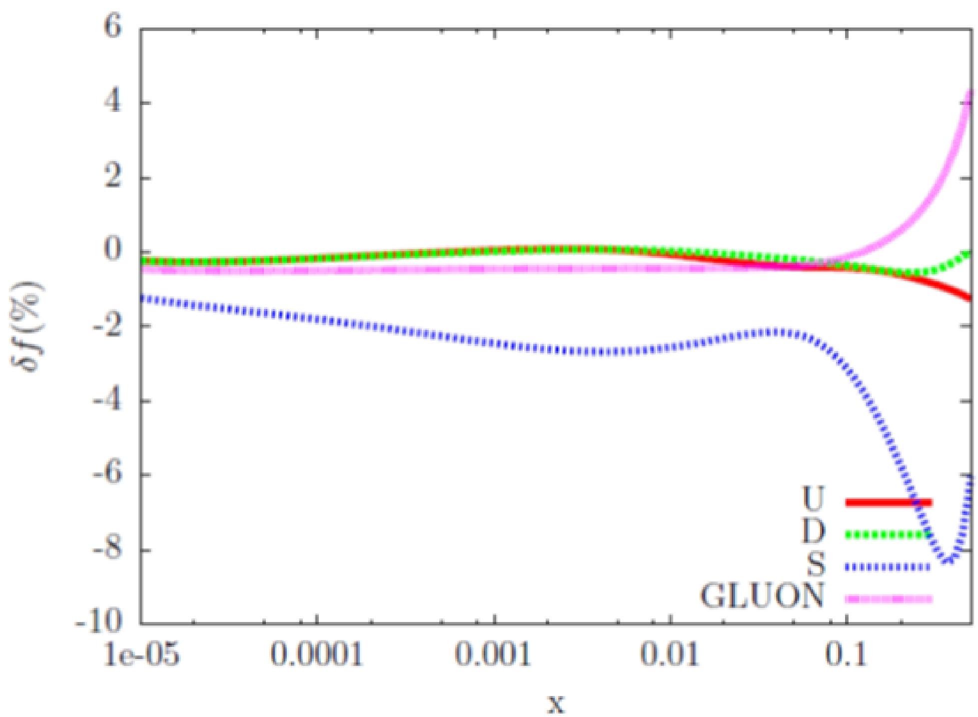


Gluon affected mainly at high $x$, loss of momentum.

Small $x$ flavour rearrangement in quarks – less strange. Well within uncertainty.

Quarks lose momentum at high $x$ from QED evolution, but reduction in high $Q^2$ up quark less as compensated for by input.

Modern LUX-based PDFs all in excellent agreement with very small uncertainty.

Historical photon PDFs have much more variation.

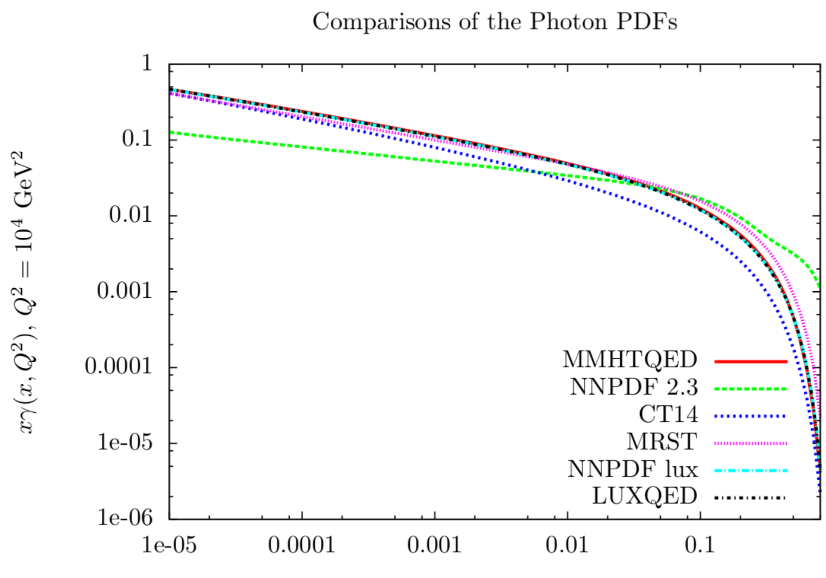


MMHTqed photon largely in good agreement with LUXqed.

Main differences (slightly larger at small $x$, smaller for $x \sim 0.5$) due to differences in quarks – PDFs not exactly the same as MMHT2014.

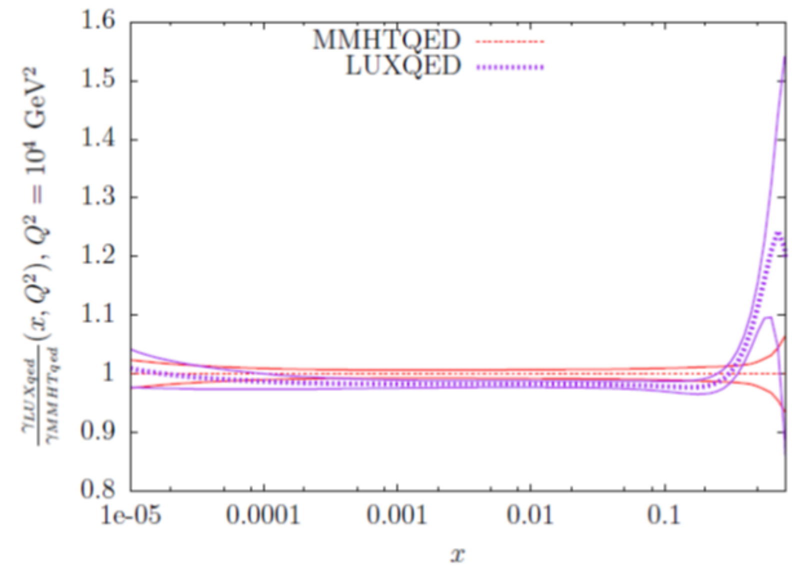

## Uncertainties in Photon Distribution

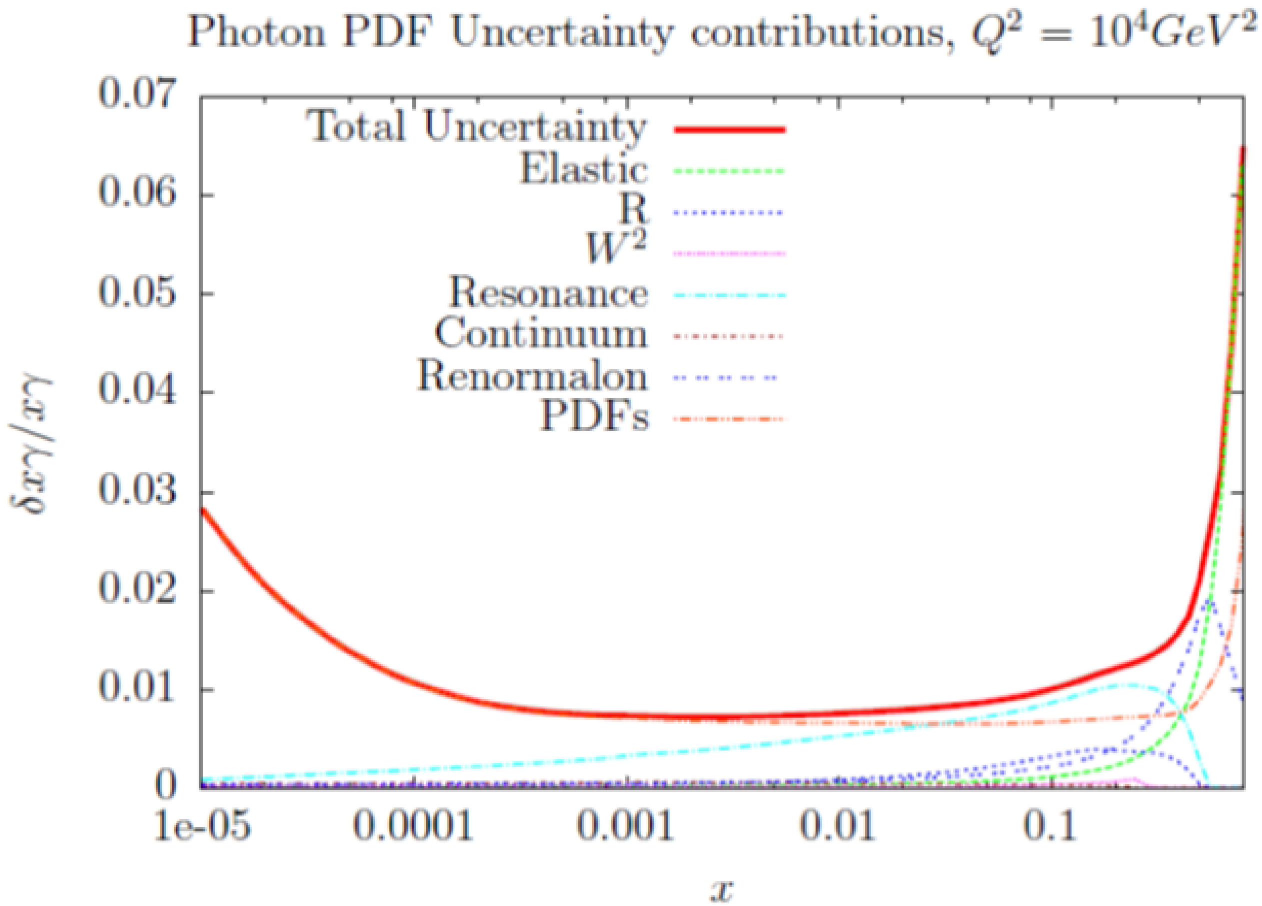


As with LUXqed mainly due to PDFs and elastic contribution and the resonance region.

Large high-$x$ component from higher twist contributions for $Q^2 > Q_0^2$.

# Inelastic and Elastic contributions provided separately.

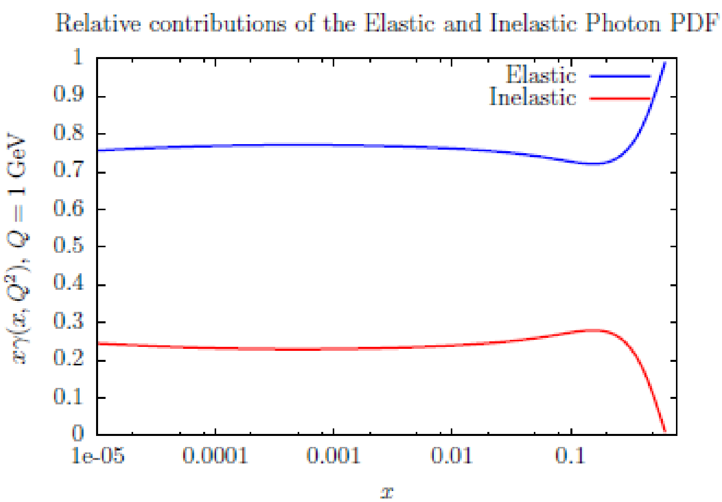


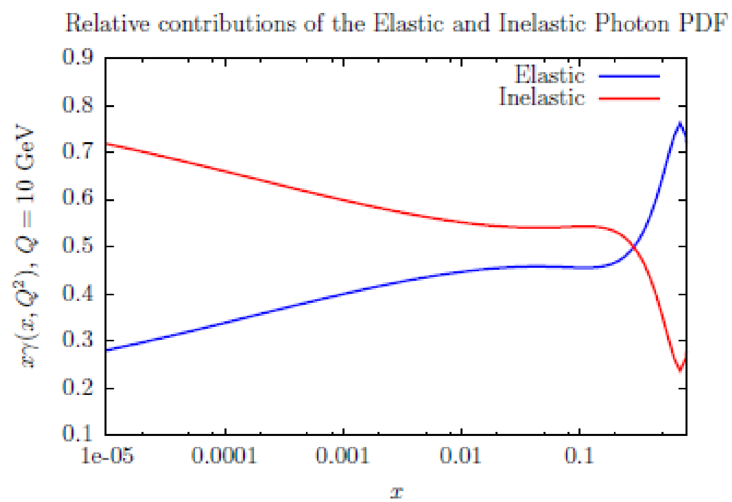


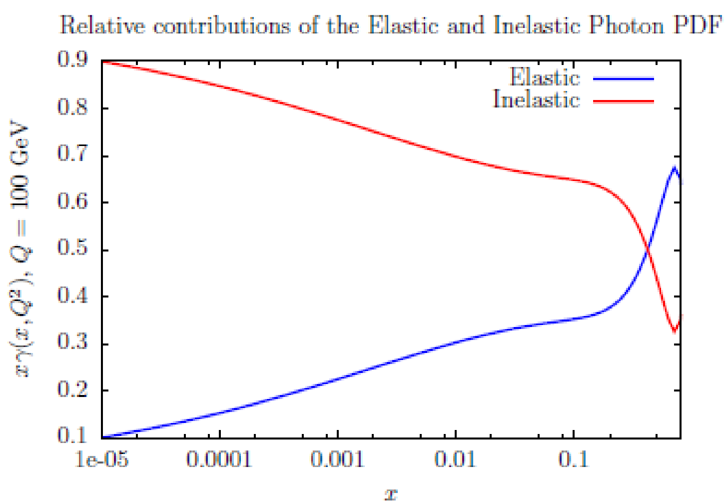

Impact on fit to ATLAS high-mass Drell-Yan data.

This data no longer constrains the photon in any meaningful way. Fit quality including photon contributions $\chi^2/\mathrm{Npts} = 65/48$.

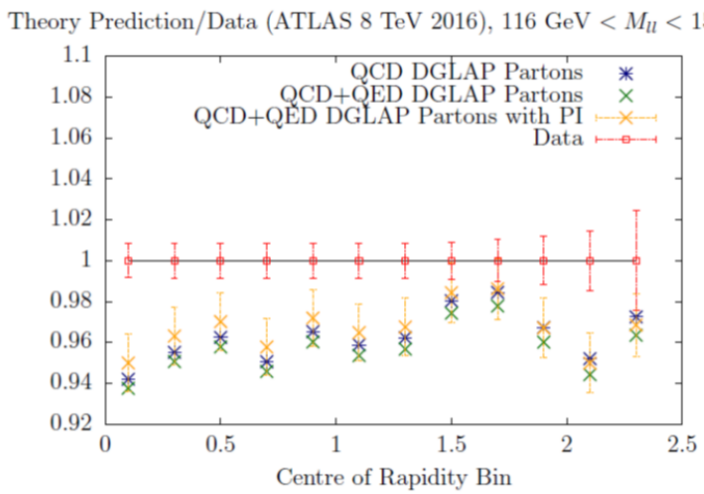


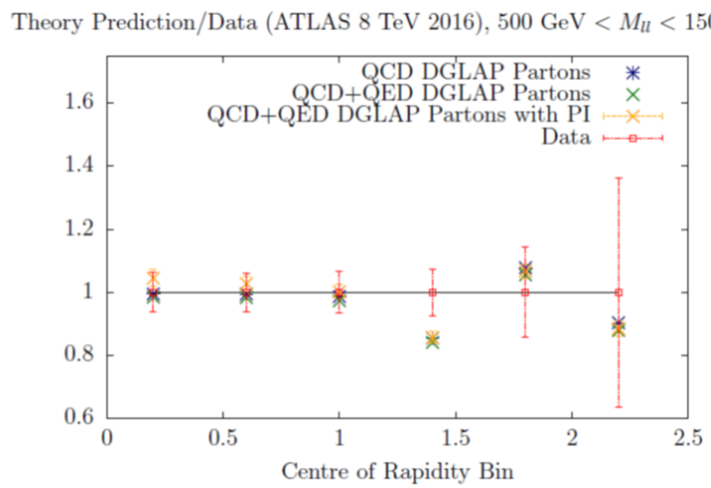


In some bins QED-altered evolution of quarks more important than photon contribution.

## Some dedicated studies on best-fit $\alpha_S(M_Z^2)$

# DETERMINING ALPHAS FROM A GLOBAL FIT

[1802.03398]

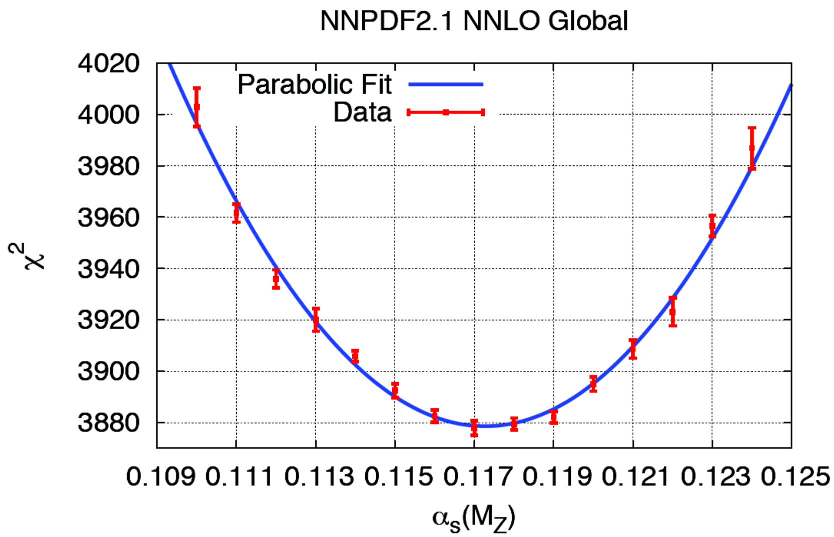


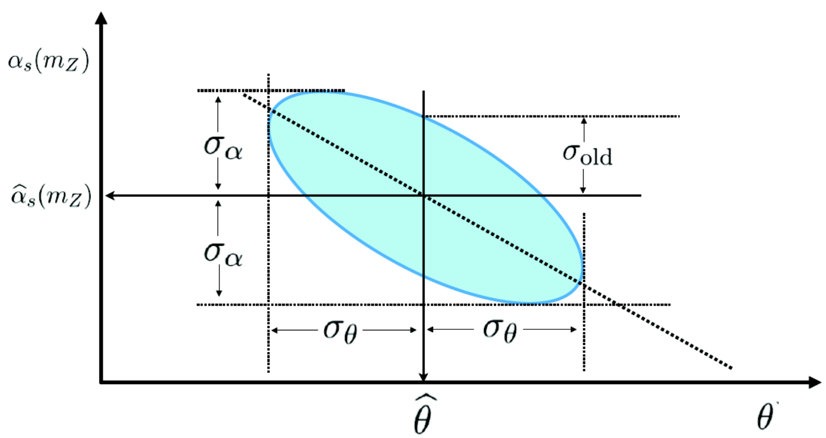


***Previous NNPDF determination***
***Based on a scan of NNPDF2.1***
**[1110.2483]**

Measure the $\chi^2$ of best fit PDF parameters as a function of $\alpha_S$

Neglects correlations with PDF fit parameters ($\theta$) - important when experimental uncertainties are small

***Ideally one should minimise PDFs and $\alpha_S$ simultaneously***

# RESULTS

[1802.03398]

$$\alpha_s^{\mathrm{NNLO}}(m_Z) = 0.1185 \pm 0.0005^{\mathrm{exp}} \pm 0.0001^{\mathrm{meth}} \pm 0.0011^{\mathrm{th}} = 0.1185 \pm 0.0012 \ (1\%)$$

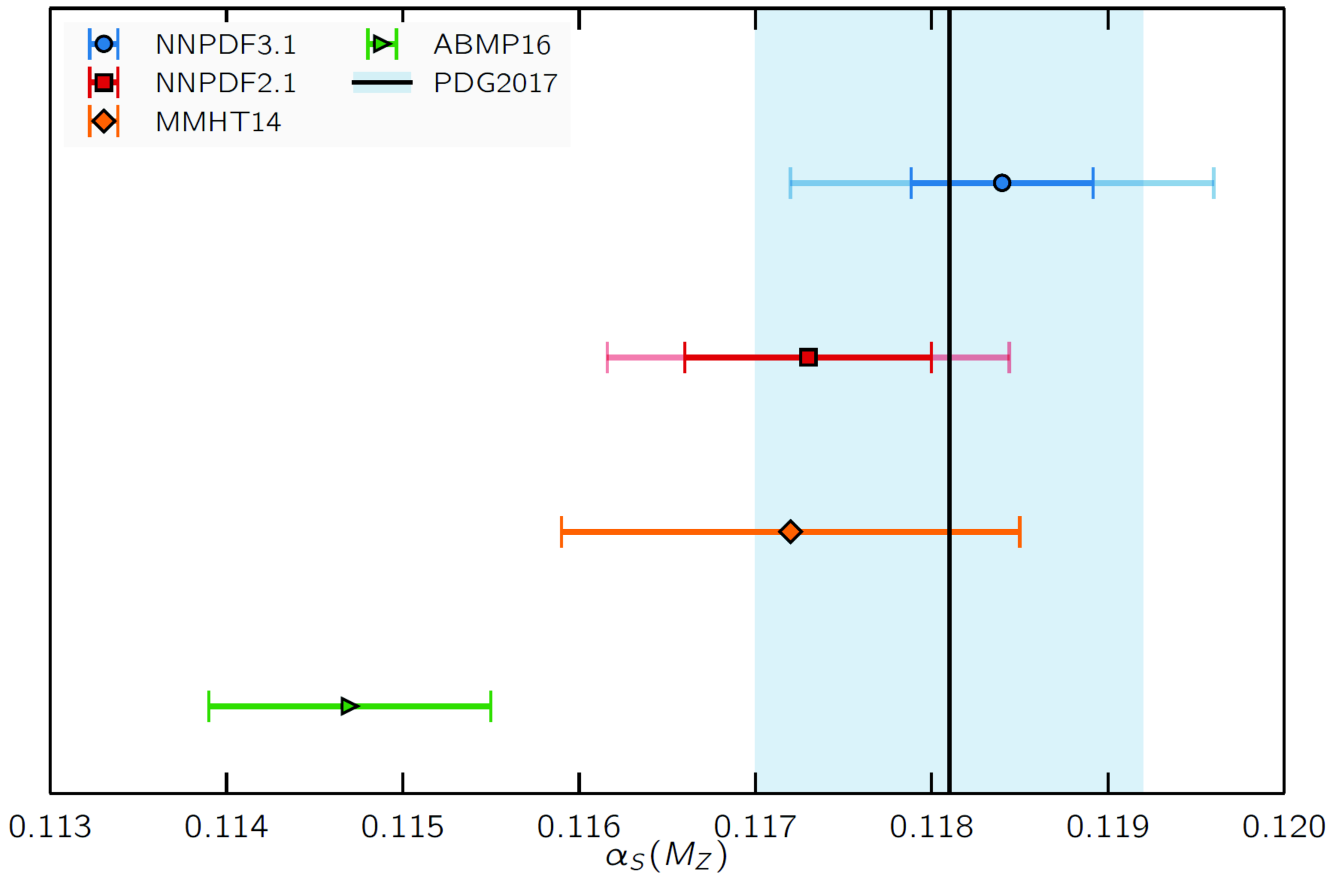


Note ABMP lower at $\alpha_S(M_Z^2) = 0.1147 \pm 0.0008$.

For MMHT2014 $\alpha_S(M_Z^2) = 0.1172 \pm 0.0013$ ($\alpha_S(M_Z^2) = 0.1178$ when world average added as data point). With 8 TeV data on $\sigma_{\bar{t}t}$ and final HERA data went to $\alpha_S(M_Z^2) = 0.118$.

Addition of LHC jets and removal of Tevatron jet data gives $\alpha_S(M_Z^2) = 0.1164$. When Tevatron jets also added back $\alpha_S(M_Z^2) = 0.1173$

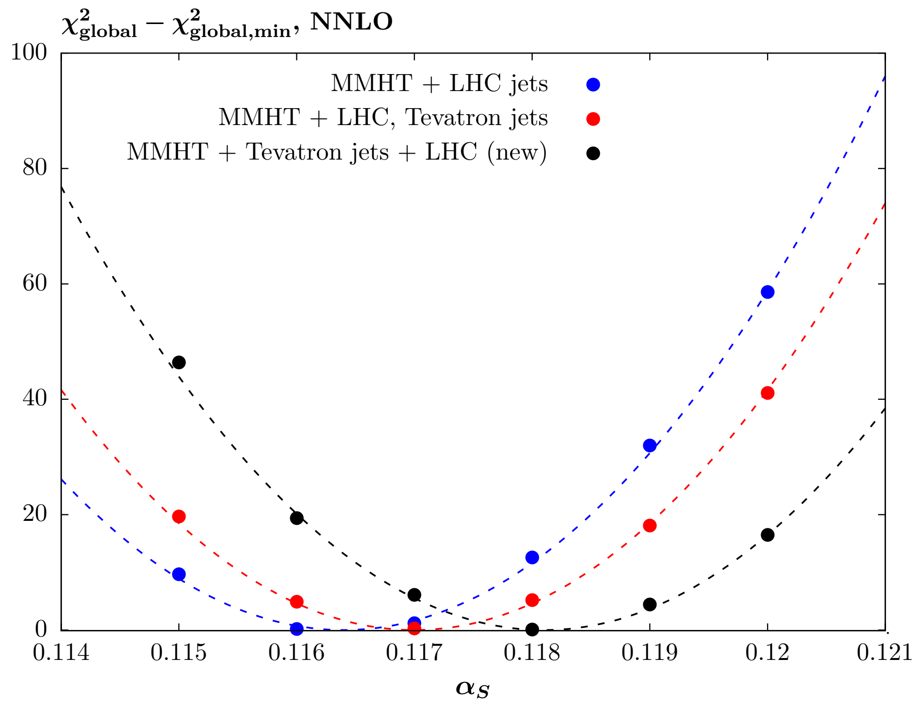


Also look at inclusion of newer $W, Z$ data from ATLAS, CMS, LHCb. Without newer LHC jet data $\alpha_S(M_Z^2) = 0.1179$ but with these data $\alpha_S(M_Z^2) = 0.1176$.

# CT see lots of tension between data sets.

## $\alpha_s$ (Mz ) for CT18

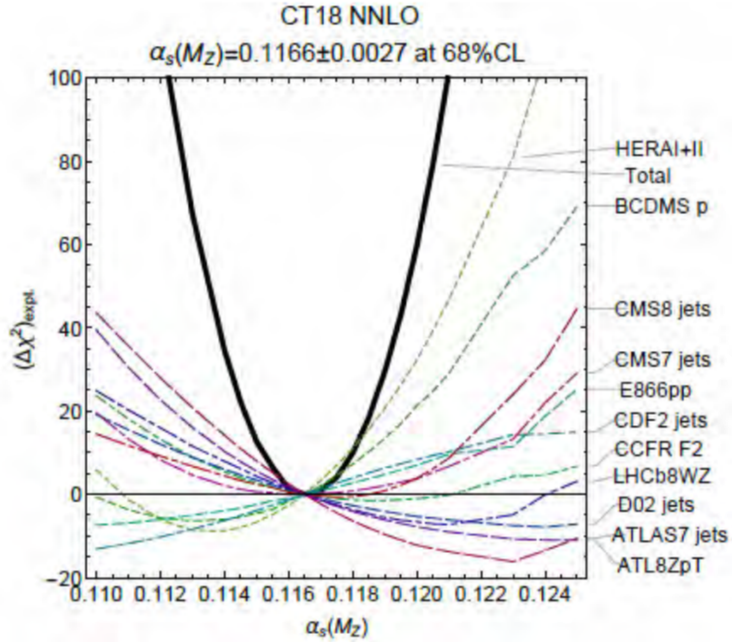


HERA I+II

Lagrange Multiplier scan

ATLAS 7 jet

ATLAS 8 Z pT

- The fixed target F2 data and HERA DIS data prefer smaller αs value.
- The ATLAS 8TeV Z pT and ATLAS 7 TeV incl. jet data, bring the central value of αs (Mz ) from $0.115^{+0.006}_{-0.004}$ (CT14) to 0.1166 ± 0.0027 (CT18).

Yuan DIS 2019

# HERAPDF include DIS jet data with NNLO calculation.

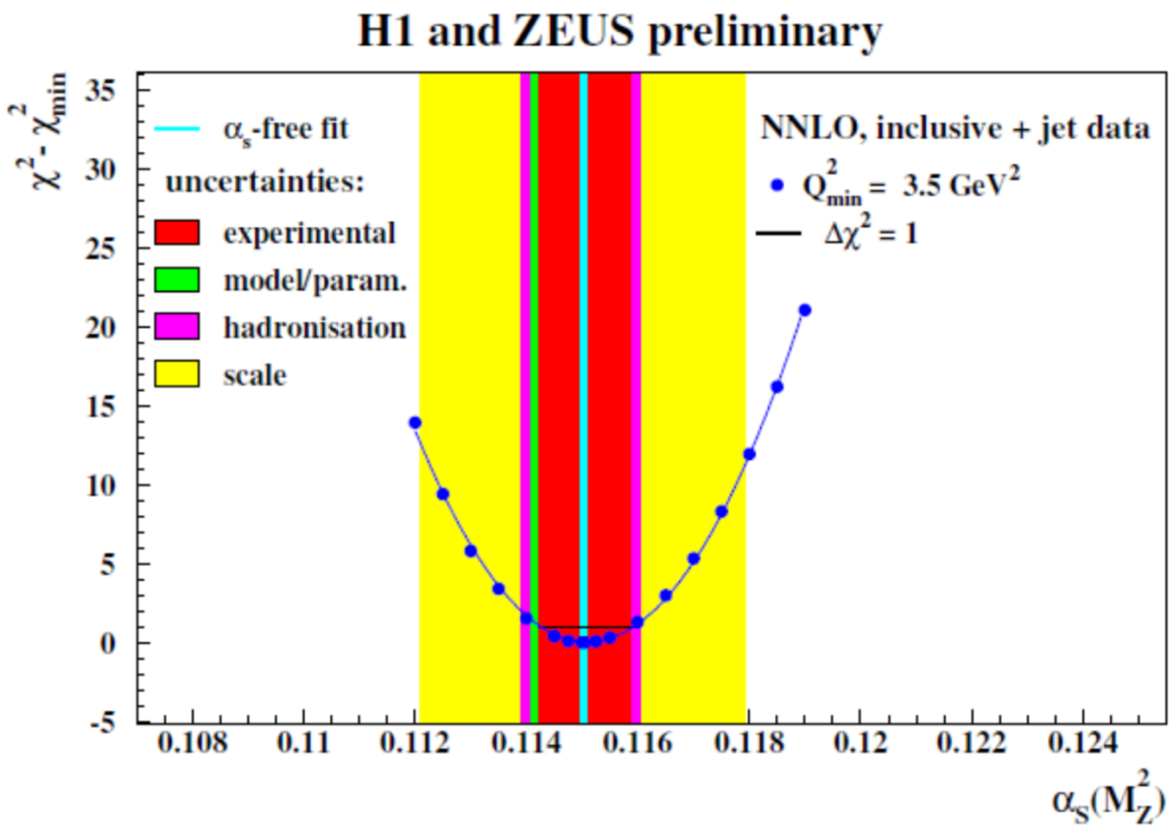


$\alpha_s(M_Z)=0.1150 \pm 0.0008_{(exp)}\, ^{+0.0002}_{-0.0005(model/param)} \pm 0.0006_{(had)} \pm 0.0027_{(scale)}$

Cooper-Sarkar DIS 2019

**Reaching the point where PDF uncertainties related to theory becoming vital.** First attempts by NNPDF tries varying scales.

## Theory covariance matrix

- In a PDF fit we use data $D_i$ and experimental covariance matrix $C_{ij}$
- Want to include theory covariance matrix $S_{ij}$
- $C_{ij} \to C_{ij} + S_{ij}$ [R. D. Ball & A. Desphande, arXiv:1801.04842]
- Nuisance parameters: $\Delta_i^{(n)} = T_i^{(n)} - T_i$, $n = 1, ..., N_{nuis}$
- $S_{ij} = \frac{1}{N_{nuis}} \sum_{n=1}^{N_{nuis}} \Delta_i^{(n)} \Delta_j^{(n)}$
- Treat theory errors like experimental systematics

| | $C$ | $C + S^{(3\mathrm{pt})}$ | $C + S^{(9\mathrm{pt})}$ |
|---|---|---|---|
| $\chi^2$ | 1.139 | 1.139 | 1.109 |
| $\phi$ | 0.314 | 0.310 | 0.315 |

TABLE II: The central $\chi^2$ per datapoint and the average uncertainty reduction $\phi$ for the 3-point and 9-point fits.

Voisey DIS 2019

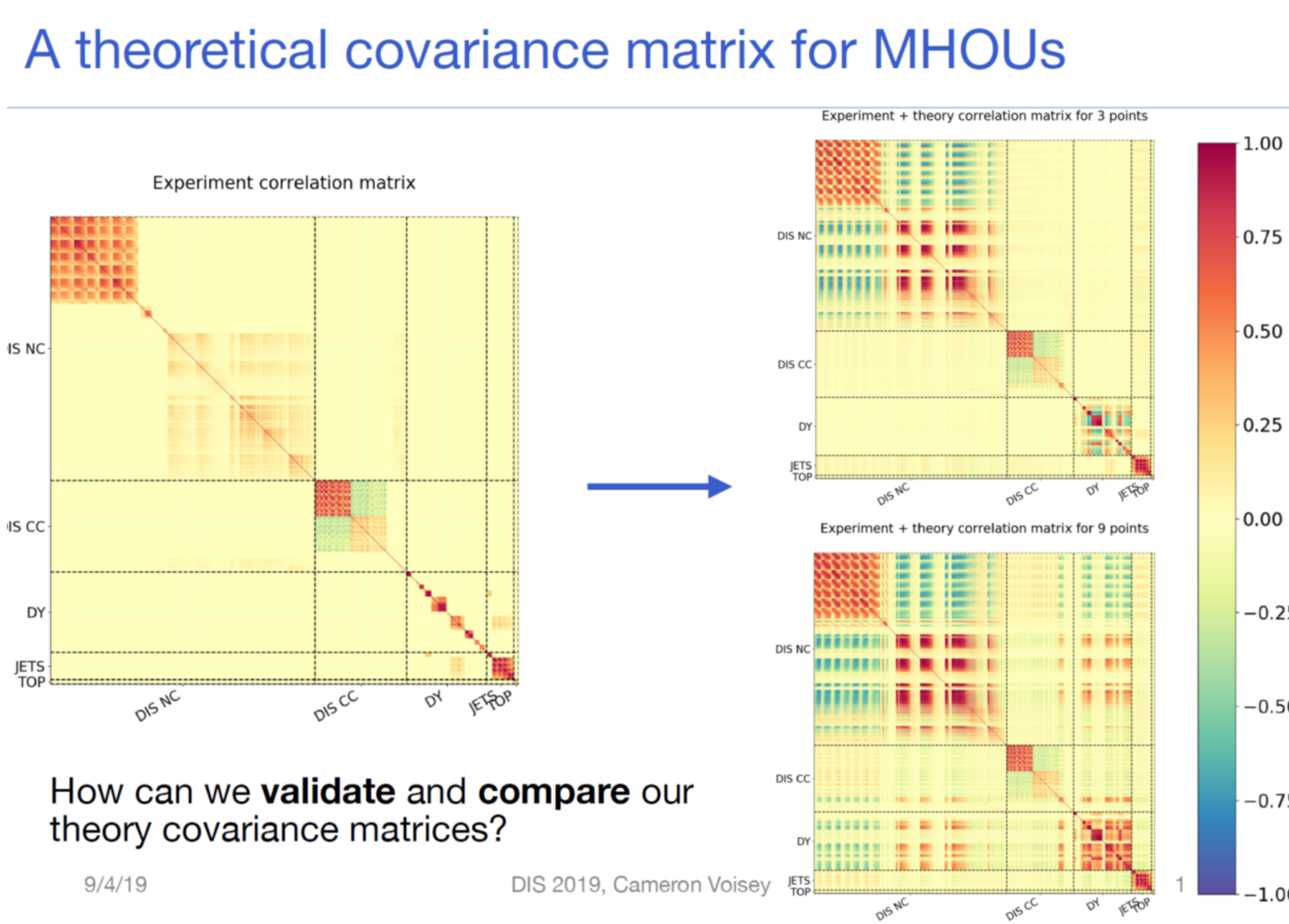


Uncertainties **related to** PDFs not the same as uncertainties **on** PDFs.

Change in PDFs and in the uncertainty.

The uncertainty is hardly changed.

Scale variations highly correlated.

Data constrains variation in scales.

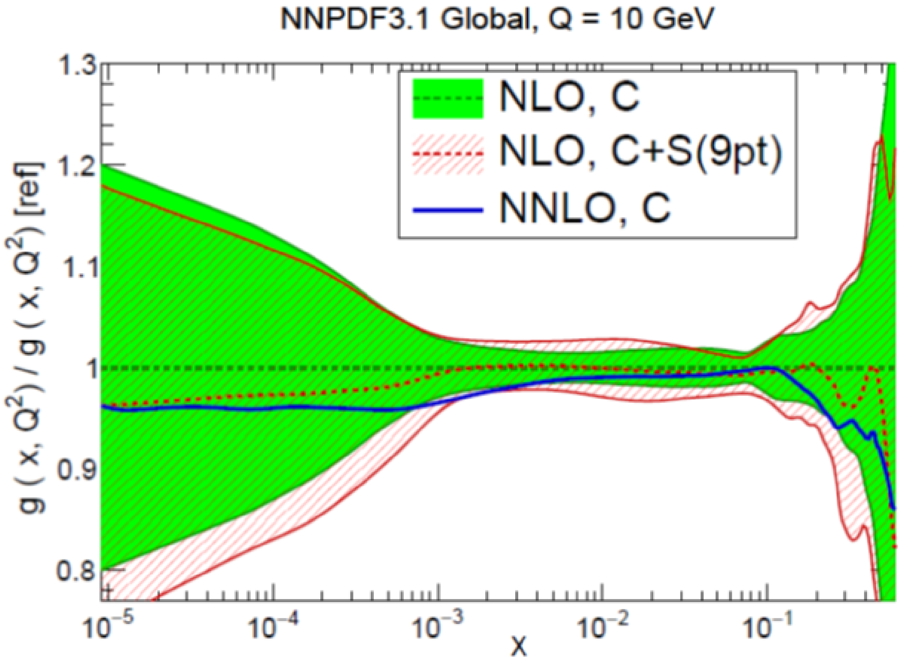


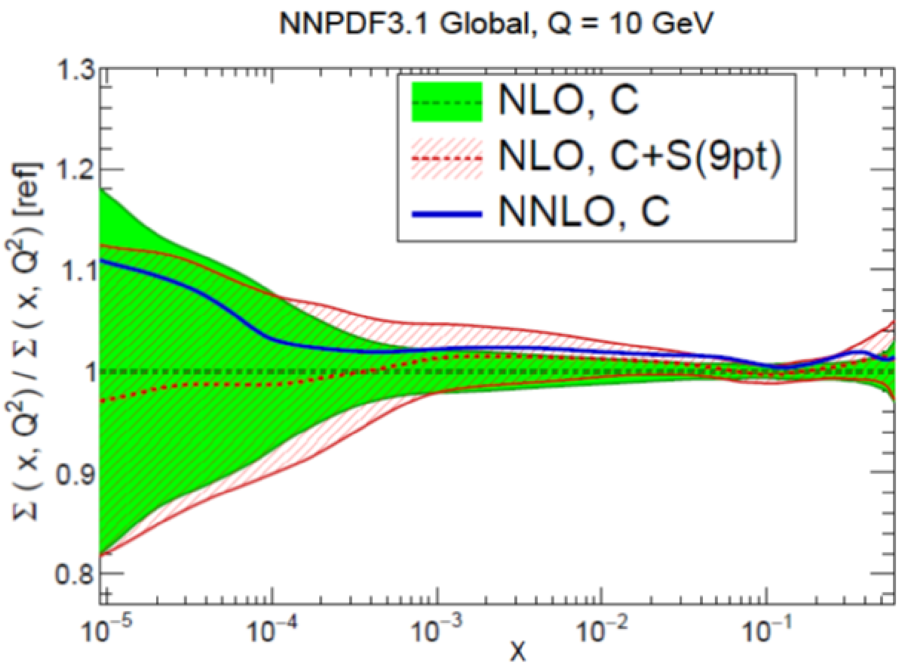

## Theory Uncertainties – Factorization Scale Variation

http://arxiv.org/abs/arXiv:1811.08434 Harland-Lang, RT.

Scale variation of a fixed factor often used as a basis for estimation of theory uncertainty (not necessarily good).

Parton distributions not physical. In practice measure one physical quantity, determine PDF (vary scale $a_i = Q^2/\mu_F^2$), and predict another physical quantity (vary scale $a_f = Q^2/\mu_F^2$).

If both physical quantities determined in terms of only one type of PDF then in practice

$$F'_{\rm NS}(x,Q^2) = F_{\rm NS}(x,aQ^2) + \tilde{\alpha}_S \left(C_q'^{(1)} - C_q^{(1)}\right) \otimes F_{\rm NS}(x,aQ^2) - \tilde{\alpha}_S \ln a P_{qq}^{(0)} \otimes x F_{\rm NS}(x,aQ^2)$$

where $a = a_f/a_i$, i.e. only really one relative scale factor. Extends to higher orders.

In so much that a fixed scale variation means something, varying in fit and prediction is double counting – could just do either.

In general More complicated, but when considering quarks and gluons evolution splits into two eigenvectors. Fit to two quantities $F$ and $H$

$$F(Q^2) = \Sigma_+(\mu^2) \left(\frac{Q^2}{\mu^2}\right)^{\tilde{\alpha}_S \gamma_+} F_+ + \Sigma_-(\mu^2) \left(\frac{Q^2}{\mu^2}\right)^{\tilde{\alpha}_S \gamma_-} F_- \ ,$$

$$H(Q^2) = \Sigma_+(\mu^2) \left(\frac{Q^2}{\mu^2}\right)^{\tilde{\alpha}_S \gamma_+} H_+ + \Sigma_-(\mu^2) \left(\frac{Q^2}{\mu^2}\right)^{\tilde{\alpha}_S \gamma_-} H_-$$

Predicting a third physical quantity $K$

$$K(Q^2) \sim \left(K_1 + \tilde{\alpha}_S \ln\left(\frac{a_f}{a_k}\right) K_2 + \tilde{\alpha}_S \ln\left(\frac{a_h}{a_f}\right) K_3\right) F\left(\frac{a_k}{a_f} Q^2\right) + \begin{array}{l} F \leftrightarrow H \\ a_f \leftrightarrow a_h \end{array}$$

Now have dependence on $a_h/a_f$ (disappears if factorization scales correlated in fit). Independent of scale in prediction.
In practice things often simplify.

$$F(Q^2) = \Sigma_+(\mu^2) \left(\frac{Q^2}{\mu^2}\right)^{\tilde{\alpha}_S \gamma_+} F_+ + \Sigma_-(\mu^2) \left(\frac{Q^2}{\mu^2}\right)^{\tilde{\alpha}_S \gamma_-} F_- \ ,$$

★ High $x$ : $\begin{array}{l} \Sigma_+(j,\mu^2) = g(j,\mu^2) \\ \Sigma_-(j,\mu^2) = \Sigma_q(j,\mu^2) \end{array}$ ★ Low $x$ : $g(j,\mu^2) \sim q(j,\mu^2) \sim \Sigma_+(j,\mu^2)$

In this limit same conclusion as the case of a single PDF.

## Revival of studies with $\ln(1/x)$ resummation (Fit in Eur.Phys.J. C78 (2018) no.4, 321.)

### PDFs with BFKL resummation

- Ultimately, the need for (or lack of) BKFL resummation can only be assessed by performing a **global PDF analysis with (N)NLO+NLLx matched theory**
- Theoretical tools are now available: **HELL for NLLx resummation**, interfaced to the public **APFEL** code

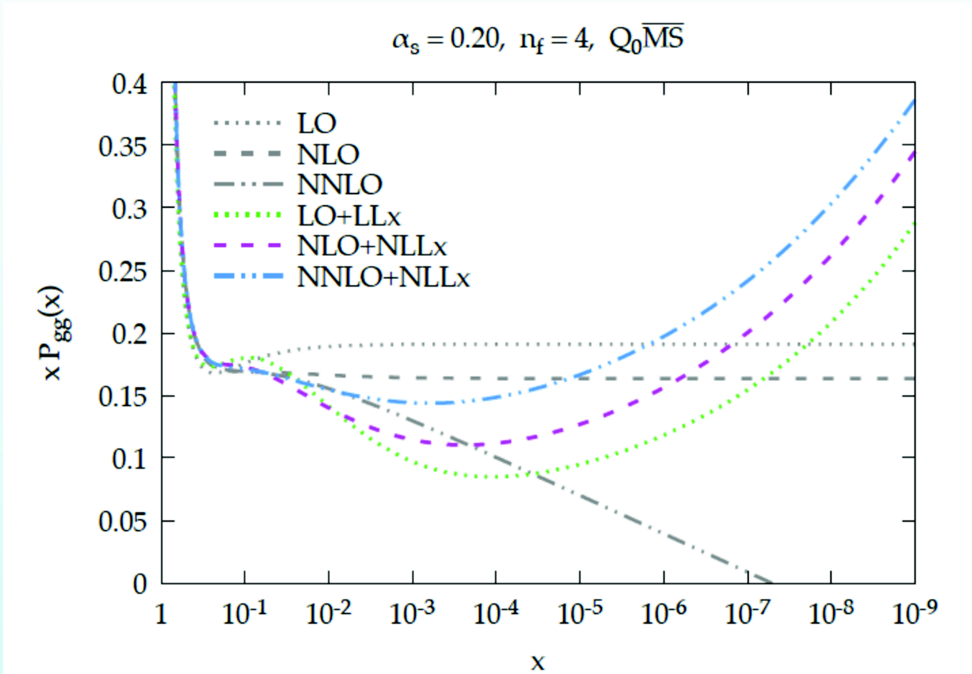


*Bonvini, Marzani, Peraro 16*
*Bonvini, Marzani, Muselli 17*

$$P_{ij}^{\mathrm{N}^k\mathrm{LO}+\mathrm{N}^h\mathrm{LL}x}(x) = P_{ij}^{\mathrm{N}^k\mathrm{LO}}(x) + \Delta_k P_{ij}^{\mathrm{N}^h\mathrm{LL}x}(x),$$

*https://www.ge.infn.it/~bonvini/hell/*

**Juan Rojo** 13 **PDF4LHC WG meeting, CERN, 06/08/2017**

Based on results previously obtained from studies by Altarelli, Ball, Forte, Ciafaloni, Colferai, Salam, Stasto and RT, White.

# Comparison with HERA data

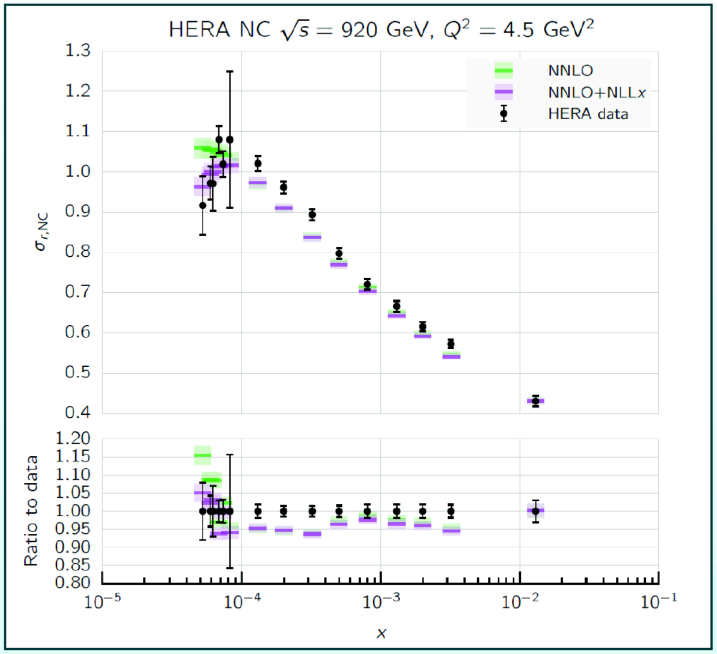


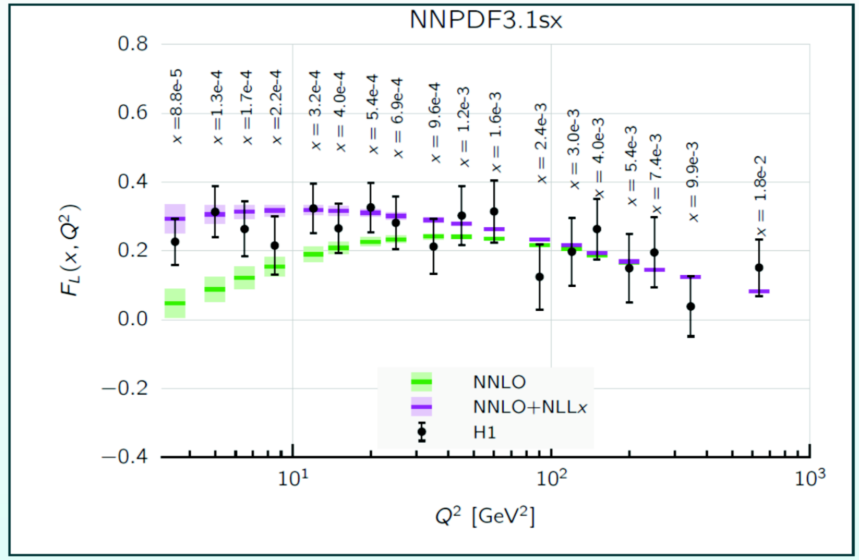


Using **NNLO+NLL*x* theory,** improved description of the **small-x NC cross-sections**, in particular of the change of slope

Also **improved description of $F_L$,** which moreover remains markedly **positive** down to the smallest values of *x* and Q probed

**Juan Rojo** 18 **PDF4LHC WG meeting, CERN, 06/08/2017**

Also resolves problems in fitting charm data at NNLO.

General results also found by xFitter Eur.Phys.J. C78 (2018) 621, but no issue with fit to charm data in this instance.

## Data vs theory

| | NNLO fit | NNLO+NLL$x$ fit |
|---|---|---|
| Total $\chi^2$/d.o.f | 1446/1178 | 1373/1178 |
| subset NC 920 $\tilde{\chi}^2$/n.d.p | 446/377 | 413/377 |
| subset NC 820 $\tilde{\chi}^2$/n.d.p | 70/70 | 65/70 |
| subset charm $\tilde{\chi}^2$/n.d.p | 48/47 | 49/47 |
| correlated shifts inclusive | 102 | 77 |
| correlated shifts charm | 15 | 11 |
| log term inclusive | 20 | −3 |
| log term charm | −2 | −1 |

$$\chi^2 = \sum_i \frac{\left[D_i - T_i\left(1 - \sum_j \gamma^i_j b_j\right)\right]^2}{\delta^2_{i,\mathrm{unc}} T_i^2 + \delta^2_{i,\mathrm{stat}} D_i T_i} + \sum_j b_j^2 + \sum_i \ln \frac{\delta^2_{i,\mathrm{unc}} T_i^2 + \delta^2_{i,\mathrm{stat}} D_i T_i}{\delta^2_{i,\mathrm{unc}} D_i^2 + \delta^2_{i,\mathrm{stat}} D_i^2},$$

→ largest improvements in the $\chi^2$ are observed for the precise $E_p = 920$ GeV set as well as for correlated systematic uncertainties and log-penalty term.

Bertone, DIS 2018

# LHCb heavy flavour data potentially constrains this region

Open charm production

JHEP03(2016)159, JHEP05(2017)074, JHEP06(2017)147

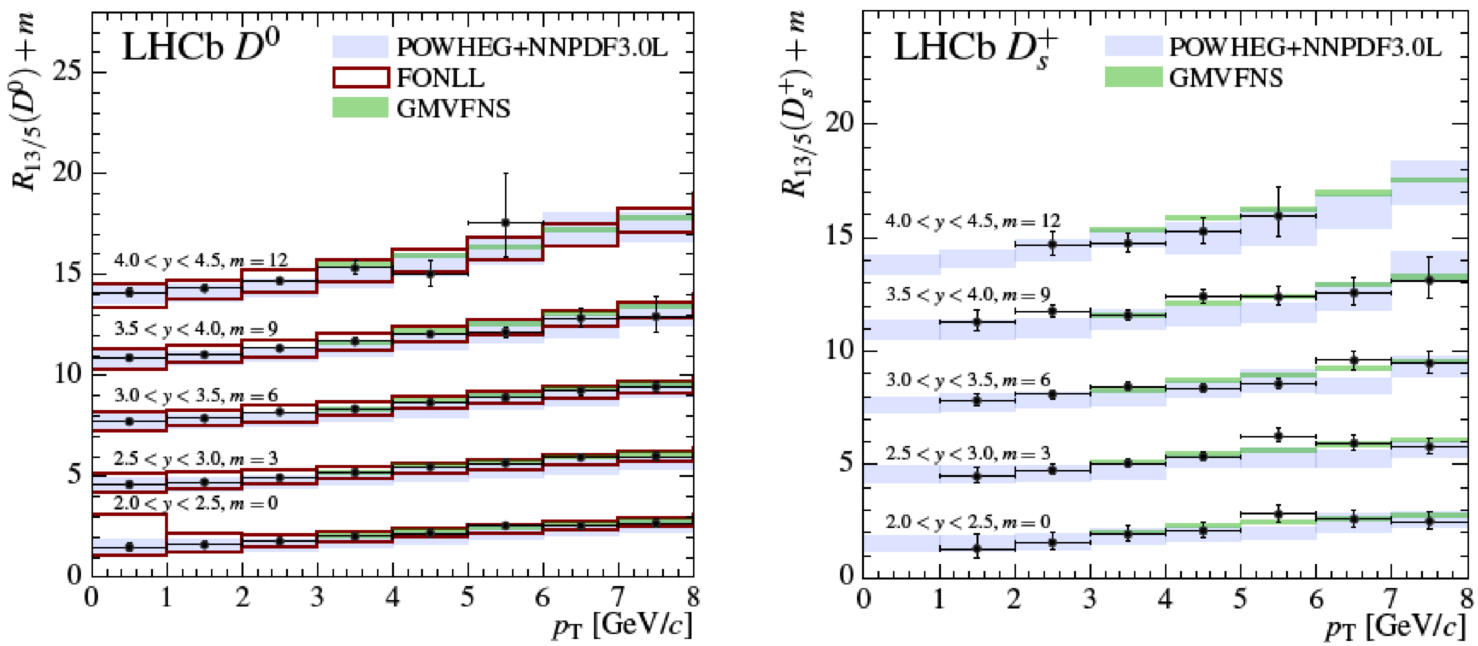


Theory for cross section not as well-understood.

Known at NLO - potential large corrections at small $x$.

**PDFs the dominant uncertainty source for $M_W$ determination.**
Bozzi *et al*, Phys. Rev. D91 (11) (2015) 113005.

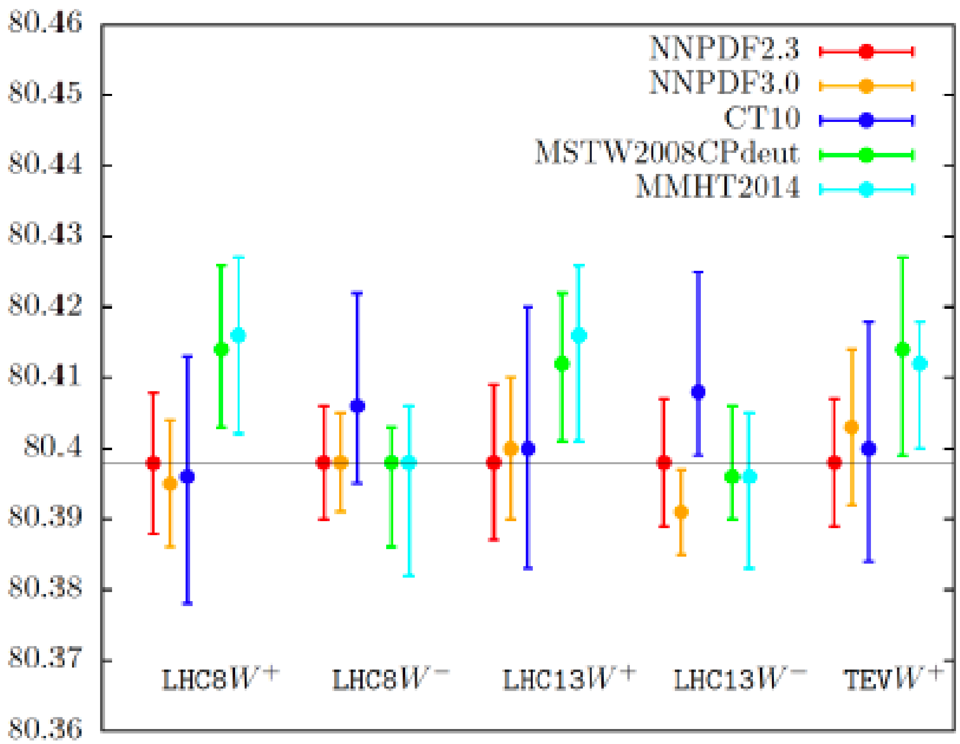


Significant variation between some PDF sets depending on whether $W^+$ or $W^-$ used.

There will be some impact for the most recently incorporated LHC data, and from some methodology changes.

## Also playing and important role in $\sin^2\theta_W$ extraction.

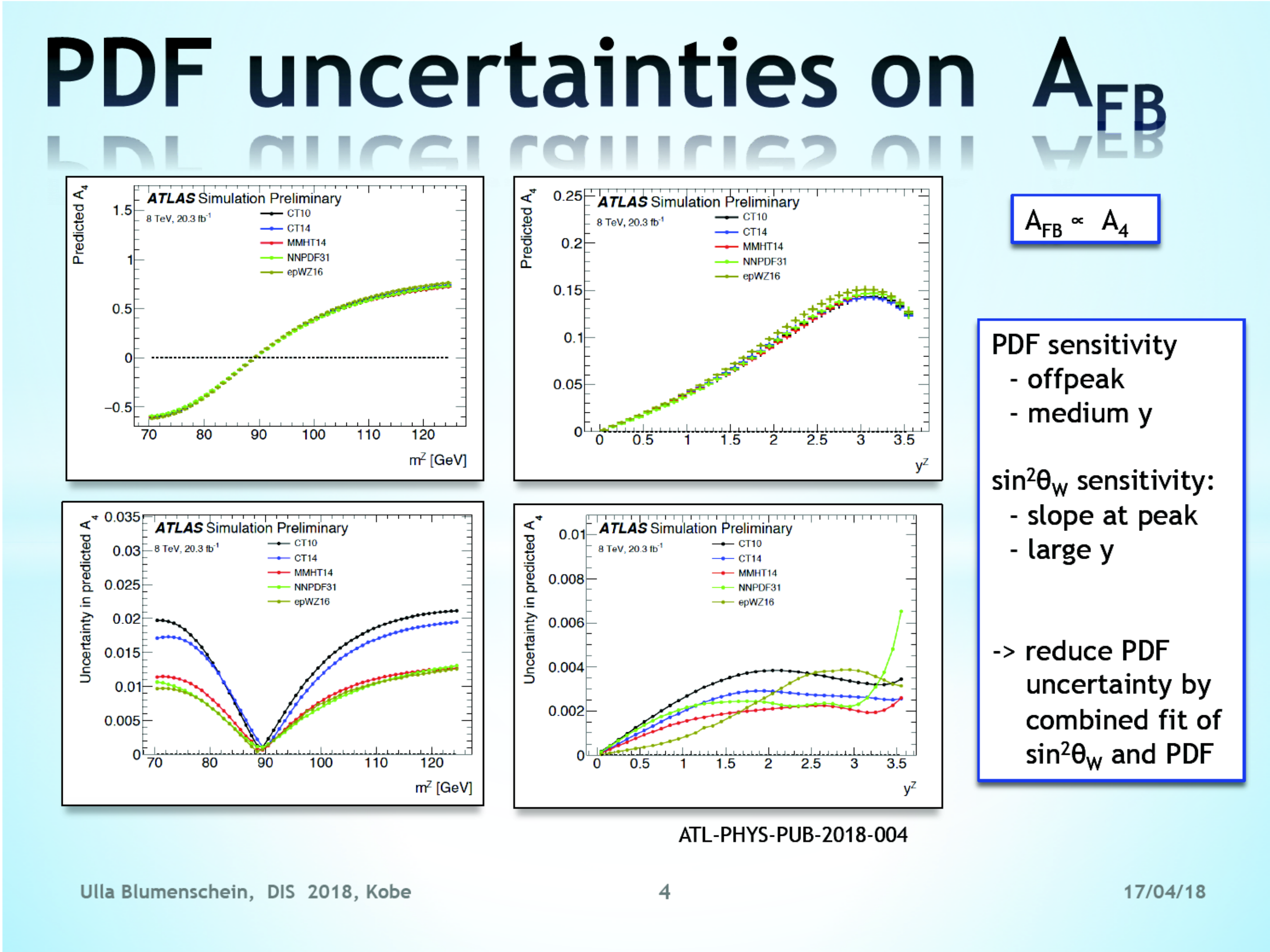

## Very recent study on potential impact of High Lumi LHC on PDFs – Bailey, Gao, Harland-Lang, Khalek, Rojo.

# PDF-sensitive processes at the HL-LHC

Our analysis is based on a **non-exhaustive** list of **PDF-sensitive processes** at the HL-LHC, with emphasis on **high-$p_T$ region,** and on measurements that are not already **limited by systematic uncertainties**

| Process | Kinematics | $N_{\text{dat}}$ | |
|---|---|---|---|
| $Z\ p_T$ | $20\,\text{GeV} \leq p_T^{ll} \lesssim 3.5$ TeV<br>$12\,\text{GeV} \leq m_{ll} \leq 150$ GeV<br>$\lvert y_{ll}\rvert \leq 2.4$ | 130 | $\longrightarrow$ *medium-x gluon* |
| high-mass Drell-Yan | $m_{ll} \geq 116\,\text{GeV},\ \lvert\eta_l\rvert < 2.5$<br>$p_T^{l1(2)} \geq 40\ (30)$ | 21 | $\longrightarrow$ *antiquarks* |
| top quark pair | $m_{t\bar{t}} \lesssim 5$ TeV, $\lvert y_t\rvert \leq 2.5$ | 26 | $\longrightarrow$ *large-x gluon* |
| $W$+charm (central) | $p_T^{\mu} \geq 26\,\text{GeV},\ p_T^{c} \geq 5\,\text{GeV},$<br>$\lvert\eta^{\mu}\rvert \leq 2.4$ | 6 | $\longrightarrow$ *strangeness* |
| $W$+charm (forward) | $p_T^{\mu} \geq 20\,\text{GeV},\ p_T^{c} \geq 20\,\text{GeV},\ p_T^{\mu+c} \geq 20\,\text{GeV},$<br>$2 \leq \eta^{\mu} \leq 2.4,\ 2.2 \leq \eta^{c} \leq 3.2$ | 12 | $\longrightarrow$ *strangeness* |
| Direct photon | $E_T^{\gamma} \lesssim 3$ TeV, $\lvert\eta_\gamma\rvert \leq 2.5$ | 60 | $\longrightarrow$ *medium-x gluon* |
| Forward $W, Z$ | $p_T^{l} \geq 20\,\text{GeV},\ 2.0 < \eta_l < 4.5$<br>$60 < m_{ll} < 120\,\text{GeV},\ 2.0 < y_{ll} < 4.5$ | 90 | $\longrightarrow$ *antiquarks* |
| Inclusive jets ($R = 0.4$) | $\lvert y_{\text{jet}}\rvert \leq 3,\ p_T^{\text{jet}} \lesssim 4$ TeV | 54 | $\longrightarrow$ *large-x gluon* |

# Parton distributions at the HL-LHC

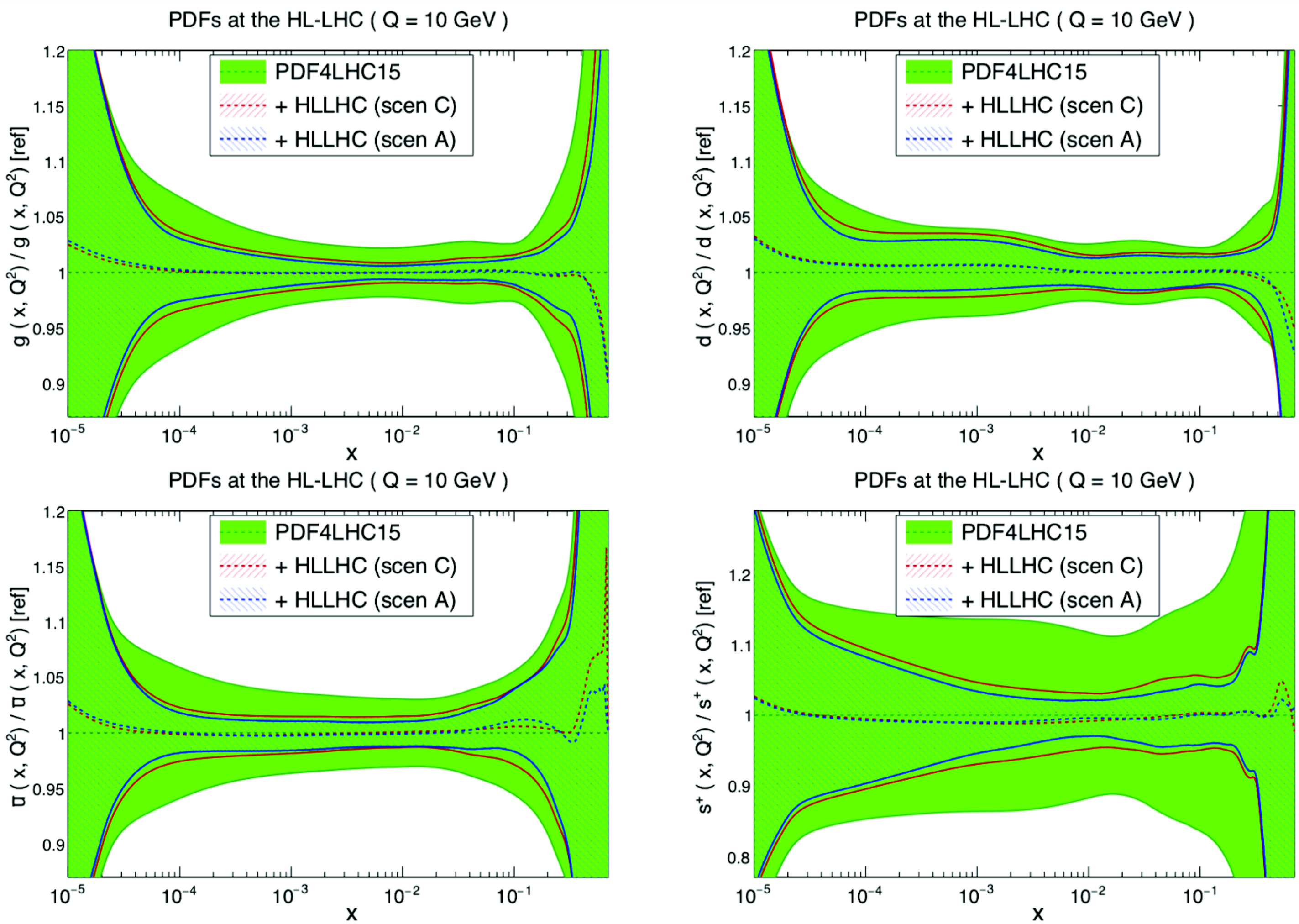


- **Scenario A: optimistic** (assume systematic uncertainty reduction by factor 2.5)
- **Scenario B: Conservative** (assume no reduction in systematic errors)

10

**Juan Rojo** **CERN TH Institute, 17/07/2018**

# Complementarity between HL-LHC and LHeC.

## LHeC

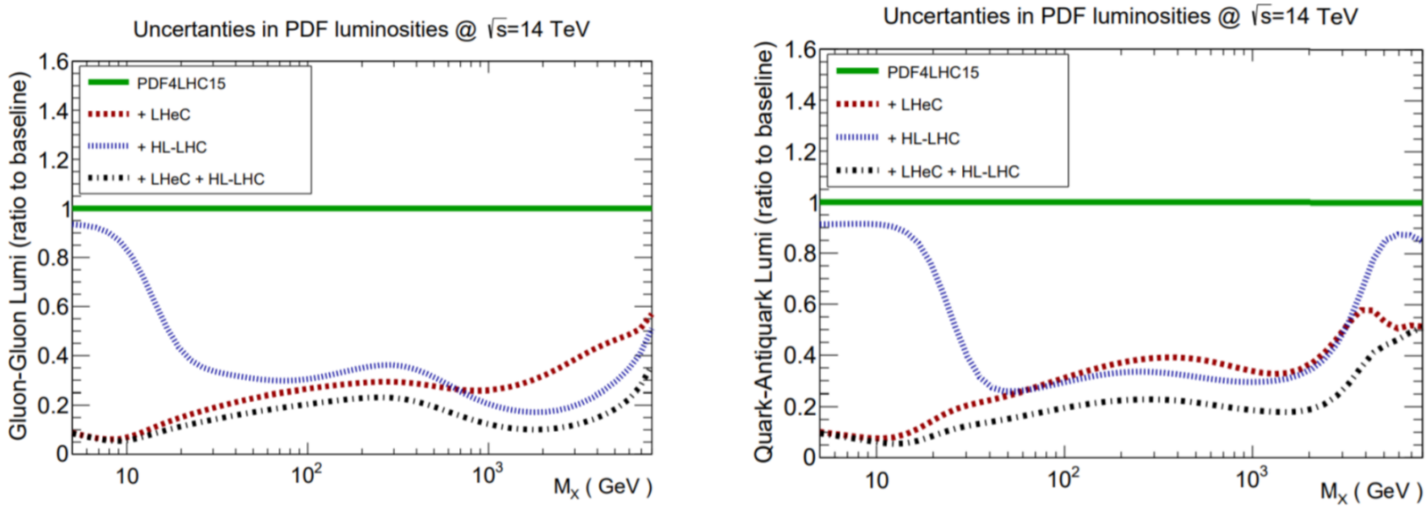


- HL-LHC and LHeC complementary, reducing errors in different regions
- e.g. HL-LHC reduces high-x gluon, while LHeC reduces low-x gluon
- However, not all data-sets chosen to concentrate on these regions and others such as jets at LHeC can constrain high-x gluon

Bailey DIS 2019

# Partonic luminosities at the HL-LHC

*Uncertainty reduction in PDF luminosities as compared to the baseline (current situation)*

| PDF uncertainties HLLHC / Current | 10 GeV < $M_X$ < 40 GeV | 40 GeV < $M_X$ < 1 TeV | 1 TeV < $M_X$ < 6 TeV |
|---|---|---|---|
| g-g luminosity | 0.58 (0.49) | 0.41 (0.29) | 0.38 (0.24) |
| q-g luminosity | 0.71 (0.65) | 0.49 (0.42) | 0.39 (0.29) |
| quark-quark luminosity | 0.78 (0.73) | 0.46 (0.37) | 0.60 (0.45) |
| quark-antiquark luminosity | 0.73 (0.70) | 0.40 (0.30) | 0.61 (0.50) |
| up-strange luminosity | 0.73 (0.67) | 0.38 (0.27) | 0.42 (0.38) |

- In the region $\mathbf{M_X > 40}$ **GeV**, the constraints from the HL-LHC can lead to a reduction of the PDF uncertainties in the partonic lumis of **up to a factor 4 in the optimistic scenario**
- Even with rather conservative assumptions, a **PDF error reduction between a factor 2 and 3** can be expected
- Moreover, these results are mostly likely **upper bounds** on the HL-LHC potential, since we have not included other PDF-sensitive processes (dijets, single top, low-mass DY, charged meson production, …)

# Calculating PDFs in a complete different manner, i.e. lattice.

| Mom. | Collab. | Ref. | $N_f$ | Status | Disc | QM | FV | Ren | ES | | Value |
|---|---|---|---|---|---|---|---|---|---|---|---|
| $\langle x \rangle_{u^+ - d^+}$ | LHPC 14 | [249] | 2+1 | P | ■ | ★ | ★ | ★ | ★ | | 0.140(21) |
| | ETMC 17 | [250] | 2 | P | ■ | ★ | ■ | ★ | ★ | * | 0.194(9)(11) |
| | RQCD 14 | [251] | 2 | P | ■ | ■ | ○ | ★ | ★ | ** | 0.217(9) |
| $\langle x \rangle_{u^+}$ | ETMC 17 | [250] | 2 | P | ■ | ★ | ■ | ★ | ★ | *▷ | 0.453(57)(48) |
| $\langle x \rangle_{d^+}$ | ETMC 17 | [250] | 2 | P | ■ | ★ | ■ | ★ | ★ | *▷ | 0.259(57)(47) |
| $\langle x \rangle_{s^+}$ | ETMC 17 | [250] | 2 | P | ■ | ★ | ■ | ★ | ★ | *▷ | 0.092(41)(0) |
| $\langle x \rangle_{g}$ | ETMC 17 | [250] | 2 | P | ■ | ★ | ■ | ○ | ★ | * | 0.267(22)(27) |

* Study employing a single physical pion mass ensemble.
** Study employing a single ensemble with $m_\pi = 150$ MeV.
▷ Nonsinglet renormalization is applied.

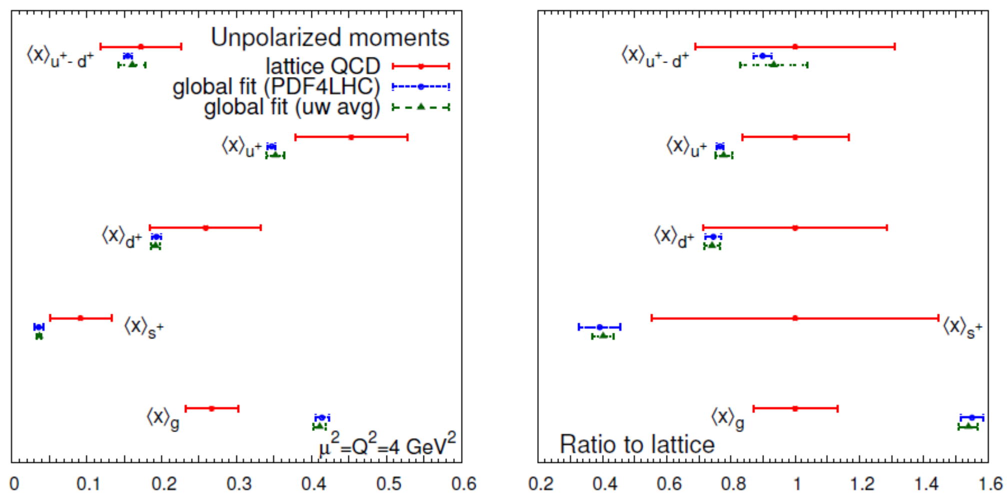


Figure 3.2: A comparison of the unpolarized PDF benchmark moments between the lattice QCD computations and global fit determinations. Results are displayed both in terms of absolute values (left) and ratios to the lattice values (right) at $\mu^2 = 4$ GeV$^2$.

## Conclusions

LHC data starting to have a significant impact on PDF extractions.

Theory catching up for fitting precision data, e.g NNLO jets, differential top, ....

Significant changes in strange distribution most likely first major change.

Many new tools becoming available – practical and potentially theoretical.

Precision data and theory throwing up problems in cases where correlated systematics are important. Improved interplay between theory/experiment on these seems a priority.